BRADLEY GRAHAM WAGNER

MODELING VACCINATION STRATEGIES FOR THE CONTROL AND ERADICATION OF CHILDHOOD INFECTIOUS DISEASE

By
BRADLEY G. WAGNER, MSc BSc

A Thesis
Submitted to the School of Graduate Studies
in Partial Fulfilment of the Requirements
for the Degree
Doctor of Philosophy

McMaster University

DOCTOR OF PHILOSOPHY (2008) McMaster University

TITLE: Modeling Vaccination Strategies for the Control and Eradication of Childhood Infectious Disease

AUTHOR: Bradley G. Wagner, MSc (McMaster University)
BSc (University of British Columbia)

SUPERVISOR: Professor David J.D. Earn

NUMBER OF PAGES: xi, 199

Inclusion of Previously Published Material

Chapter 2 of this thesis represents previously published co-authored material (Wagner B.G. and Earn, D.J.D . *Circulating Vaccine Derived Polioviruses and their Impact on Global Polio Eradication.* Bulletin of Mathematical Biology.(2008) 70:253-280.) For this co-authored work B.G. Wagner was responsible for global stability proofs, numerical work, and served as the primary author. The article is reprinted with the permission of the Society for Mathematical Biology and D.J.D. Earn.

Abstracts

The main body of this thesis deals with three related concepts pertaining to vaccination strategies for childhood infectious disease. Chapter 2 deals with the implications of reversion in the Oral Polio Vaccine on global polio eradication programs. Chapter 3 explores the phenomenon of contact or secondary vaccination in the use of live-attenuated virus vaccines. Chapter 4 explores the importance of demographic stochasticity in pulse vaccination campaigns, largely focusing on measles dynamics. Abstracts for each chapter are given below.

Chapter 2 Abstract

Poliomyelitis vaccination via live Oral Polio Vaccine (OPV) suffers from the inherent problem of reversion: the vaccine may, upon replication in the human gut, mutate back to virulence and transmissibility resulting in circulating vaccine derived polio viruses (cVDPVs). We formulate a general mathematical model to assess the impact of cVDPVs on prospects for polio eradication. We find that for OPV coverage levels below a certain threshold, cVDPVs have a small impact in comparison to the expected endemic level of the disease in the absence of reversion. Above this threshold, the model predicts a small but significant endemic level of the disease, even where standard models predict eradication. In light of this, we consider and analyze three alternative eradication strategies involving a transition from continuous OPV vaccination to either continuous Inactivated Polio Vaccine (IPV), pulsed OPV vaccination, or a one-time IPV pulse vaccination. Stochastic modeling shows continuous IPV vaccination is effective at achieving eradication for moderate coverage levels, while pulsed OPV is effective if higher coverage levels are maintained. The one-time pulse IPV method may also be a viable strategy, especially in terms of the number of vaccinations required and time to eradication, provided that a sufficiently large pulse is practically feasible. More investigation is needed regarding the frequency of revertant virus infection resulting directly from vaccination, the ability of IPV to induce gut immunity, and the potential role of spatial transmission dynamics in eradication efforts.

Chapter 3 Abstract

Viruses contained in live-attenuated virus vaccines (LAVV) can be transmitted between individuals, resulting in secondary or *contact vaccinations*. This fact has been exploited successfully in the use of the Oral Polio Vaccine (OPV) to better control wild polio viruses. In this work we analyze general LAVV vaccination models for infections that confer lifelong immunity. We consider both standard (continuous) vaccination strategies and pulse vaccination programs (where mass vaccination is carried out at regular intervals). For continuous vaccination, we provide a complete global analysis of a very general compartmental ordinary differential equation LAVV model. We find that the threshold vaccination level required for eradication of wild virus depends on the basic reproduction numbers of both the wild and vaccine viruses, but is otherwise independent of the distributions of the durations in each of the sequence of stages of disease progression (e.g., latent, infectious, *etc.*). Furthermore, even for vaccine viruses with reproduction numbers below one, which would naturally fade from the population upon cessation of vaccination, there can be a significant reduction in the threshold vaccination level. The dependence of the threshold vaccination level on the virus reproduction numbers largely generalizes to the pulse vaccination model. For shorter pulsing periods there is negligible difference in threshold vaccination level as compared to continuous vaccination campaigns. Thus, we conclude that current policy in many countries to employ annual pulsed OPV vaccination does not significantly diminish the benefits of contact vaccination.

Chapter 4 Abstract

In the last two decades, many countries have implemented pulse vaccination for infectious diseases (mass vaccination campaigns repeated annually or at other regular intervals). Based on deterministic mathematical models, previous work has shown that the total expected cost of control or eradication (measured by the number of vaccine doses required) is identical for pulse vaccination (with any pulse interval) and for traditional, continuous vaccination. We reconsider this problem using stochastic epidemic models (both by direct simulation and by employing a moment closure approximation). We focus on measles and show that demographic stochasticity has a large impact on the relative success of pulse and continuous vaccination programs, even for well-mixed populations as large as 10 million.

Acknowledgements

I would like to thank my family for their support through my many years of study, my supervisor David Earn for his invaluable guidance, and my friends.

Contents

List of Figures

List of Tables

Chapter 1

Preliminaries

1.1 Introduction

Childhood infectious disease has a significant impact on morbidity and mortality, particularly, in the developing world. Measles infections can result in pneumonia and encephalitis while poliomyelitis infections may leave individuals with lifelong paralysis [9, 10, 11]. The commonality between these and many other childhood diseases is that they are largely preventable through vaccination.

Without a doubt the greatest achievement of modern vaccination programs is the global eradication of smallpox. Traceable as far back as 6000 BC the first true smallpox vaccinations were originated in 1726 using cowpox virus [38] . Despite this, it was not until 1978 that the last naturally occurring smallpox infection was recorded in Somalia, marking the eradication of the disease [12]. The lessons of smallpox underscore that eradication can only be achieved through a well organized global vaccination program.

To date the World Health Organization has aggressively pursued vaccination campaigns in the developing world for polio and measles. Measles remains highly endemic in the developing world (and endemic in the developed world) accounting for roughly 1 million deaths per year [9, 10]. Naturally occurring polio, though eliminated in the developed world, persists at low but significant levels in the developing world [11]. As long as the threat of transmission remains, worldwide vaccination levels must be maintained. Should vaccination wane, introduction of a handful of infectious individuals in an otherwise infection free population can result in epidemics.

Global eradication represents the ultimate goal of any vaccination campaign. Only at this point may vaccination be ceased. This goal is important not only from the standpoint of the alleviation of human suffering, but also from an economic standpoint. The WHO estimates polio eradication alone would save $1.5 billion per year in vaccination and treatment costs [11].

Mathematical modelling has an important role to play in the development of global vaccination strategies. There is a rich history of mathematical contributions to epidemiology. A good place to begin is with the seminal paper of Kermack and McKendrick [27]. This work established that the density of susceptible individuals must exceed a critical threshold in order for an epidemic to occur. Though a standard idea today, it forms the basis for all (deterministic) vaccination models.

Models of the type posed by Kermack and Mckendrick are phrased in the language of differential equations, dividing the population into homogeneous

compartments such as susceptible, infectious or immune. The rate of appearance of new infections (incidence rate) is, in its simplest form, proportional to the product of the densities of susceptible and infectious individuals. This proportionality is commonly referred to as *mass action mixing*. Systems of increased complexity may be considered by adding additional classes that may, for example, be based on age [7, 39], presence of maternal antibodies, multiple stages of infection [17], or geographic heterogeneities. Time varying transmission rates may also be considered reflecting the natural seasonality of disease transmission [16, 35], and more generalized versions of the mass action interaction can be used to reflect the effect of population density on transmission rates [30]. Such compartmentalized mathematical models have been used successfully to explain a variety of epidemiological phenomena. These phenomena include changes in the time patterns of recurrent epidemics [14] as well as the paradoxical increase in magnitude of some epidemics associated with increased hygiene in the 19th and 20th centuries [8].

Compartmental epidemiological models are not limited strictly to childhood disease. From a mathematical standpoint the childhood disease is differentiated from other disease models by two qualities; ideally infection (and vaccination) result in complete and lifelong immunity, and (in the absence of vaccination) transmission rates are sufficiently high that the average age of infection is during childhood. Of course in reality previous infection and vaccination do not guarantee immunity. However this represents a reasonable approximation and further complexity may be straightforwardly added to

models to take into account vaccine failures and less than perfect immunity when appropriate.

Though differential equation based compartmental models often give great insight into the dynamics of epidemiological systems, analysis cannot be limited to these methods. As differential equations deal with continuous flow between compartments they ignore the fact that populations are made up of a discrete finite number of individuals, and infection and recovery are random processes. While compartmental models may be sufficiently predictive at large populations, for smaller populations this demographic stochasticity may have significant effects on the system dynamics.

The effects of demographic stochasticity were first observed by field epidemiologists who noted that for small, isolated populations, recurrent measles epidemics may be prevented by random extinctions [5]. The first mathematical treatments of this phenomena were given in the influential work of Barlett [5, 6]. These works established the idea of the *critical community size* (CCS); the minimum population size required to prevent stochastic extinction (for some fixed finite time). The topic of stochastic extinction and critical community sizes remains an important topic of research to this day [1, 2, 24, 25, 33, 34, 36], and has important implications for vaccination strategies.

In this work we analyze a number of different vaccination strategies with respect to their ability to control disease spread and ultimately achieve complete eradication. We approach these problems using both deterministic com-

partmental differential equation models as well as stochastic methods. We begin with a review of some of the standard epidemiological models on which this work is based.

1.1.1 Standard Models

SEIR Model with Continuous Vaccination

The $SEIR$ model with continuous vaccination represents one of the simplest possible predictive models of childhood infectious disease transmission [19]. Vaccinations are assumed to be performed as soon as maternal antibodies have waned. The model is given by

$$\frac{dS}{dt} = (1-p)\nu N - \frac{\beta}{N} IS - \mu S \tag{1.1a}$$

$$\frac{dE}{dt} = \frac{\beta}{N} IS - (\mu + \sigma)E \tag{1.1b}$$

$$\frac{dI}{dt} = \sigma E - (\mu + \gamma)I \tag{1.1c}$$

$$\frac{dR}{dt} = p\nu N + \gamma I - \mu R \tag{1.1d}$$

$$\frac{dN}{dt} = (\nu - \mu)N \tag{1.1e}$$

The compartments S, E, I, R represent respectively the number of susceptible, infected but not yet infectious (latent), infectious, and immune individuals. The total population is given by $N = S + E + I + R$. The parameters ν and μ represent the *per capita* birth and death rates, while $\frac{1}{\sigma}$ and $\frac{1}{\gamma}$ represent the mean latent and infectious periods. The parameter p represents the

newborn vaccination proportion.

From Eq. (1.1c) we see that the population may undergo exponential growth. As we are concerned with the proportion of the population which is infected or infectious, it is convenient to transform the model(1.1) via

$$X \to \widetilde{X} = \frac{X}{N}. \tag{1.2}$$

Noting that

$$\frac{d\widetilde{X}}{dt} = \frac{1}{N}\frac{dX}{dt} - \frac{(\nu-\mu)X}{N^2}, \tag{1.3}$$

Eq. (1.1) may be rewritten in terms of proportions [18, 19] as

$$\frac{d\widetilde{S}}{dt} = (1-p)\nu - \beta\widetilde{I}\widetilde{S} - \nu\widetilde{S} \tag{1.4a}$$

$$\frac{d\widetilde{E}}{dt} = \beta\widetilde{I}\widetilde{S} - (\nu+\sigma)\widetilde{E} \tag{1.4b}$$

$$\frac{d\widetilde{I}}{dt} = \sigma\widetilde{E} - (\nu+\gamma)\widetilde{I} \tag{1.4c}$$

$$\frac{d\widetilde{R}}{dt} = p\nu + \gamma\widetilde{I} - \nu\widetilde{R} \tag{1.4d}$$

The long time behaviour of system (1.4) is determined by two parameters, the vaccination proportion p and the basic reproduction number which is defined to be the average number of secondary infections resulting from a single infectious individual in an otherwise susceptible population. The basic

reproduction number for the model (1.4) is given by

$$\mathcal{R}_0 = \frac{\beta\sigma}{(\sigma+\nu)(\gamma+\nu)}, \tag{1.5}$$

In the case of constant population, (1.5) may be understood as a product of the transmission rate β, the mean time spent in the infectious class $\frac{1}{(\nu+\gamma)}$, and the probability that an individual will move to the infectious class I from the exposed class E before death $\frac{\sigma}{(\sigma+\nu)}$. System (1.4) has two equilibria: an endemic equilibrium given by

$$S^* = 1 - \frac{1}{\mathcal{R}_0} \tag{1.6a}$$

$$E^* = \frac{\nu}{(\nu+\gamma)}\left(1 - \frac{1}{\mathcal{R}_0} - p\right) \tag{1.6b}$$

$$I^* = \frac{\nu\sigma}{(\nu+\sigma)(\nu+\gamma)}\left(1 - \frac{1}{\mathcal{R}_0} - p\right), \tag{1.6c}$$

and a *disease free equilibrium* (DFE) given by

$$S^0 = 1 - p \tag{1.7a}$$

$$E^0 = 0 \tag{1.7b}$$

$$I^0 = 0. \tag{1.7c}$$

Lyapnuov function methods may be used to establish that the *endemic equi-*

librium is globally asymptotically stable when it exists [29], i.e., if

$$p \geq p_{\text{crit}} = 1 - \frac{1}{\mathcal{R}_0}, \tag{1.8}$$

while the *disease free equilibrium* is globally asymptotically stable above this threshold vaccination level. For this deterministic model, p_{crit} gives the critical vaccination proportion for eradication. The use of Lyapunov functions for epidemic models is expanded on in chapter 3 . Analogous results for the continuous vaccination SIR model, which lacks the latent class E are given in chapter 2

Pulse vaccination SIR model

In pulse vaccination strategies, mass vaccinations are performed at regular intervals rather than continuously. This strategy is currently utilized for measles and polio vaccination in a number of countries, though often in conjunction with standard continuous vaccination [4, 43] . In its simplest form, the pulse vaccination strategy can be represented by an SIR model

[40, 42] of the type

$$\frac{dS}{dt} = \nu - \beta IS - \nu S - p_{\text{pulse}} \sum_{n=0}^{\infty} \delta(t - nT) S(nT^-) \tag{1.9a}$$

$$\frac{dI}{dt} = \beta IS - (\nu + \gamma) I \tag{1.9b}$$

$$\frac{dR}{dt} = p_{\text{pulse}} \sum_{n=0}^{\infty} \delta(t - nT) S(nT^-) - \nu R \tag{1.9c}$$

$$S(nT^-) = \lim_{\varepsilon \to 0^+} S(nT - \varepsilon) \tag{1.9d}$$

Eq. (1.9) is phrased in terms of proportions of the population as in Eq. (1.1). The parameter p_{pulse} represents the proportion of susceptibles vaccinated in each pulse, while T is the pulse interval. As in (1.1), ν represents the *per capita* birth rate while $\frac{1}{\gamma}$ is the mean infectious period. Note that unlike the $SEIR$ model there is no latent period included in (1.9).

System (1.9) possesses a unique T periodic *disease free solution* which can be straightforwardly computed. For $0 \leq t \leq T$ the solution is given by [40]

$$\widetilde{S}(t) = 1 - \frac{p_{\text{pulse}} e^{\nu T}}{e^{\nu T} - (1 - p_{\text{pulse}})} e^{-\nu t} - p_{\text{pulse}} \left(1 - \frac{p_{\text{pulse}} e^{\nu T}}{e^{\nu T} - (1 - p_{\text{pulse}})} e^{-\nu T} \right) \int_0^t \delta(t - T) \tag{1.10a}$$

$$\widetilde{I}(t) = 0 \tag{1.10b}$$

Local stability analysis shows that the T-periodic DFS will be asymptotically

stable whenever

$$\frac{1}{T}\int_0^T \widetilde{S}(t)dt \leq \frac{\nu+\gamma}{\beta} = \frac{1}{\mathcal{R}_0} \tag{1.11}$$

Full details of the local stability analysis computations are given in [40], §4.1. The condition (1.11) actually implies global stability of the DFS as is proved in [13]. Substituting the expression for $\widehat{S}(t)$ (1.10) into condition (1.11) yields the result that for any given pulse vaccination proportion p_{pulse}, there exists a maximal pulsing interval $T_{\max}$ below which the T-periodic DFS is (globally) asymptotically stable. An approximation for $T_{\max}$ is explicitly worked out in [40] §4.1 and is given by

$$T_{\max} \approx \frac{\gamma p_{\text{pulse}}}{\beta\nu(1-p_{\text{pulse}}/2-\gamma/\beta)} \tag{1.12}$$

For $T > T_{\max}$ the disease persists and periodic epidemics as well as chaotic behaviour can be observed [40]. Note that chaotic behaviour something that is impossible for the continuous vaccination SIR model. In this work we also investigate pulse vaccination models based on the $SEIR$ model in which a latent or exposed class is included.

1.1.2 Focus of this Work

This work concentrates on three primary topics, all related to feasibility of disease control and eradication under different vaccination programs.

Reversion in the Oral Polio Vaccine

The Oral Polio Vaccine (OPV) is recommended for use in developing countries [21]. OPV provides a strong immune response with long lasting immunity [3]. Unlike the inactivated vaccine (IPV) OPV is composed of live attenuated viruses (LAVVs). These viruses may, via mutation, regain virulence and transmissibility [22]. Polio outbreaks of revertant virus have been documented, some in regions that were previously certified as polio free [20]. As wild poliovirus eradication gets closer, the impact of these revertant viruses may be a significant obstacle to the eventual cessation of vaccination programs.

We construct and analyze a compartmental model to analyze the impact of revertant viruses on polio eradication for continuous vaccination OPV campaigns. We then provide and analyze a number of possible transition or endgame strategies to achieve complete eradication and allow for the cessation of vaccination.

Contact Vaccination in Live-Attenuated Virus Vaccines

Live-attenuated virus vaccines (LAVVs) differ from inactivated viruses in that they are live viruses, which can be transmitted person to person. Although this transmission can have unwanted consequences in the form of reversion or back mutation to virulence, there are also potential benefits. In the absence of mutation, transmission of vaccine virus results in secondary or contact vaccinations enhancing vaccination coverage. Contact vaccination

is observed in the use of OPV as well as smallpox vaccines [37] , and is cited by the WHO as a reason for the use of OPV in the developing world [23]. We investigate the significance of contact vaccination in the control of wild virus spread. We construct and analyze a general compartmental ordinary equation model for continuous vaccination LAVV campaigns. We then extend our results to pulse vaccination campaigns.

Pulse Vaccination and Stochastic Eradication

Pulse vaccination campaigns, whereby mass vaccinations are performed at regular intervals, are currently used in numerous countries for both measles and polio [41, 43]. We analyze the effect of demographic stochasticity on disease eradication in pulse vaccination strategies in comparison to continuous vaccination strategies. Analytical as well as Monte-Carlo simulation methods are used in our analysis.

Chapter 2

Circulating Vaccine Derived Polioviruses

2.1 Introduction

[1] Vaccination for a number of diseases is currently performed through administration of live-attenuated virus vaccines. Attenuation means that the virus has been altered genetically into a state of low virulence and low transmissibility. Attenuation is often accomplished by passage through successive animal host tissues in which there is selective pressure for mutations that reduce the virulence and transmissibility in humans; this differs from inactivated virus vaccines where the virus is killed by treatment with a chemical

[1]Previously published material: Wagner, B.G and Earn, D.J.D. .*Circulating Vaccine Derived Polioviruses and their Impact on Global Polio Eradication.* Bulletin of Mathematical Biology (2008) 70:253-280.
Printed with permission of Society for Mathematical Biology and D.J.D. Earn

agent or some physical process [29]. An intrinsic problem with live-attenuated virus vaccines is that of back mutation or reversion, whereby the live virus, upon replicating in its human host, may regain its virulence and transmissibility, potentially causing infection in the vaccinee and his or her contacts. Reversion to higher transmissibility is a potentially serious barrier to disease eradication.

An important and well documented example in which reversion takes place is in the use of Oral Polio Vaccine (OPV). Poliovirus is an RNA virus, and may appear in one of three antigenic types. Transmission may be either fecal to oral, or oral to oral. Initially the virus resides in the pharynx and intestines of the host. Subsequently it may invade the local lymphoid tissue, entering the blood stream and eventually invading the motor neurons. Damage to these neurons may result in varying degrees of paralysis. It should be noted that there is no cross immunity between antigenic types. As well, the standard formulation of OPV is *trivalent*: it contains attenuated versions of all three types (each of which is capable of undergoing reversion and potentially causing paralysis [4]).

In cases where OPV vaccination results in paralysis, this effect is commonly referred to as vaccine associated paralytic polio (VAPP). Vaccine viruses which have regained transmissibility and neurovirulence are referred to as circulating vaccine derived polioviruses (cVDPVs) [17].

Though largely replaced in the developed world by the Salk injectable inactivated polio virus vaccine (IPV) [6], OPV is still the primary vaccine in

the developing world. Since 1988, the World Health Organization (WHO) has advocated the exclusive use of OPV for polio eradication, citing five primary factors: (1) low cost, (2) simple administration (oral), (3) high effectiveness for a small number of doses, (4) ability to induce a high level of intestinal immunity, and (5) the possibility of contact vaccination whereby vaccinated individuals may spread the vaccine virus resulting in secondary immunizations [17].

While the efficacy of OPV is generally excellent, it has been shown to induce a reduced immune response in some individuals living in regions where diahrreal disease is highly endemic. Recent work has traced the problem to the use of trivalent OPV. Studies now show that monovalent OPV can be used to achieve a high level of efficacy in the regions where standard trivalent OPV has been problematic [14]. Consequently, vaccine efficacy should not presently represent a concern for OPV.

The drawbacks of OPV are the risk of VAPP and the creation of cVDPVs. IPV, on the other hand, involves no risk of reversion as it is a killed virus. However, IPV has the disadvantages that it is roughly five times more expensive to produce [25], must be injected, cannot produce contact vaccinations, and is believed to induce a lower level of intestinal immunity [20]. Intestinal immunity is important as vaccinated individuals with no intestinal immunity can still have polio virus replicating in their intestines, and thus serve as carriers of the disease (in spite of being immune themselves). Recent studies show enhanced potency IPV (eIPV) provides improved intestinal immunity,

but eIPV is still believed to be inferior to OPV in this respect [20].

The creation of cVDPVs from OPV poses an obstacle to eventual polio eradication. Since 2000, four outbreaks of cVDPVs have been identified in Madagascar, the Philippines, Hispaniola and China [16]. In the cases of China and Hispaniola, these outbreaks occurred more than five years after the regions had been certified as polio free. It is important to note that detection of cVDPVs is complicated by the fact that most polio infections cause little or no illness: the ratio of paralytic to inapparent or asymptomatic polio has been estimated to be 1:200 [6, 16].

In this work we investigate an infectious disease transmission model that includes the possibility of reversion. We provide tools to assess the epidemiological impact of reversion, and the creation of cVDPVs, assuming the present polio vaccination strategy in developing countries (continuous OPV vaccination). We then address the problem of polio eradication, presenting three alternative polio eradication strategies involving both IPV and OPV and comparing their effectiveness. The mathematical model is built from the basic SIR model, which we review first. Although we focus on polio here, we emphasize that the model is relevant to many diseases for which live virus vaccines exist.

2.2 The Basic SIR Model

The basic Susceptible-Infected-Removed or SIR model is the simplest transmission model for diseases that confer lifelong immunity. In spite of its simplicity, it successfully predicts the shape of epidemic curves [18] and yields useful quantitative predictions of eradication thresholds [3].

We will assume initially that the population is sufficiently large that we can treat the number of individuals who are susceptible ($\tilde{S}$), infected ($\tilde{I}$) or removed ($\tilde{R}$) as continuous variables. Note that "infected" individuals are assumed to be infectious and "removed" individuals are immune to the pathogen. If a vaccine exists and a fixed proportion of individuals is vaccinated as soon as any maternally-acquired immunity has waned, the model can be written

$$\frac{d\tilde{S}}{dt} = (1-p)\nu N - \frac{\beta}{N}\tilde{I}\tilde{S} - \mu\tilde{S} \tag{2.1a}$$

$$\frac{d\tilde{I}}{dt} = \frac{\beta}{N}\tilde{I}\tilde{S} - (\mu+\gamma)\tilde{I} \tag{2.1b}$$

$$\frac{d\tilde{R}}{dt} = p\nu N + \gamma\tilde{I} - \mu\tilde{R} \tag{2.1c}$$

Here, the total population is $N = \tilde{S} + \tilde{I} + \tilde{R}$. The parameters of the model are the proportion vaccinated (p), the birth rate (ν, for *natality*), the transmission rate (β), the recovery rate (γ) and the natural death rate (μ, for *mortality*). The mean infectious period is $1/\gamma$. The model assumes that immunity is lifelong and that there is no disease-induced mortality (or that

disease-induced mortality is sufficiently rare that its dynamical effect is negligible). It should also be noted that individuals may be asymptomatic for part (or all) of the infectious period.

Equation (2.1) is forward invariant in the non-negative orthant $\{(\tilde{S}, \tilde{I}, \tilde{R}) \mid \tilde{S} \geq 0, \tilde{I} \geq 0, \tilde{R} \geq 0\}$, so initially non-negative solutions can never become negative. To see this, note that if $\tilde{S} = 0$ then $d\tilde{S}/dt \geq 0$ (and similarly for $\tilde{I}$ and $\tilde{R}$).

It is more convenient to work with the SIR model in terms of proportions of the population, so we apply the variable transformations

$$S = \frac{\tilde{S}}{N}, \qquad I = \frac{\tilde{I}}{N}, \qquad R = \frac{\tilde{R}}{N}. \tag{2.2}$$

If the population is constant (i.e., $\nu = \mu$, which is an excellent approximation when looking at short time scales) then equation (2.2) simply represents scaling by a constant. More generally, N will grow (or decay) at exponential rate $\nu - \mu$. Noting that

$$\frac{dX}{dt} = \frac{1}{N}\frac{d\tilde{X}}{dt} - \frac{\tilde{X}}{N^2}\frac{dN}{dt}, \tag{2.3}$$

where X is S, I or R, we obtain the SIR model in terms of proportions:

$$\frac{dS}{dt} = (1-p)\nu - \beta IS - \nu S \tag{2.4a}$$

$$\frac{dI}{dt} = \beta IS - \gamma I - \nu I \tag{2.4b}$$

$$\frac{dR}{dt} = p\nu + \gamma I - \nu R \tag{2.4c}$$

The forward invariance of equation (2.1) in the non-negative orthant implies that equation (2.1) is forward invariant in the simplex $\{(S,I) \mid 0 \leq S \leq 1, 0 \leq I \leq 1, 0 \leq S+I \leq 1\}$. Furthermore, as $S+I+R=1$, one of these equations is redundant, so we drop equation (2.1c).

In subsequent sections we will employ equations (2.1) to model continuous IPV vaccination, as reversion is not an issue for the killed virus vaccine.

2.2.1 Analysis of the basic SIR model

A key characteristic of an infectious disease in a given population is its basic reproductive ratio, $\mathcal{R}_0$, which is defined to be the average number of secondary infections caused by a single infected individual in a population with no immunity. $\mathcal{R}_0$ is the product of the transmission rate and the mean time that an individual is infectious, hence for the model given by equation (2.1) (with constant population)

$$\mathcal{R}_0 = \frac{\beta}{\gamma+\nu}. \tag{2.5}$$

System (2.4) has two equilibria. Denoting the equilibrium proportions of individuals that are susceptible and infected by S^* and I^*, respectively, the *disease free equilibrium* (DFE) is

$$S_1^* = 1 - p, \qquad I_1^* = 0\,. \tag{2.6}$$

The *endemic equilibrium* is

$$S_2^* = \frac{1}{\mathcal{R}_0}, \qquad I_2^* = \frac{\nu}{\gamma + \nu}\left(1 - \frac{1}{\mathcal{R}_0} - p\right)\,. \tag{2.7}$$

It is convenient to define two further dimensionless quantities in terms of the model parameters:

$$f = \frac{\nu}{\gamma + \nu}\,. \tag{2.8}$$

which is the mean time spent in the infected class as a fraction of mean life-span (assuming a constant population) and

$$p_{\text{crit}} = 1 - \frac{1}{\mathcal{R}_0}\,. \tag{2.9}$$

We can then express the endemic equilibrium as

$$S_2^* = \frac{1}{\mathcal{R}_0}, \qquad I_2^* = f\,(p_{\text{crit}} - p)\,, \tag{2.10}$$

from which we see that p_{crit} is the *critical vaccination level*: the endemic equilibrium exists (i.e., is positive and hence biologically meaningful) if and

only if $p < p_{\text{crit}}$. It can be shown that if the vaccination proportion $p \geq p_{\text{crit}}$ then the DFE is globally asymptotically stable (states near the DFE stay near the DFE and every solution eventually approaches the DFE). Similarly, if $p < p_{\text{crit}}$ then any initial condition with $I(0) > 0$ eventually converges to the endemic equilibrium [15, 19]. Biologically, p_{crit} is an eradication threshold: the disease will persist if and only if $p < p_{\text{crit}}$. Note that this critical vaccination proportion is determined solely by the basic reproductive ratio $\mathcal{R}_0$. The proportion of the population that is immune at a given time is often called the degree of *herd immunity*. Thus, p_{crit} is the level of herd immunity that must be maintained to prevent persistence should an eradicated disease be re-introduced.

2.3 The Live-Attenuated Vaccine Model: Modeling OPV

To account for the effects of a live-attenuated virus vaccine such as OPV, we assume a fixed proportion of those vaccinated will become infected by the revertant virus. All other vaccinations are taken to be successful at conferring immunity without illness. Leaving the other aspects of the SIR model intact, the new model can be depicted graphically as in Figure 2.1 and expressed

mathematically (in terms of *proportions* S, I and R) via

$$\frac{dS}{dt} = (1-p)\nu - \beta IS - \nu S \tag{2.11a}$$

$$\frac{dI}{dt} = \phi p\nu + \beta IS - \gamma I - \nu I \tag{2.11b}$$

$$\frac{dR}{dt} = (1-\phi)p\nu + \gamma I - \nu R \tag{2.11c}$$

Here ϕ is the *reversion factor*, i.e., the proportion of those vaccinated who become infected by the revertant virus ($0 < \phi \leq 1$). As in equation (2.4), equation (2.11c) is superfluous and we deal with the two-dimensional system defined by equations (2.11a) and (2.11b). Note that since the three types of polio do not interact immunologically, we have not included any strain structure in the model.

There has been considerable recent interest in models that include a separate compartment for vaccinated individuals [9], rather than simply the proportion vaccinated as specified by p in equation (2.11). A separate vaccinated compartment can be important if the vaccine has limited efficacy (or if vaccine-induced immunity wanes) because vaccinated individuals may remain (or become) partially susceptible. The "breakthrough infections" that occur in this situation typically lead to multiple endemic equilibria and backward bifurcations [9]. However, as mentioned in the introduction, OPV is highly efficacious and yields lifelong immunity, so we have not included a separate vaccinated compartment. Our reversion model formalizes the effect of immediate infection that results occasionally from vaccination, as opposed to

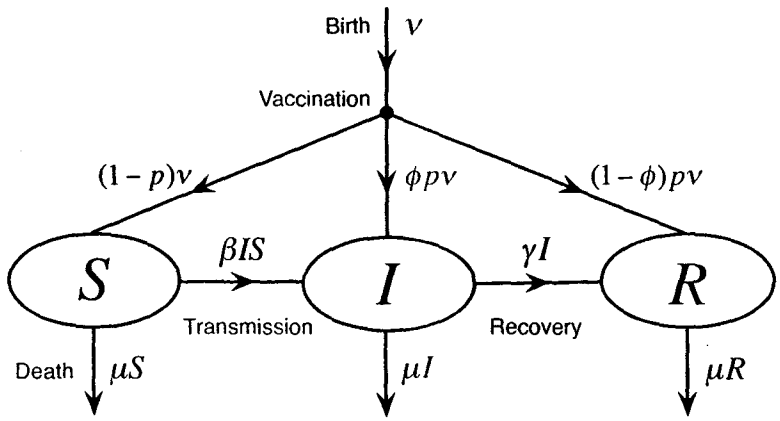

Figure 2.1: Flow diagram for the live-attenuated vaccine model that we use to investigate the effects of OPV on polio transmission. The flow diagram for the basic SIR model (equation 2.1) is obtained by setting the reversion factor ϕ to zero. The model (for any value of ϕ) is expressed in equation (2.11) in terms of *proportions* of the population that are susceptible, infectious or removed.

susceptibility to infection from subsequent exposures following vaccination.

2.3.1 Epidemiological parameters for Poliomyelitis

Epidemiological parameter estimates for poliomyelitis and OPV are given in Table 2.1. The vaccine reversion factor (ϕ) is estimated indirectly from two parameters that have been estimated previously: the mean number of paralytic polio cases as a proportion of total polio cases (π_{para}) and the incidence of paralytic polio in newly vaccinated infants (V_{infant}). Assuming that VAPP in infants really does result directly from vaccination (as opposed to contact with an infected individual) and that any increase in π_{para} with age can be

Table 2.1: Epidemiological Parameter estimates for Poliomyelitis.

Parameter	Symbol	Estimate	Source
Basic Reproductive Ratio	$\mathcal{R}_0$	6	[3]
Mean Infectious Period	$1/\gamma$	16 days	[3]
Birth Rate, developed countries	ν	$0.02\,\text{year}^{-1}$	[23, 5]
Birth Rate, developing countries	ν	$0.04\,\text{year}^{-1}$	[5]
$\frac{\nu}{\gamma+\nu}$, developed countries	f	8.76×10^{-4}	Equation 2.8 (§2.2.1)
$\frac{\nu}{\gamma+\nu}$, developing countries	f	1.75×10^{-3}	Equation 2.8 (§2.2.1)
Infant VAPP Incidence	V_{infant}	1/1400000	[6]
Paralytic Polio/Total Polio Cases	π_{para}	1/200	[6, 4]
OPV Reversion proportion	ϕ	10^{-4}	Equation 2.12 (§2.3.1)

ignored, the reversion proportion for OPV is

$$\phi = \frac{V_{\text{infant}}}{\pi_{\text{para}}} \approx 10^{-4}. \tag{2.12}$$

Note that since OPV contains attenuated versions of all three antigenic types, any of which may revert, we may treat ϕ as an upper bound for reversion in each type.

2.4 Analysis of the OPV model

2.4.1 Equilibria

Unlike typical epidemiological models, the OPV model (2.11) has no DFE. Instead, for any parameter set with $\phi > 0$, there is a single (endemic) equilibrium. Indeed, setting the derivatives to zero in equations (2.11a) and (2.11b)

and summing the resulting two equations yields

$$S^* = 1 - p(1-\phi) - \frac{1}{f} I^*, \tag{2.13}$$

where S^* and I^* denote equilibrium values. Inserting (2.13) into (2.11b) (set to zero) then yields

$$\frac{1}{f} I^{*2} - (p_{\text{crit}} - p(1-\phi))\, I^* - \frac{p\phi f}{\mathcal{R}_0} = 0. \tag{2.14}$$

Solving this quadratic for I^* (and insisting that it be non-negative) yields the unique solution

$$I^* = \frac{1}{2} f\,(p_{\text{crit}} - p(1-\phi)) + \sqrt{\left[\frac{1}{2} f\,(p_{\text{crit}} - p(1-\phi))\right]^2 + \frac{p\phi f^2}{\mathcal{R}_0}} \tag{2.15}$$

Note that $p_{\text{true}} = p(1-\phi)$ is the *true vaccination proportion*, i.e., the proportion of vaccinations that are successful. It is convenient to define

$$\Delta p = p_{\text{crit}} - p(1-\phi). \tag{2.16}$$

The equilibrium defined by equations (2.13) and (2.15) may then be more simply expressed as

$$S^* = 1 - p(1-\phi) - \frac{1}{2}\Delta p - \sqrt{\left[\frac{1}{2}\Delta p\right]^2 + \frac{p\phi}{\mathcal{R}_0}} \tag{2.17a}$$

$$I^* = f\left[\frac{1}{2}\Delta p + \sqrt{\left[\frac{1}{2}\Delta p\right]^2 + \frac{p\phi}{\mathcal{R}_0}}\right] \tag{2.17b}$$

This equilibrium is always biologically meaningful: it can be shown that (S^*, I^*) lies in the region $\{(S, I) : S > 0, I > 0, S + I < 1\}$ if $0 < p < 1$ and $0 < \phi \leq 1$ (see appendix 2.7).

2.4.2 Stability

In this section we show that the equilibrium (2.17) is globally asymptotically stable. Biologically, this means that regardless of the proportions of the population that are susceptible (S), infectious (I) and immune (R), the model predicts the virus will persist and approach the endemic prevalence level given by (2.17b).

We begin by considering how the system behaves if it is perturbed slightly away from the equilibrium. We show that the equilibrium (S^*, I^*) is not only locally stable but always hyperbolic, i.e., that the Jacobian matrix of the system at (S^*, I^*) never has eigenvalues with zero real parts. Hyperbolic stability implies that for any initial conditions sufficiently close to the equilibrium, the solution trajectory converges exponentially to the equilibrium.

Local Stability

Linearizing equations (2.11a) and (2.11) about the equilibrium (2.17) and computing the Jacobian matrix we find

$$J = \begin{pmatrix} -\beta I^* - \nu & -\beta S^* \\ \beta I^* & \beta S^* - (\gamma + \nu) \end{pmatrix} \tag{2.18}$$

If $\phi = 0$, the system (2.11) reduces to the standard SIR model (2.1) and the equilibrium given by equations (2.) corresponds to either the endemic equilibrium (2.6) of the standard SIR model (for $p < p_{\text{crit}}$) or the DFE (2.10) of the standard SIR model (for $p \geq p_{\text{crit}}$). In either case, the equilibrium in question is locally asymptotically stable and, provided $p \neq p_{\text{crit}}$, it is hyperbolic [15] (J has no eigenvalues on the imaginary axis). If $p = p_{\text{crit}}$ then the DFE of the standard SIR model ($\phi = 0$) is locally asymptotically stable but non-hyperbolic.

The eigenvalues of J can be written

$$\lambda_{\pm} = \frac{\gamma + \nu}{2} \Big\{ -(1+f) + \mathcal{R}_0(S^* - I^*) \pm \sqrt{[\mathcal{R}_0(S^* + I^*) - (1-f)]^2 - 4\mathcal{R}_0^2 S^* I^*} \Big\}. \tag{2.19}$$

Note that the dependence of these eigenvalues on ϕ is hidden in the expressions for S^* and I^* (equation 2.17). Since $\lambda_{\pm}$ depend continuously on ϕ, to prove hyperbolic stability of the equilibrium (2.17) for any $\phi > 0$ and

$p \neq p_{\text{crit}}$ it suffices to show that no eigenvalue of J crosses the imaginary axis as ϕ is varied, for an arbitrary fixed $p \neq p_{\text{crit}}$. Given this, and the fact that the eigenvalues of J are also continuous functions of p, it will follow that the equilibrium is hyperbolically stable also for $p = p_{\text{crit}}$ if we can show that J cannot have an eigenvalue with zero real part for any $\phi > 0$.

Eigenvalues may cross the imaginary axis either at 0 or at Ai where $A \neq 0$. We treat these cases separately. Suppose first that 0 is an eigenvalue of J. Then the determinant of J must be zero, i.e.,

$$\beta I^*(\nu + \gamma) - \nu\beta S^* + \nu(\nu + \gamma) = 0\,. \tag{2.20}$$

Using equation (2.13) to write S^* in terms of I^*, and after some algebraic manipulation, we find

$$\frac{2}{f} I^* = \Delta p\,. \tag{2.21}$$

Inserting (2.17b) for I^* into (2.21) yields

$$\sqrt{\left(\frac{1}{2} f \Delta p\right)^2 + \frac{p\phi f^2}{\mathcal{R}_0}} = 0 \tag{2.22}$$

But this is impossible for $\phi > 0$, so J does not have a zero eigenvalue.

Now suppose that J has a purely imaginary eigenvalue Ai. Then

$$\det(J - Ai\mathbb{I}) = (-\beta I^* - \nu - Ai)(\beta S^* - (\nu + \gamma) - Ai) = 0\,, \tag{2.23}$$

where $\mathbb{I}$ is the 2×2 identity matrix. Examining the imaginary part of equation (2.23) and simplifying yields

$$-I^* - \frac{\nu}{\beta} + S^* - \frac{1}{\mathcal{R}_0} = 0 \tag{2.24}$$

Using (2.13) to express S^* in terms of I^* and rearranging yields

$$(1 + \frac{1}{f})I^* + \frac{\nu}{\beta} = p_{\text{crit}} - p_{\text{true}}. \tag{2.25}$$

As $I^* > 0$, the left hand side of (2.25) is strictly positive. Thus if $p_{\text{crit}} \leq p_{\text{true}}$ we have a contradiction. If $p_{\text{crit}} > p_{\text{true}}$ then from equation (2.17b) it is apparent that if $\phi > 0$ then $I^* > f\Delta p = f(p_{\text{crit}} - p_{\text{true}})$. Substituting this inequality into equation (2.25) gives a left hand side that is strictly greater than $p_{\text{crit}} - p_{\text{true}}$, and we have a contradiction.

Thus, the eigenvalues of J do not cross the imaginary axis for any $\phi > 0$, and the endemic equilibrium given by equation 2.17 is hyperbolically, and hence locally asymptotically stable.

Global Stability

As the system is two-dimensional, global asymptotic stability can be established by applying Poincaré-Bendixson theory and Dulac's Criterion [26].

Consider an autonomous system of ordinary differential equations,

$$\frac{dx}{dt} = f(x, y) \tag{2.26a}$$

$$\frac{dy}{dt} = g(x, y) \tag{2.26b}$$

where f and g are continuously differentiable, and suppose that D is a bounded region in the plane such that there exists a single stable equilibrium point of (2.26) in the closure of D. If a given orbit remains in D for all $t > 0$ then the Poincaré-Bendixson theorem says that the orbit must either have a non-trivial periodic orbit as its ω-limit set or tend asymptotically to the equilibrium.

Dulac's Criterion states that given a simply connected region D in the plane, with f and g continuously differentiable as above, if there exists a continuously differentiable function $C(x, y)$ such that the divergence of the vector field $\partial_x(Cf) + \partial_y(Cg)$, is not identically zero and does not change sign in D, then there can be no non-trivial periodic orbits contained in D.

Our live-attenuated virus model is a two-dimensional system with orbits bounded (in forward time) in the closure of the triangular region whose boundary is formed by the lines $S \equiv 0$, $I \equiv 0$ and $S + I = 1$ (as discussed for the basic SIR model in §2.2). In fact, we have the stronger condition that the interior of this set, which we denote as $\mathcal{B} = \{(S, I) \mid S > 0, I > 0, S + I < 1\}$, is forward invariant and for all initial conditions on its boundary the flow is into $\mathcal{B}$ (see Appendix 2.9). There is one (hyperbolically) stable equilibrium

point in the closure of $\mathcal{B}$, located in $\mathcal{B}$ itself (see Appendix 2.7), and given by equation (2.17). The functions $f(S, I)$ and $g(S, I)$ given by (2.11a) and (2.11b) are infinitely differentiable with respect to both S and I. Therefore, applying the Poincaré-Bendixson theory, any orbit must be periodic, have another non-trivial periodic orbit as its ω-limit set, or tend asymptotically to the equilibrium (2.17). To establish that every orbit must in fact tend to the equilibrium, we rule out the existence of periodic orbits in the closure of $\mathcal{B}$ using the Dulac function

$$C(S, I) = \frac{1}{I} \tag{2.27}$$

Notice that $C(S, I)$ is infinitely differentiable in $\mathcal{B}$. Therefore, applying Dulac's criterion yields

$$\partial_S\Big(C(S, I)\frac{dS}{dt}\Big) + \partial_I\Big(C(S, I)\frac{dI}{dt}\Big) = -\frac{(I^2\beta + \nu I + p\phi\nu)}{I^2} \tag{2.28}$$

Equation (2.28) is strictly negative for all points in $\mathcal{B}$. Hence, no periodic orbits can exist and by the Poincaré-Bendixson theorem, all orbits must converge to the (hyperbolically) stable equilibrium (2.17).

Damping Frequencies and Rate of Convergence for Polio

Damping Frequencies Figure 2.2 shows the frequency of damped oscillations onto the equilibrium (2.17) as a function of the vaccination proportion p. The birth rate used is representative of developed countries (Table 2.1). The dashed curve shows the results in the case of zero reversion ($\phi = 0$),

corresponding to the standard SIR model, while the solid curve shows results for the estimated OPV reversion proportion ($\phi = 10^{-4}$, Table 2.1). The damping frequency F_{damp} is given by

$$F_{\text{damp}} = \left| \Im \left(\frac{\lambda}{2\pi} \right) \right| , \tag{2.29}$$

where λ is either of the two eigenvalues given in equation (2.19).

Figure 2.2 illustrates that for the estimated value of ϕ and other epidemiological parameters corresponding to polio (Table 2.1), the difference in the frequency of damped oscillations compared to zero reversion is negligible. The maximum difference occurs near the SIR model's eradication threshold, $p \approx 0.83$. As p is increased , the DFE ( ) changes from unstable to globally asymptotically stable. The solid curve in Figure 2.2 shows a frequency $F_{\text{damp}} = 0$ for $p \geq 0.83$. Note that the DFE is never approached by damped oscillations.

While the unique equilibrium of the live-attenuated vaccine model (2.17) is always endemic (and stable), the manner in which it is approached parallels the distinct behaviours near each of the stable equilibria of the standard SIR model. Figure 2.2 shows that there is a threshold level of vaccination below which the endemic equilibrium is reached by damped oscillations, and above which there is no oscillatory behaviour. This threshold is lower than the SIR model's threshold ≈ 0.83, though for $\phi = 10^{-4}$ the difference between the thresholds is only 0.4%. Numerical explorations like in Figure 2.2 for a

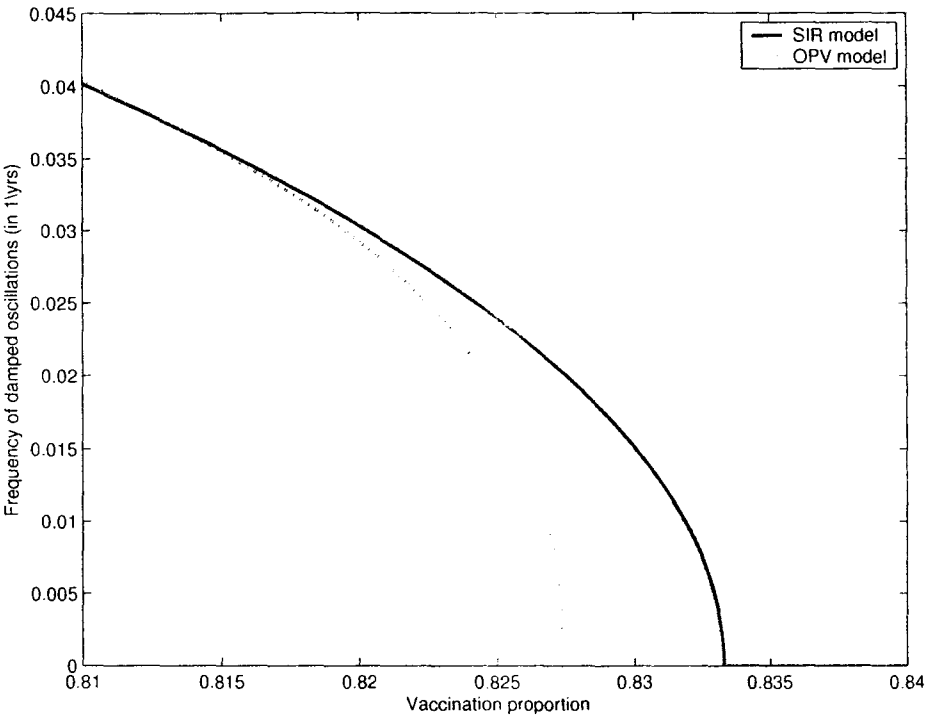

Figure 2.2: Frequency of damped oscillations (F_{damp}, Eq. 2.29) about the globally asymptotically stable endemic equilibrium (2.17) of the OPV model (2.11) and the reversion-free SIR polio model, as a function of vaccination proportion (p). The curves are shown only over the narrow range of p for which there is a non-negligible difference in the damping frequencies for the two models. Parameter values, including the estimated OPV reversion proportion (ϕ), are given in Table 2.1 (the birth rate is that listed for developed countries). For these parameters both models exhibit a vaccination threshold beyond which the globally stable equilibrium is no longer reached by damped oscillations. The threshold is slightly below p_{crit} for the SIR model. Increasing the value of the reversion proportion ϕ leads to a decrease in this threshold value. For the estimated value of $\phi \simeq 10^{-4}$ (Table 2.1) this decrease represents only a 0.4% reduction from $p \approx 0.83$ in the reversion-free model. Similar results are obtained if the OPV reversion proportion is taken an order of magnitude higher: $\phi \simeq 10^{-3}$ yields a threshold of $p \simeq 0.81$.

wide range of reversion proportions ($10^{-6} \leq \phi \leq 10^{-2}$) indicate that there is a threshold value p_{damp} such that damped oscillations occur if and only if $p < p_{\text{damp}}$. Moreover, p_{damp} decreases as ϕ is increased.

Rate of Convergence To quantify the attractivity of the (globally stable) equilibrium of the OPV model (2.11), Figure 2.3 shows the minimal rate of convergence of solutions in a sufficiently small neighbourhood of the equilibrium (2.17), as a function of the vaccination proportion p. The dashed curve shows the convergence rate for the estimated OPV reversion proportion ϕ (Table 2.1), while the solid curve shows the convergence rate for the case of no reversion ($\phi = 0$), which corresponds to the standard SIR model. The minimal rate of convergence is calculated as

$$r_{\text{min}} = \min\{-\Re(\lambda_+), -\Re(\lambda_-)\} \tag{2.30}$$

where $\lambda_\pm$ are the eigenvalues given in Eq. (2.19). Note that in the zero reversion case, the convergence rate shown is always to the globally asymptotically stable equilibrium (the endemic equilibrium for $p < p_{\text{crit}}$ and the DFE for $p \geq p_{\text{crit}}$).

Figure 2.3 shows that for the estimated value of the OPV reversion proportion (Table 2.1) the rate of convergence onto the globally asymptotically stable equilibrium (2.17) differs negligibly from the rate for the standard SIR polio model when the vaccination proportion is either significantly greater or significantly smaller than the theoretical SIR eradication threshold p_{crit}.

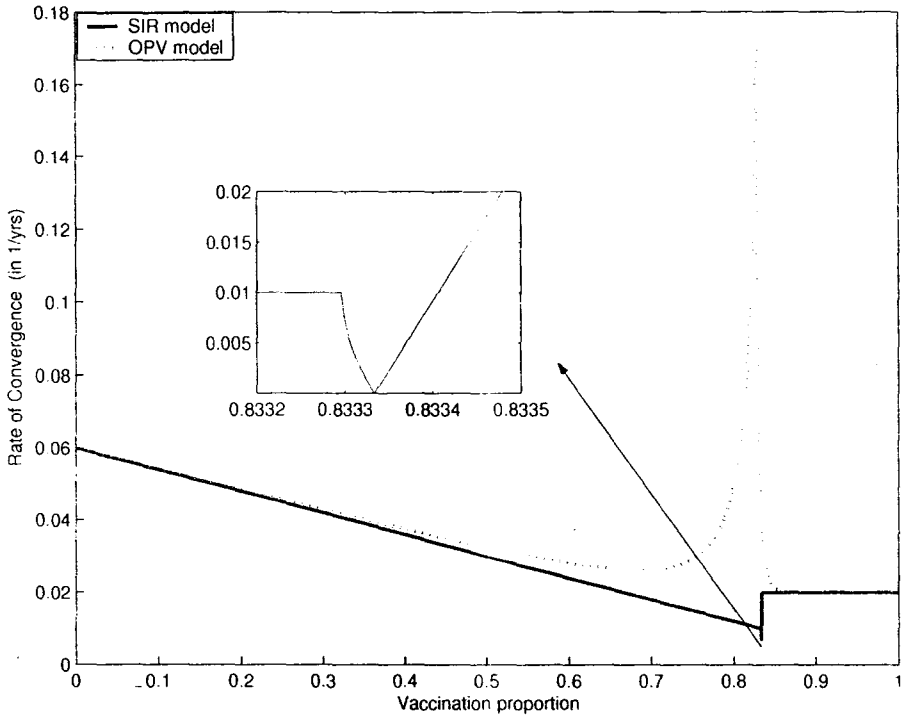

Figure 2.3: Local minimum rate of convergence ($r_{\min}$, Eq. 2.30) of solutions to the globally asymptotically stable equilibrium for the OPV polio model and the standard SIR polio model without vaccine reversion, as a function of vaccination proportion p. Values of parameters, including the estimated OPV reversion proportion ϕ are given in Table 2.1. Birth rates used are for developed countries. For high and low levels of vaccination the local rates of convergence are very similar. However, as the vaccination proportion is increased towards the theoretical vaccination threshold for the SIR polio model, $p_{\text{crit}} \approx 0.83$, the rate for OPV increases sharply to a maximum followed by an equally sharp decrease to rates comparable to those in the SIR polio model. It should be noted that as $p = p_{\text{crit}}$ is a point of stability exchange between the endemic equilibrium and disease free equilibrium in the SIR model, the rate of convergence is zero at this point.

However, when p approaches p_{crit}, the rate of convergence for the OPV model increases sharply, attaining a maximum, and then sharply decreases to the levels of the SIR polio model. In contrast, in the SIR model, as there is an exchange of stability between the endemic and the disease free equilibrium at $p = p_{\text{crit}}$, the rate of convergence is near zero for p in a neighbourhood of p_{crit}. When the reversion proportion ϕ is taken orders of magnitude higher or lower, results are qualitatively similar. As ϕ is increased, the maximum value of the rate r_{min} is increased and attained at a lower vaccination proportion p.

2.4.3 Implications for Continuous OPV Vaccination

Figure 2.4 shows, as a function of the vaccination proportion p, the predicted equilibrium number of infectives and annual expected cases of paralytic polio in a (constant) population of one hundred million (i.e., I^*N with I^* from Eq. (2.17b) and $N = 10^8$). Since the mean time spent in the infected class is $1/(\gamma + \nu)$, and the probability that polio will become paralytic is π_{para} (Table 2.1), the number of cases of paralytic polio expected in time T as a proportion of the population is

$$P(T) = \pi_{\text{para}} I^* (\gamma + \nu) T \tag{2.31}$$

The solid curve in Figure 2.4 is based on the parameter estimates in Table 2.1 (birth rates used are for developed countries), whereas the dotted (dashed)

curve uses a value of ϕ that is an order of magnitude below (above) the estimated value. Note that the range of p shown in Figure 2.4 is mostly beyond the eradication threshold for the standard SIR ($p_{\text{crit}} \approx 0.83$).

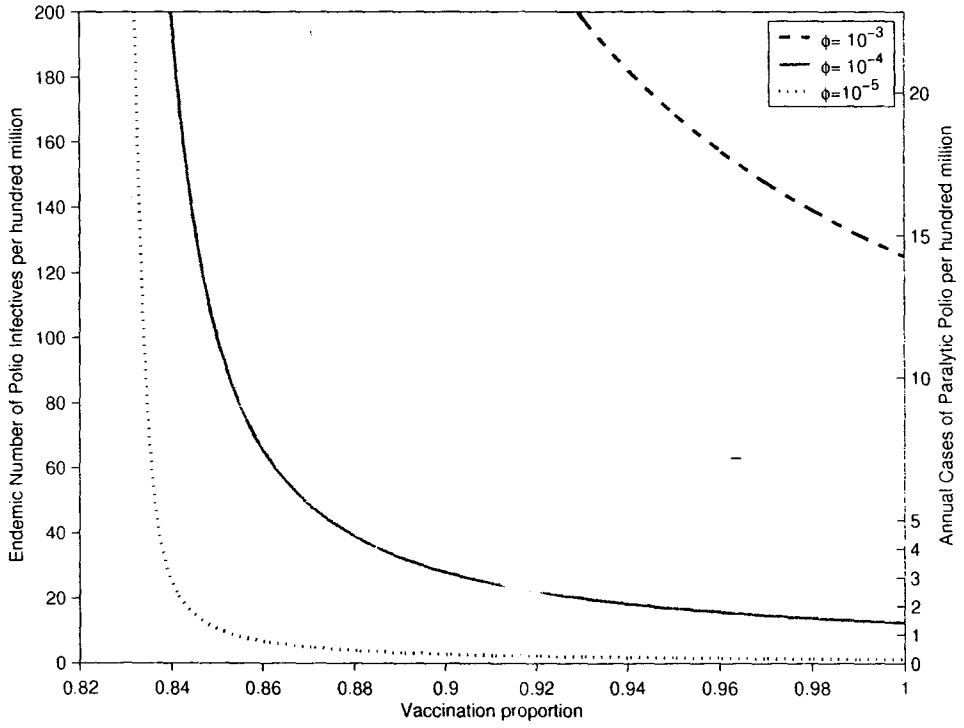

Figure 2.4: Equilibrium number of infectives and expected cases of Paralytic Polio annually per hundred million population as a function of OPV vaccination proportion p, for $p > 0.82$ The solid line represents results for the estimated value of the reversion proportion, $\phi \approx 10^{-4}$. A small but significant endemic level of the disease is predicted. Dashed lines represent reversion proportions an order of magnitude above and below the estimated value (10^{-3} and 10^{-5}). Note that for the standard SIR model, eradication of the disease is predicted for all $p > p_{\text{crit}} \approx 0.83$.

For the estimated value of the reversion factor ($\phi \sim 10^{-4}$), Figure 2.4 indicates that even in a population with 90–95% vaccination coverage the

model predicts persistence of the disease at an endemic level of 20 to 30 infected individuals per hundred million, and an event rate of two or three cases of paralytic polio per hundred million per year. This prediction agrees closely with the observed event rate in the United States from 1988 to 2000 when OPV was in use (8–10 cases of paralytic polio annually in a population $\sim$ 300 million; [6]). This agreement suggests that the estimated ϕ is of the right order of magnitude, since the event rate predicted in Figure 2.4 is sensitive to ϕ.

The main purpose of the OPV model (2.11) is to help understand the significance of emergent cVDPVs. This is perhaps best illustrated in Figure 2.5, which shows the difference between the endemic number of infectives predicted by the OPV model, Eq. (2.15), and the number of infectives predicted by the standard SIR model, Eq. (2.6) or (2.10) (the SIR endemic level is also plotted for comparison). For $p \lesssim 0.75$, the difference is negligible (two orders of magnitude smaller than the number of infectives predicted by the standard SIR model). The difference is maximal ($\sim$ 380 per hundred million population) for $p = 0.83 \approx p_{\text{crit}}$, the eradication threshold in the absence of reversion.

We infer that for levels of vaccination even five percent below the theoretical eradication threshold in the absence of reversion (p_{crit}), the impact of cVDPVs is likely to be negligible compared to the impact of the native viruses. Consequently, if coverage levels cannot be brought close to p_{crit} then use of OPV is likely to be easy to justify. However, in situations like the

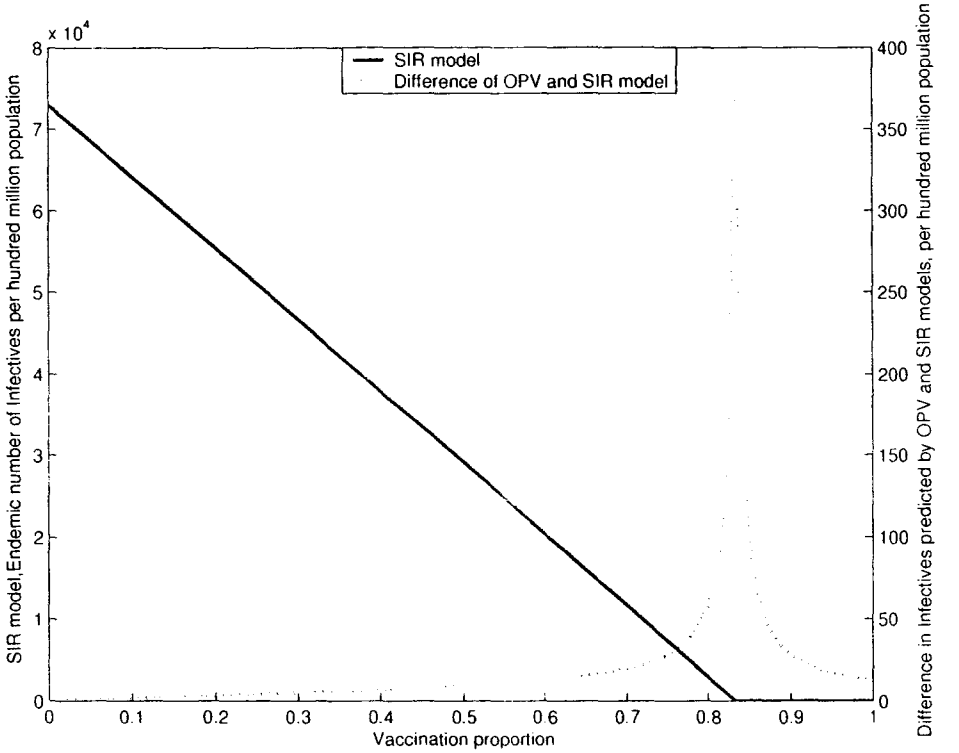

Figure 2.5: Effects of reversion on the endemic number of infective individuals at equilibrium. The solid line shows, as a function of vaccination proportion p, the predicted endemic equilibrium for the standard SIR model (2.1) (which may be thought of as a model of IPV vaccination or a theoretical OPV that never reverts). The dotted curve shows the difference between the predicted endemic number of infectives in the (continuous) OPV vaccination model (2.17) (with reversion) and the standard SIR model. For vaccination levels even five percent below $p_{\text{crit}} \approx 0.83$, the effect of reversion is negligible. As the vaccination level approaches p_{crit}, the reversion-free SIR model predicts eradication of the disease, while the OPV model with reversion predicts a small but significant endemic level of the disease (note the different scales on the left and right axes of the plot). For the estimated parameters in Table 2.1, the difference between the models is maximized near p_{crit}, though this is not the case for much larger values of the reversion proportion ϕ.

present, where coverage levels reaching p_{crit} are plausibly within reach, it appears that OPV can itself become the primary impediment to eradication.

It should be noted that although Figures 2.4 and 2.5 are plotted using birth rates for developed countries (Table 2.1), the shape of the curves is practically invariant to the birth rate ν. To see this, note that the equations for the proportion of infected individuals at the endemic equilibrium in the SIR model (2.6) and the equilibrium in the OPV model (2.17b) scale linearly with f (2.8) and are otherwise independent of ν (notwithstanding the negligible dependence of $\mathcal{R}_0$ on ν). Thus Figures 2.4 and 2.5 will scale essentially linearly with birth rates (for birth rates in a realistic range). For example, to produce these figures for birth rates representative of developing countries (Table 2.1) one need only scale both vertical axes by a factor of 2.

Sensitivity to Distribution of Infectious Period

In both the SIR model (2.4) and our OPV reversion model (2.17), there is an implicit assumption that infectious periods are exponentially distributed. This assumption is usually made in epidemiological modelling because it greatly simplifies the mathematical formulation, yielding a small system of ordinary differential equations. For arbitrary distributions of stage durations, the models become more complex systems of integro-differential equations [22].

In general, real distributions of infectious periods are not well-fitted by exponential distributions [21]. In the context of OPV, there is one poten-

tially advantageous aspect of the exponential distribution: its extremely long tail, i.e., finite probability of individuals remaining infectious for an extremely long time. This may be reasonable for polio because some individuals (with severely compromised immune systems) have been observed to shed poliovirus for extremely long periods [7]. Nevertheless, the existence of chronic shedders is unlikely to result in a precisely exponential distribution of infectious periods.

Does the implicit assumption of an exponential distribution of infectious periods affect our conclusions? To address this, we examine how the predicted endemic level of infectives (2.17b) changes as the shape of the infectious period distribution is changed from extremely broad (exponential) to extremely narrow (almost no variation about the mean infectious period, $1/\gamma$).

We suppose the distribution of infectious periods is a Gamma distribution Gamma$(n, \frac{1}{n\gamma})$, with mean $1/\gamma$ and shape parameter n. The probability density for the distribution Gamma$(n, \frac{1}{n\gamma})$ is

$$g(x; n, \frac{1}{n\gamma}) = \frac{x^{n-1}(n\gamma)^n e^{-n\gamma x}}{\Gamma(n)}, \qquad x > 0. \tag{2.32}$$

For $n = 1$ we obtain the exponential distribution and the limit $n \to \infty$ yields a Dirac delta distribution. The probability densities for several values of n are shown in Figure 2.6a.

For integer n, a standard trick [2, 8, 21] allows us to express our OPV

model as a system of $n+1$ ordinary differential equations:

$$\frac{dS}{dt} = (1-p)\nu - \beta IS - \nu S \tag{2.33a}$$
$$\frac{dI_1}{dt} = \phi p\nu + \beta IS - (n\gamma + \nu)I_1 \tag{2.33b}$$
$$\frac{dI_2}{dt} = n\gamma I_1 - (n\gamma + \nu)I_2 \tag{2.33c}$$
$$\vdots \qquad\qquad \vdots$$
$$\frac{dI_n}{dt} = n\gamma I_{n-1} - (n\gamma + \nu)I_n \tag{2.33d}$$
$$\frac{dR}{dt} = (1-\phi)p\nu + n\gamma I_n - \nu R \tag{2.33e}$$

Here, the proportion of infectious individuals is $I = \sum_{k=1}^{n} I_k$ and the new infectious subclasses I_k represent a mathematical device with no intended biological interpretation.

In Appendix 2.8, we show that Eq. (33) has a unique endemic equilibrium for any n (not just the case $n = 1$ as considered in previous sections). We computed this endemic equilibrium using the estimated OPV parameters (Table 2.1), for a large range of shape parameters from $n = 1$ to 1000. For each n, we verified that the equilibrium is locally stable by numeric computation of the eigenvalues (using the MATLAB function `eig`).

Figure 2.6b shows the relationship between the equilibrium endemic level of infection (I^*) and the shape parameter (n) for a specific vaccination proportion ($p = 0.85$). For this particular p. it is clear that the effect of distribution shape on I^* is negligible. More generally, for any $p \in [0, 1]$, I^* varies

by less than 0.1% if n is varied from 1 to 1000. Thus the predicted endemic level appears to be robust with respect to the distribution of the infectious period.

2.5 Final Eradication Strategies

It is not likely to be possible to eradicate polio using a continuous OPV vaccination strategy, because a continuous source of infectives is inevitable (as a result of reversion). We therefore explore the benefits of several alternative polio vaccination strategies that may eliminate the continuous source of new infectious individuals:

1. Pulsed OPV vaccination. Mass vaccinations are to be performed at regular intervals such as every year or every other year [1, 24]. A revised model incorporating pulsed vaccination is described below.

2. Switch to continuous IPV vaccination. The standard SIR model is appropriate for IPV because there is no reversion.

3. One-time mass vaccination with IPV. While continuous IPV vaccination at a high level may not be financially and logistically feasible, given a high level of herd immunity following a broad OPV vaccination program, a single mass IPV campaign might be sufficient to extinguish the disease. The model required is just a simplification of the pulsed vaccination model (without repeats).

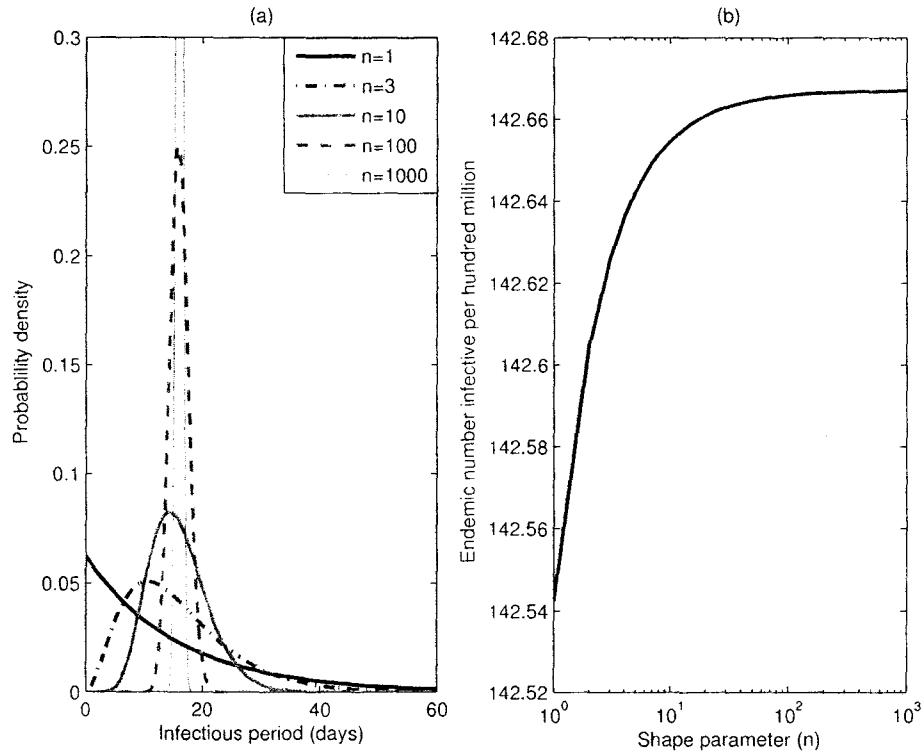

Figure 2.6: The effect of the shape of the infectious period distribution on the endemic level of infection in the OPV model (see §2.1.3 and Appendix 2.8). (a) Probability density functions for Gamma distributions with mean $\frac{1}{\gamma} = 16$ days and shape parameter n (see Eq. 2.32). Note that $n = 1$ yields the exponential distribution. For $n = 1000$ the peak density value is 0.789. (b) Endemic number of polio infectives per hundred million as a function of distribution shape, for fixed vaccination proportion $p = 0.85$. Epidemiological parameters are as given in Table 2.1 for developing countries. For fixed mean infectious period, the shape of the full distribution of infectious periods has a negligible effect on the endemic level of polio infection.

Since genuine eradication means reducing the infective population to zero, the problem can be properly addressed only in a stochastic setting with finite populations. After introducing a model for pulsed vaccination, we turn to stochastic simulations to investigate the above three proposed polio eradication strategies.

2.5.1 Pulse Vaccination Models

A pulsed version of our live-attenuated vaccine model (2.11) can be expressed as the following set of impulsive differential equations.

$$\frac{dS}{dt} = \nu - (\beta I + \nu)S - p_{\text{pulse}} \sum_n S(nT^-)\delta(t - nT) \tag{2.34a}$$

$$\frac{dI}{dt} = \beta IS - (\nu + \gamma)I + \phi p_{\text{pulse}} \sum_n S(nT^-)\delta(t - nT) \tag{2.34b}$$

$$\frac{dR}{dt} = \gamma I + (1 - \phi)p_{\text{pulse}} \sum_n S(nT^-)\delta(t - nT) - \nu R \tag{2.34c}$$

$$S(nT^-) = \lim_{\varepsilon \to 0^+} S(nT - \varepsilon) \tag{2.34d}$$

where the sums are over all non-negative integers n. In this pulsed model, vaccinations are performed only at intervals of period T, not continuously. At each pulse time, a proportion p_{pulse} of the susceptible population receives the vaccine. The above equations generalize the pulse vaccination model of Stone and colleagues [27] to include the reversion factor ϕ.

If there is only one pulse (at time T), and we consider IPV (no reversion),

then the equations simplify to

$$\frac{dS}{dt} = \nu - (\beta I + \nu)S - p_{\text{pulse}} S(T^-)\delta(t-T) \tag{2.35a}$$

$$\frac{dI}{dt} = \beta IS - (\nu + \gamma)I \tag{2.35b}$$

$$\frac{dR}{dt} = \gamma I + p_{\text{pulse}} S(T^-)\delta(t-T) - \nu R \tag{2.35c}$$

$$S(T^-) = \lim_{\varepsilon \to 0^+} S(T-\varepsilon) \tag{2.35d}$$

2.5.2 Stochastic Simulations

Eqs. (2.4),(2.31), and (2.35), represent deterministic models that can be used to explore the three proposed alternative vaccination strategies. However, integrating the differential equations will not allow us to estimate the probability that a given strategy will successfully lead to polio eradication. To that end, we recast these models as continuous time Markov processes, which are fully stochastic and involve finite populations. We use the standard Gillespie algorithm [13], in which the various terms in the differential equations are interpreted as event rates for the various Markov processes involved. (Figure 2.1 shows all the state transitions that occur, with their rates.)

We are thinking of each of the three proposed strategies as final eradication strategies after a normal, continuous OPV vaccination program has come as close as possible to eradication. Therefore, we take as the initial conditions for our simulations the equilibrium of our model (2.11) with an assumed OPV coverage level $p = 0.85$ (slightly above the eradication thresh-

old in the absence of reversion, $p_{\text{crit}} \simeq 0.83$). In all simulations we used a population of one hundred million ($N = 10^8$), and the birth rate was taken to be representative of the developing world (Table 2.1). The pulsing period was taken to be one year ($T = 1\,\text{yr}$) and the first pulse was applied immediately after ceasing the continuous OPV program. The one-time IPV vaccination was also applied immediately after ceasing OPV vaccination. The pulse vaccination proportion p_{pulse} in Eq. (2.34) was varied over the range 0–0.35 while p_{pulse} in Eq. (2.35) was varied over the range 0–0.40.

Pulsed OPV versus continuous IPV.

Figure 2.7 shows, for the strategies of pulsed OPV and continuous IPV vaccination in a developing region, the probability of polio eradication within four years as a function of the effective number of vaccinations performed. Here we define the effective number to be the number of vaccinations performed on susceptible individuals, noting that under a realistic pulse vaccination strategy one might expect the true number of vaccinations to exceed the effective number due to duplicate vaccinations. It should be noted that this definition of effective number has no relationship to reversion. In order to simplify the comparison of the continuous and pulse vaccination strategies, we introduce the idea of the effective vaccination *proportion* for a pulse vaccination strategy, which can be expressed as follows:

$$p_{\text{eff}} = \frac{\overline{V}(T)}{TN\nu} \tag{2.36}$$

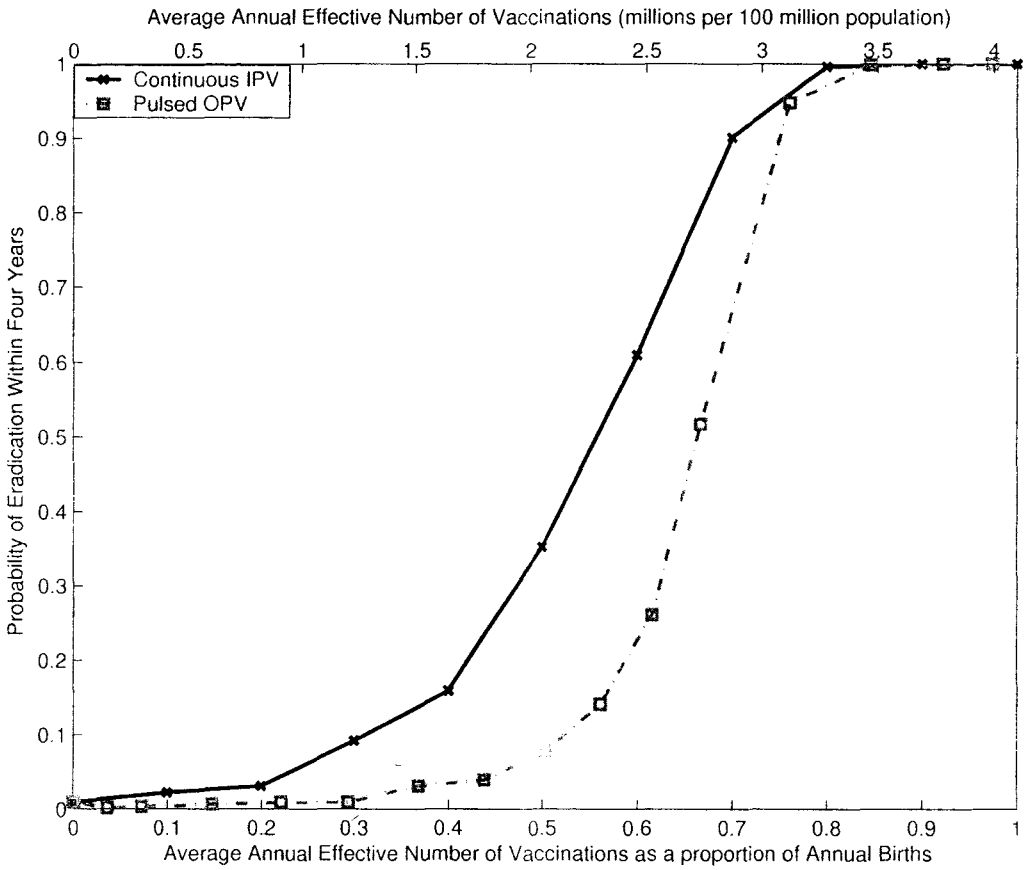

Figure 2.7: Probability of Polio eradication within 4 years as a function of the average annual effective number of vaccinations, for annually pulsed OPV (dashed curve) and continuous IPV vaccination (solid curve) in a population of one hundred million (with birth rates typical of developing countries; Table 2.1). The lower horizontal axis gives the average annual effective number of vaccinations as a proportion of the average annual births as defined by p_{eff} in Eq. (2.36) (for $T = 1$). For continuous vaccination this reduces to the vaccination proportion p in Eq. (2.1). The upper horizontal axis gives the raw annual average number of vaccinations (in millions per 100 million population). Continuous IPV campaigns are successful for moderate vaccination coverage ($p_{\text{eff}} \gtrsim 0.7$). For very low vaccination coverage ($p_{\text{eff}} \lesssim 0.3$) pulsed OPV campaigns are no better than ceasing vaccination altogether, due in part to the introduction of infectives through vaccination. However, pulsed OPV can also be successful if a moderate coverage level is achieved ($p_{\text{eff}} > 0.75$), though the vaccination level required is greater than that required for continuous IPV.

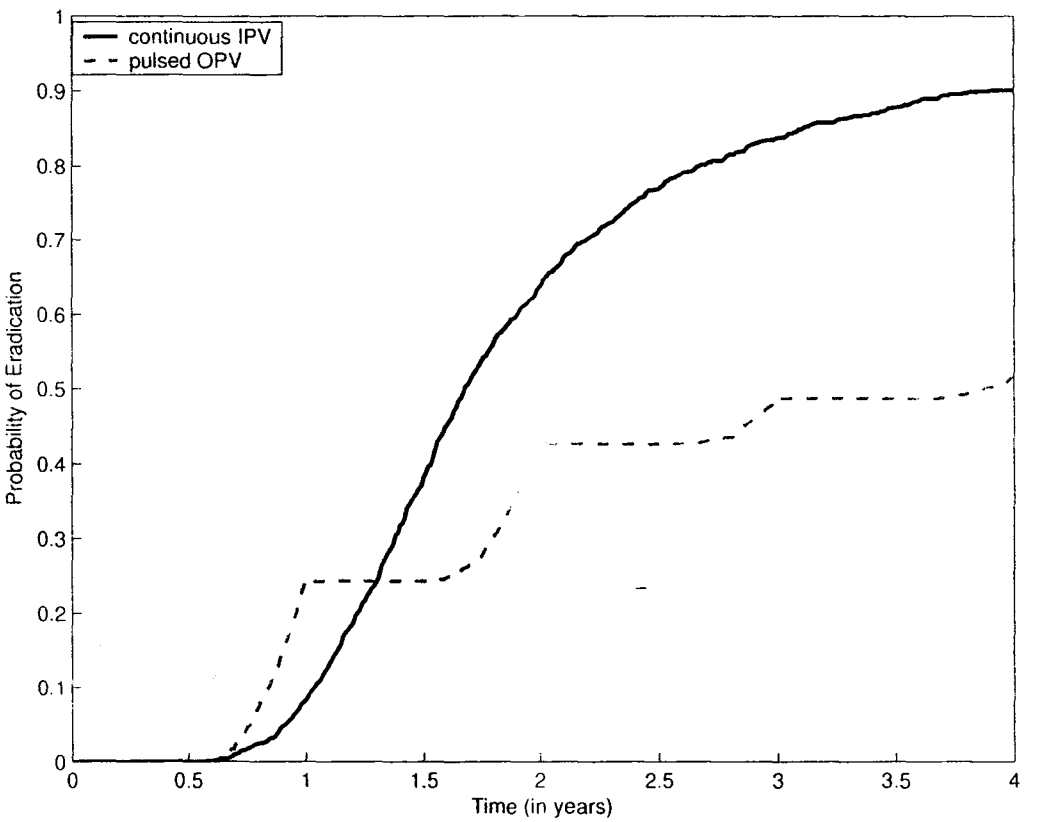

Figure 2.8: Probability of Polio eradication as a function of time for a 4 year continuous IPV vaccination program with vaccination proportion $p = 0.7$ (solid curve) and pulse OPV with vaccination parameter $p_{\text{pulse}} = 0.2$ and pulse period $T = 1\text{yr}$, corresponding to $p_{\text{eff}} \simeq 0.7$ (see Eq. 2.36). The population size is one hundred million with birth rates typical of developing countries (Table 2.1). Nonzero probability of eradication is apparent slightly after half a year for both strategies. For OPV pulses, there is little increase in eradication probability for roughly half a year following each pulse, due to the pulse introducing a significant number of infectives via vaccine reversion. It should be noted that both strategies exhibit quickly diminishing returns, with the bulk of eradications occurring within the first two years of simulations.

where T is the pulsing period, $\overline{V}(T)$ is the average effective number of vaccinations per pulsing period, N is the population size and ν is the birth rate. Thus, under this definition, a continuous vaccination strategy with vaccination proportion $p = p_{\text{eff}}$ would vaccinate the same number of individuals as the corresponding pulse strategy in a given pulsing period.

Substantial effects of stochasticity are evident in Figure 2.7. Even if we cease vaccination altogether (left limit of Figure 2.7) there is a non-zero probability that polio will go extinct within four years. In developing countries (the situation depicted in Figure 2.7) this fadeout probability is very small (less than one percent) but it should be noted that the probability of fadeout after stopping vaccination altogether is much greater for smaller birth rates; in particular, for birth rates typical of developed countries (Table 2.1), the one-year fadeout probability upon ceasing vaccination is 17%. Sensitivity of fadeout probabilities to birth rates occurs for two reasons: the birth rate determines the rate at which new susceptible individuals are recruited into the population and the equilibrium number of infected individuals is (approximately) proportional to the birth rate Eq. (2.17b)].

Continuing to focus on birth rates appropriate for developing countries, we see from Figure 2.7 that for any $p_{\text{eff}} < 0.3$ the four-year fadeout probability remains negligible if pulsed OPV is employed, and small ($\sim 10\%$) if continuous IPV is used. However, moderate vaccination levels ($p_{\text{eff}} \sim 0.7$) yield great improvement. The four-year fadeout probability reaches 90% for $p_{\text{eff}} \sim 0.75$ using OPV or $p_{\text{eff}} \sim 0.7$ with IPV.

In general, pulsed OPV vaccination is less effective than the corresponding IPV strategies with the same number of doses. For small OPV pulses, the probability of eradication is no better than if no OPV vaccination is performed at all (due to the introduction of infectives via reversion). However, for sufficiently large OPV pulses, increased herd immunity outweighs the input of infectives and switching from continuous OPV vaccination to pulsing is likely to be very helpful. In particular, Figure 2.7 indicates that switching from 85% continuous OPV vaccination to 85% pulsed OPV vaccination once per year will change the probability of fadeout within four years from zero to nearly 1 using the same number of doses.

Single pulse OPV versus single pulse IPV.

The most effective strategy might be the application of one large pulse of IPV, following a successful continuous OPV vaccination campaign. Figure 2.9 shows the probability of eradication within one year as a function of the effective number of IPV or OPV vaccinations in a one-time pulse. As an example, note from the figure that an application of five million effective doses, representing less than 35% of the susceptible population, leads to a one-year fadeout probability of less than 80% if OPV is used but greater than 95% if IPV is used. Furthermore, as illustrated by Figure 2.10, eradication is witnessed in shorter time intervals following IPV vaccination as compared to an equivalent OPV pulse. Thus, a one-time IPV pulse may be desirable both from the perspectives of total number of vaccinations and time to eradication.

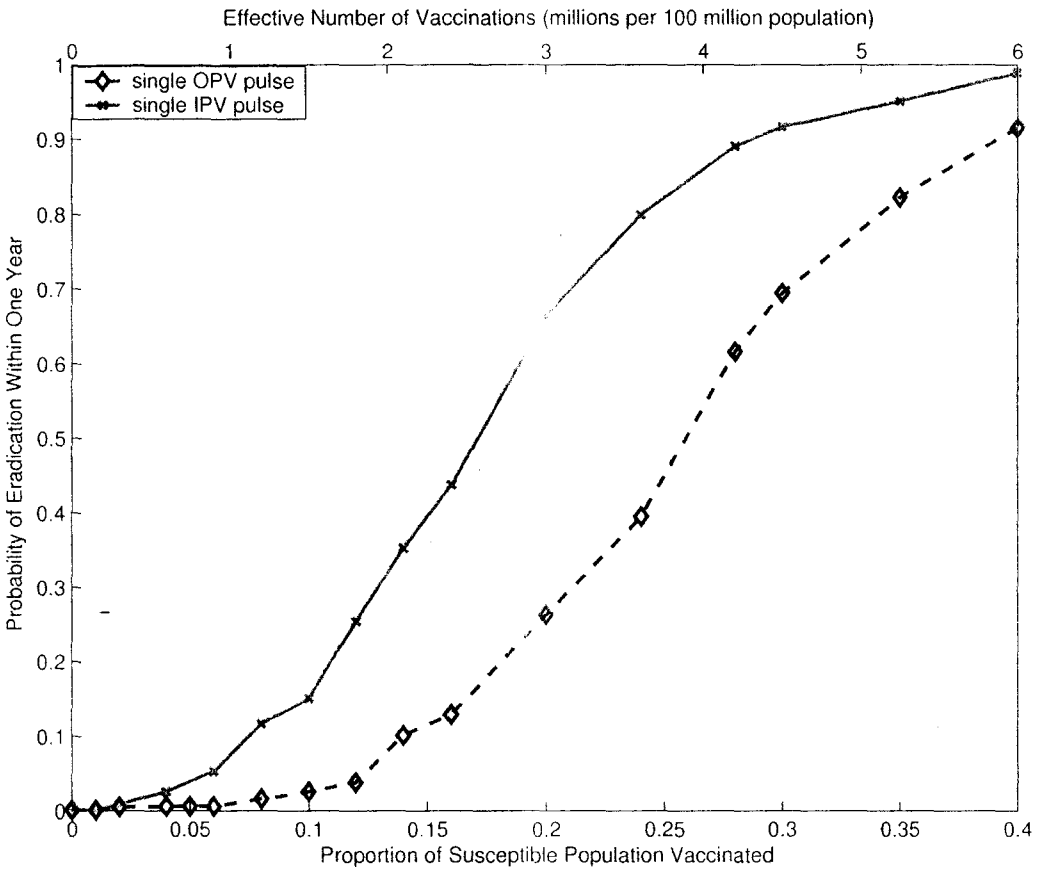

Figure 2.9: Probability of Polio eradication within one year, as a function of the effective number of vaccinations for a single vaccine pulse of IPV or OPV in a population of one hundred million (with birth rates typical of developing countries; Table 2.1). The lower horizontal axis shows the proportion of susceptibles vaccinated (parameter p_{pulse} in Eq. (2.35); note that $\phi = 0$ for IPV as there is no reversion). The upper horizontal axis shows the total number of vaccinations given. IPV achieves superior eradication probabilities in comparison to OPV for equivalent numbers of vaccinations. Note that for less than five million IPV vaccinations, corresponding to less than 35% of the susceptible population (as given by Eq. [illegible]a), the probability of eradication within one year is 95%.

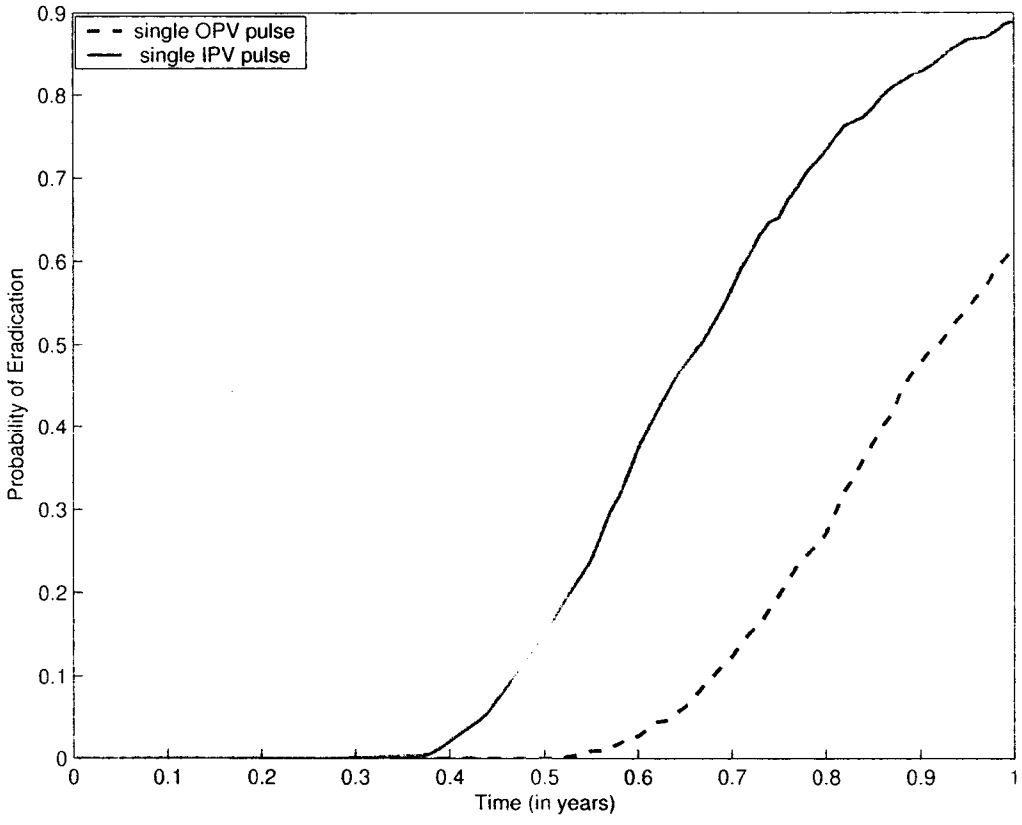

Figure 2.10: Probability of polio eradication as a function of time, for a single vaccine pulse of IPV ($\phi = 0$) or OPV (ϕ as in Table 2.1) with $p_{\text{pulse}} = 0.28$ (where p_{pulse} is the susceptible vaccination proportion in Eq. 2.35). The population is one hundred million (with birth rates typical of developing countries; Table 2.1). For IPV, nonzero probability of eradication is apparent for shorter time intervals in comparison to OPV. Nonzero probability of eradication for OPV is observed almost two months later than for IPV.

Rational policy options

Our models indicate that one-time mass and continuous IPV coverage are effective eradication strategies, even at moderate coverage levels, while pulsed OPV vaccination may be a viable option as long as a sufficiently high level of coverage is maintained. Note that while OPV is much cheaper and easier to administer than IPV, the logistical advantage of needing to reach a much smaller proportion of the population for the same payoff in probability of eradication is an important benefit of IPV.

It should also be noted that in this discussion the IPV model assumes full intestinal immunity of the vaccinated individual. This is of course a simplification, and IPV is generally thought to induce lower levels of intestinal immunity compared to OPV [20]. Consequently, it is likely that the eradication probabilities that we have predicted for the IPV programs are overestimated (by an unknown amount). The significance of lowered gut immunity is still an open question, though as previously mentioned, recent studies suggest that enhanced potency IPV (eIPV) induces an improved level of intestinal immunity over previous IPV offerings [20].

2.6 Discussion

We have presented a compartmental model that takes into account the possibility of reversion in live attenuated virus vaccines (Figure 2.1 and Eqs. (2.11)). For a nonzero reversion proportion of the vaccine ($\phi > 0$), the model has one

biologically meaningful (endemic) equilibrium, which is globally asymptotically stable.

We applied the model to polio dynamics, assuming oral polio vaccine (OPV) is given to a fixed proportion of newborns (p), and investigated the impact of circulating vaccine derived polio viruses (cVDPVs). For our estimated value of the reversion proportion ($\phi \sim 10^{-4}$; Table 2.1), we found that for vaccination levels (p) less than 75% the effect of cVDPVs is negligible compared to the expected endemic level of the disease in the absence of reversion. We concluded that if OPV coverage levels are below the critical level required for eradication in the absence of reversion ($p < p_{\text{crit}} \simeq 0.83$) then it is best to focus on trying to increase OPV coverage levels (the benefits of increased coverage far outweigh the negative impact of vaccine reversion). However, if p can be brought close to p_{crit} then other strategies should be considered to increase the probability of eradication (the inevitable input of new cVDPVs resulting from continuous OPV vaccination must be avoided).

We considered three alternative eradication strategies that eliminate continuous input of cVDPVs: pulsed OPV vaccination, continuous injectable polio vaccine (IPV) vaccination, and one-time mass IPV vaccination. Based on simulations of stochastic models, we found that continuous or mass IPV vaccination achieves a higher probability of eradication (per dose) than pulsed OPV. In spite of the much greater cost per dose for IPV, we expect that investment in IPV vaccination following a successful continuous OPV campaign will be more effective because the time to eradication is likely to be

substantially shorter (Figures 2.8 and 2.9).

The key parameter in our models is the reversion factor ϕ, which can be estimated only crudely. Our modeling would benefit from a more precise estimate of ϕ, noting that by reversion we mean regaining both virulence and transmissibility. Revertant vaccine viruses probably do not always regain full transmissibility, so an estimate of $\mathcal{R}_0$ for revertant strains would be helpful.

We have ignored the benefit of contact vaccination via OPV: because the vaccine is live, vaccinated individuals can transmit the vaccine and thereby immunize non-vaccinated individuals. This effect should (slightly) lower the predicted endemic number of infectives below that predicted by our model.

With respect to final eradication strategies, a more thorough understanding of IPV's effectiveness in inducing gut immunity is needed. In addition, polio models accounting for spatial heterogeneity and seasonality in transmission rates should be investigated, since synchronization of fadeouts could increase the probability of eradication [10, 11, 12].

2.7 Appendix

We show here that if $0 < p < 1$ and $0 < \phi \leq 1$ then the equilibrium given by (2.17) is contained in the biologically relevant region $\mathcal{B} = \{(S, I) : S > 0, I > 0, S + I < 1\}$.

First, if $p\phi > 0$ then

$$\sqrt{\left[\frac{1}{2}\Delta p\right]^2 + \frac{p\phi}{\mathcal{R}_0}} > \left|\frac{1}{2}\Delta p\right| , \tag{2.37}$$

so $I^* > 0$ in Eq. (2.17b).

Second, we can re-express Eq. (2.17a) as

$$S^* = 1 - p_{\text{crit}} + \frac{1}{2}\Delta p - \sqrt{\left[\frac{1}{2}\Delta p\right]^2 + \frac{p\phi}{\mathcal{R}_0}} . \tag{2.38}$$

Since $1 - p_{\text{crit}} = 1/\mathcal{R}_0$, we therefore have

$$S^* > 0 \iff \frac{1}{\mathcal{R}_0} + \frac{1}{2}\Delta p > \sqrt{\left[\frac{1}{2}\Delta p\right]^2 + \frac{p\phi}{\mathcal{R}_0}} \tag{2.39a}$$

$$\iff \left(\frac{1}{\mathcal{R}_0} + \frac{1}{2}\Delta p\right)^2 > \left[\frac{1}{2}\Delta p\right]^2 + \frac{p\phi}{\mathcal{R}_0} \tag{2.39b}$$

$$\iff \frac{1}{\mathcal{R}_0^2} + \frac{\Delta p}{\mathcal{R}_0} > \frac{p\phi}{\mathcal{R}_0} \tag{2.39c}$$

$$\iff \frac{1}{\mathcal{R}_0} + \left(1 - \frac{1}{\mathcal{R}_0}\right) - p(1-\phi) > p\phi \tag{2.39d}$$

$$\iff p < 1 . \tag{2.39e}$$

Finally, summing Eqs. (2.17a) and (2.17b) to obtain

$$S^* + I^* = \frac{1}{\mathcal{R}_0} + \frac{1}{2}(1+f)\Delta p - (1-f)\sqrt{\left[\frac{1}{2}\Delta p\right]^2 + \frac{p\phi}{\mathcal{R}_0}} , \tag{2.40}$$

and defining

$$F(f) = 1 - (S^* + I^*)\,, \tag{2.41}$$

we must show $F(f) > 0$ for all relevant values of f (i.e., for $0 < f < 1$ from definition (2.8)). To see this, note that

$$F(1) = 1 - \frac{1}{\mathcal{R}_0} - \Delta p = p(1-\phi) \geq 0 \tag{2.42}$$

and

$$\frac{dF}{df} = -\frac{1}{2}\Delta p - \sqrt{\left[\frac{1}{2}\Delta p\right]^2 + \frac{p\phi}{\mathcal{R}_0}} \tag{2.43a}$$

$$< 0 \text{ for all } f\,. \tag{2.43b}$$

so $F(f) > 0$ for all $f < 1$.

2.8 Appendix

We formally calculate the endemic equilibrium of the Gamma distributed OPV reversion model (2.33). We use the superscript * to denote the equilibrium value and we define the dimensionless parameter

$$f_n = \frac{\nu}{n\gamma + \nu}\,. \tag{2.44}$$

For $n = 1$, f_n reduces to f, as defined in Eq. (2.8). For the Gamma distributed SIR model, the *basic reproductive number* $\mathcal{R}_0$ is given by [28]

$$\mathcal{R}_0 = \frac{\beta}{\nu}\left(1 - (1 - f_n)^n\right). \tag{2.45}$$

In terms of $\mathcal{R}_0$, the *critical vaccination proportion* (which is meaningful in the absence of reversion) is still given by the usual formula (2.9).

Setting Eq. (2.33) to zero, for $k \geq 2$ we find

$$I_k^* = (1 - f_n) I_{k-1}^* \tag{2.46}$$

and hence

$$I_k^* = (1 - f_n)^{k-1} I_1^*. \tag{2.47}$$

We therefore have

$$I^* = \sum_{k=1}^{n} I_k^* = \frac{1 - (1 - f_n)^n}{1 - (1 - f_n)} I_1^* = \frac{1 - (1 - f_n)^n}{f_n} I_1^*. \tag{2.48}$$

Summing Eqs. (2.33a) and (2.33b) at equilibrium yields

$$S^* = 1 - p(1 - \phi) - \frac{1}{f_n} I_1^*. \tag{2.49}$$

Substituting Eq. (2.49) into (2.33b) (set to zero), expressing I^* in terms of

I_1^* via (2.48) and simplifying in terms $\mathcal{R}_0$ yields the quadratic equation

$$\frac{1}{f_n} I_1^{*2} - [p_{\text{crit}} - p(1-\phi)]\, I_1^* - \frac{p\phi f_n}{\mathcal{R}_0} = 0\,. \tag{2.50}$$

This quadratic equation for I_1^* has exactly the same form as Eq. (2.14) for I^* in the case $n = 1$. As in §2.4.1, defining $\Delta p = p_{\text{crit}} - p(1-\phi)$ and solving the quadratic for I_1^* (insisting that it be non-negative) yields the unique solution

$$I_1^* = f_n \left[\frac{1}{2}\Delta p + \sqrt{\left[\frac{1}{2}\Delta p\right]^2 + \frac{p\phi}{\mathcal{R}_0}} \right] \tag{2.51}$$

from which Eqs. (2.48) and (2.49) imply

$$I^* = [1 - (1 - f_n)^n] \left[\frac{1}{2}\Delta p + \sqrt{\left[\frac{1}{2}\Delta p\right]^2 + \frac{p\phi}{\mathcal{R}_0}} \right] \tag{2.52a}$$

$$S^* = 1 - p(1-\phi) - \frac{1}{2}\Delta p - \sqrt{\left[\frac{1}{2}\Delta p\right]^2 + \frac{p\phi}{\mathcal{R}_0}}\,, \tag{2.52b}$$

As expected, for the exponential distribution ($n = 1$), Eq. (2.52) reduces to (2.17).

2.9 Appendix

Here we show that for the live attenuated virus model (2.11), if $0 < p < 1$ and $0 < \phi < 1$ then the region $\mathcal{B} = \{(S, I) : S > 0, I > 0, S + I < 1\}$ is forward invariant, and for all initial conditions along the boundary of $\mathcal{B}$ the

flow of Eq. (2.11) is into $\mathcal{B}$.

As shown in §2.3, since the model (2.11) is constructed in terms of proportions, the closure of $\mathcal{B}$ is forward invariant. Therefore it is sufficient to show that the flow of (2.11) along the boundary of $\mathcal{B}$ is into $\mathcal{B}$.

The boundary is given by the lines $S = 0$, $I = 0$ and $S + I = 1$. Along the line $S = 0$, the flow of (2.11) is given by

$$\left.\frac{dS}{dt}\right|_{S=0} = (1-p)\nu\,, \tag{2.53}$$

which is positive for any $p < 1$. Hence the flow along the line $S = 0$ is into $\mathcal{B}$. Similarly, if $I = 0$ then

$$\left.\frac{dI}{dt}\right|_{I=0} = \phi p\nu\,, \tag{2.54}$$

which is positive provided $p > 0$ and $\phi > 0$. Finally, along the line $S + I = 1$,

$$\left.\frac{d(S+I)}{dt}\right|_{S+I=1} = -(1-\phi)p\nu - \gamma I \leq -(1-\phi)p\nu\,, \tag{2.55}$$

which is negative provided $\phi < 1$ and $p > 0$. Thus, the flow along the boundary lines is into $\mathcal{B}$.

Bibliography

[1] Z. Agur, L. Cojocaru, G. Mazor, R. M. Anderson, and Y. L. Danon (1993), Pulse mass measles vaccination across age cohorts, Proceedings of the National Academy of Science USA 90, 11698–11702.

[2] D. Anderson and R. Watson (1980). On the spread of a disease with Gamma distributed latent and infectious periods, Biometrika 67(1), 191–198.

[3] R. M. Anderson and R. M. May (1991), Infectious Diseases of Humans, Dynamics and Control, Oxford Science Publications.

[4] [Anon] (1994), Polio Eradication Field Guide Techincal Paper No. 40, Technical report, Word Health Organization and Pan American Health Organization.

[5] [Anon] (2001), National Vital Statistics Report, Technical Report 49 (1), National Center for Health Statistics. URL `http://www.cdc.gov/nchs/data/natality/nvs49_1t1.pdf`.

[6] [Anon] (2005), Diseases and Conditions: Polio, Technical report, Centers for Disease Control and Prevention. URL http://www.cdc.gov/nip/publications/pink/polio.pdf.

[7] [Anon] (2005), Morb. Mortal Wkly Rep., Technical Report 41, CDC.

[8] N. Bailey (1964), Some stochastic models for small epidemics in large populations. Applied Statistics 13(1). 9–19.

[9] F. Brauer (2003), Backward Bifurcation in simple vaccination models. J. Math. Anal. Appl. 298, 418–431.

[10] D. J. D. Earn and S. A. Levin (2006). Global asymptotic coherence in discrete dynamical systems, Proceedings of the National Academy of Science USA 103(11), 3968–3971.

[11] D. J. D. Earn, S. A. Levin, and P. Rohani (2000), Coherence and conservation, Science 290(5495), 1360–1364.

[12] D. J. D. Earn, P. Rohani, and B. T. Grenfell (1998), Persistence, chaos and synchrony in ecology and epidemiology, Proceedings of the Royal Society of London Series B-Biological Sciences 265(1390), 7–10.

[13] D. T. Gillespie (1976), A General Method for Numerically Simulating the Stochastic Time Evolution of Coupled Chemical Reactions, Journal of Computational Physics 22, 403–434.

[14] N. C. Grassly, J. Wenger, S. Durrani, S. Bahl, J. M. Deshpande, R. W. Sutter, D. L. Heymann, and R. Aylward (2007), Protective efficacy of a monovalent oral type 1 poliovirus vaccine: a case- control study, Lancet 369, 1356–1362.

[15] H. W. Hethcote (2000), The Mathematics of Infectious Diseases, SIAM Review 42(4), 599–653.

[16] D. L. Heymann, R. W. Sutter, and R. B. Aylward (2005), A global call for new polio vaccines, Nature 434, 699–700.

[17] J. John (2004), A developing country perspective of vaccine associated paralytic poliomyelitis, Bulletin of the World Health Organization 82, 53–58.

[18] W. O. Kermack and A. G. McKendrick (1927), A contribution to the mathematical theory of epidemics, Proceedings of the Royal Society of London Series A 115, 700–721.

[19] A. Korobeinikov and G. C. Wake (2002), Lyapunov Functions and Global Stability for SIR, SIRS, and SIS Epidemiological Models, Applied Mathematics Letters 15, 955–960.

[20] M. Laasri, K. Lottenbach, R. Belshe, M. Wolff, M. Rennels, S. Plotkin, and K. Chumakov (2005), Effect of different vaccination schedules on excretion of oral poliovirus vaccine strains, Journal of Infectious Diseases 193, 2092–2098.

[21] A. L. Lloyd (2001), Realistic Distributions of Infectious Periods in Epidemic Models: Changing Patterns of Persistence and Dynamics. Theoretical Population Biology 60, 59-71.

[22] J. Ma and D. J. D. Earn (2006), Generality of the final size formula for an epidemic of a newly invading infectious disease, Bulletin of Mathematical Biology 68, 679–702.

[23] T. McDevitt (1999), World Population Profile: 1998, Technical report, U.S. Census Bureau, URL http://iggi.unesco.or.kr/web/iggi_docs/05/952662740.pdf.

[24] D. J. Nokes and J. Swinton (1997), Vaccination in pulses: a strategy for global eradication of measles and polio?, Trends in Microbiology 5(1), 14-19.

[25] P. A. Offit (2005), The Cutter Incident, Yale University Press.

[26] L. Perko (1996), Differential Equations and Dynamical Systems, Springer Verlag.

[27] L. Stone, B. Shulgin, and Z. Agur (2000), Theoretical Examination of the Pulse Vaccination Policy in the SIR Epidemic Model, Journal of Mathematical and Computer Modelling 31, 207–215.

[28] P. van den Driessche and J. Watmough (2002), Reproduction numbers and sub-threshold endemic equilibria for compartmental models of disease transmission, Mathematical Biosciences 180, 29–48.

[29] G. C. Woodrow and M. M. Levine (1990), New Generation Virus Vaccines, Marcel Dekker, Inc.

Chapter 3

Contact Vaccination

3.1 Introduction

Both currently and historically live-attenuated virus vaccines (LAVV) have been employed against a wide range of viral diseases. Examples include the smallpox vaccine, the Oral Polio Vaccine (OPV), measles vaccine, and HIV vaccines currently under development [6, 33].

Unlike an inactivated vaccine, a LAVV is a functioning, replicating virus which has been significantly reduced in virulence and transmissibility through the attenuation process. Typically this attenuation is achieved by passing the virus through a sequence of animal host tissues where there is selective pressure for mutations which reduce its virulence [33].

The transmission of LAVVs, so-called inadvertent or *contact vaccinations* is the focus of this work. Although the transmissibility of LAVVs is signif-

icantly reduced compared with native or virulent forms, it has long been recognized that LAVV transmission can be sufficient to have an important effect on the epidemiological dynamics at the population level. The World Health Organization (WHO) has cited contact vaccination as one of the five primary reasons for use of OPV in the developing world [18]. In this case it is seen as a benefit, as the transmission of vaccine virus lowers the proportion of the population that must be directly vaccinated to control the spread of the wild virus.

Contact vaccination may have played an important role in leading the eradication of smallpox in the 1970s. However, observed smallpox contact vaccination [27] is currently viewed negatively because it implies a risk of serious allergic reaction in individuals who haven't chosen to be vaccinated. In addition, as for any LAVV, the smallpox vaccine virus has the potential to mutate and thereby revert to the original wild form [33]. The potential to re-introduce an eradicated pathogen makes contact vaccination a very dangerous risk in this case.

We focus our attention specifically on LAVV vaccination for infectious diseases that generally confer lengthy or lifelong immunity to the infecting pathogen. These include polio and smallpox, but also childhood infectious diseases such as measles, mumps, rubella and pertussis. We investigate the significance of the role of contact vaccination in decreasing the required vaccination coverage to control pathogenic wild virus spread, specifically deriving analytical expressions for the critical vaccination coverage levels for eradica-

tion of the wild virus in terms of epidemiologically measurable quantities.

The first part of our analysis deals with LAVV programs in which vaccination takes place continuously. We begin by presenting the simplest LAVV models, which are variants of the standard Susceptible-Infected-Removed (SIR) and Susceptible-Exposed-Infectious-Removed (SEIR) models; we then proceed to expand the results to a very general staged progression model, which among other things allows us to examine more realistically distributed latent and infectious periods for both the wild and vaccine viruses.

The second part of our analysis deals with pulse vaccination LAVV programs. In such programs mass vaccinations are performed at regular time intervals. This analysis has particular relevance to polio, as some form of annual pulse OPV campaign is currently in use in 55 countries around the globe [1].

Throughout this work we make the simplifying assumption that the vaccine virus cannot undergo reversion (a return to its virulent form via mutation). While this ignores a potentially critical biological process, we have previously shown that reversion is likely to contribute significantly to the population dynamics of the pathogen only when considering strategies for vaccine cessation [32]. In this paper we focus on the eradication of the wild virus strain, minimizing the total virus transmission but not necessarily eliminating it fully due to the possibility of reversion of the vaccine strain. We do not consider the "endgame", strategies for withdrawal of vaccine coverage, in this paper. Thus ignoring reversion does not represent a significant

approximation.

Some previous mathematical modelling of LAVV transmission has been carried out for HIV [6] and OPV [12]. In the case of HIV, LAVV transmission was investigated in the context of an imperfectly attenuated vaccine, which—in addition to having limited efficacy—had the potential to cause the disease itself, irrespective of reversion. In the case of OPV, a simple LAVV model was formulated and a partial local analysis performed [12]; a full global analysis of this OPV model is a special case of the general results we derive in the following sections.

3.2 LAVV Models

The simplest LAVV model is based on the standard SIR model [2, 17] and can be represented as a flow chart (Figure 3.1) or as a set of coupled ordinary differential equations (ODEs),

$$\frac{dS}{dt} = (1-p)\nu - \beta_{\mathrm{I}} IS - \beta_{\mathrm{V}} VS - \nu S \tag{3.1a}$$

$$\frac{dI}{dt} = \beta_{\mathrm{I}} IS - (\nu + \gamma_{\mathrm{I}})I \tag{3.1b}$$

$$\frac{dV}{dt} = p\nu + \beta_{\mathrm{V}} VS - (\nu + \gamma_{\mathrm{V}})V \tag{3.1c}$$

$$\frac{dR}{dt} = \gamma_{\mathrm{I}} I + \gamma_{\mathrm{V}} V - \nu R \tag{3.1d}$$

The host population is split into homogeneous classes representing the proportions of individuals who are susceptible (S), infectious with wild virus (I),

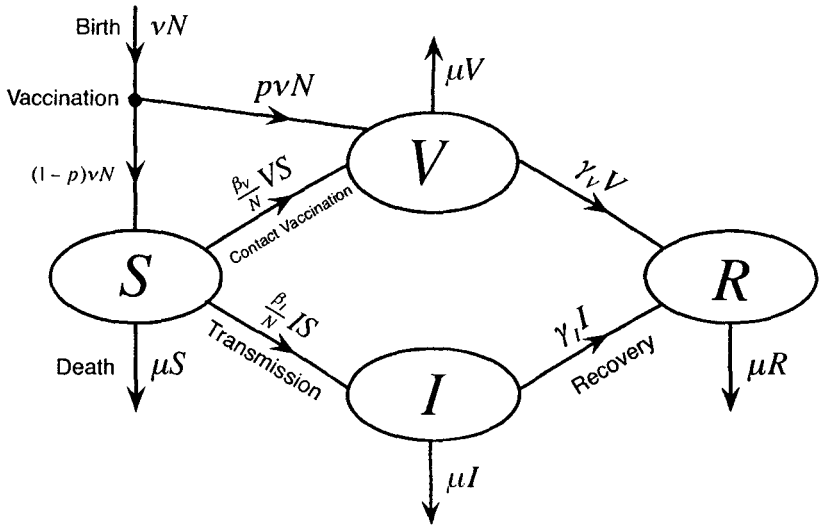

Figure 3.1: Flow diagram for the SIVR model, the simplest LAVV model. The ODE formulation of this model is given, in terms of *proportions* of the population, by system (3.1).

infectious with attenuated vaccine virus (V) or immune (R). The parameters β_{I}, β_{V}, $\frac{1}{\gamma_{\mathrm{I}}}$ and $\frac{1}{\gamma_{\mathrm{I}}}$ represent the transmission rates and mean infectious periods for the wild and vaccine viruses, respectively. In the flow chart, both birth (at *per capita* rate ν) and natural death (at *per capita* rate μ) are shown. However, because Eqs. (3.1) are written in terms of proportions rather than numbers of individuals in each compartment, only ν appears in the ODEs [16, 32]. The parameter p is the proportion of individuals who are vaccinated before entering the susceptible class (in practice, there is often a substantial delay between birth and vaccination so that maternally-acquired immunity has had a chance to wane). These vaccinated individuals then enter the attenuated-virus infectious class (V) and are able to pass the vaccine virus

to susceptible individuals, resulting in contact vaccinations. The model (3.1) assumes that there is no disease-specific mortality, that vaccination—whether direct or inadvertent—confers lifelong immunity, and that the vaccine virus does not evolve (and hence cannot revert to the virulent form). The assumption of lifelong and complete immunity is particularly valid in the case of LAVVs for childhood diseases, as they provide an active immune response very similar to natural infection [28].

We denote the basic reproduction numbers of the wild and vaccine viruses as $\mathcal{R}_0$ and $\mathcal{R}_V$, respectively. The basic reproduction number is defined in the standard manner as the average number of secondary infections (or secondary immunizations) caused by a single infectious individual in a fully susceptible population. As the vaccine virus is attenuated, substantially reducing both transmissibility as well as virulence, we impose the condition $\mathcal{R}_V < \mathcal{R}_0$. Furthermore we consider $\mathcal{R}_0 > 1$ as otherwise the virus would fade out from the population naturally without vaccination.

The ODE system (3.1) was originally proposed by Eichner and Hadeler [12] to model polio dynamics when vaccinating with Oral Polio Vaccine (OPV). They showed that system (3.1) exhibits a *disease free equilibrium* (DFE), which is (locally) asymptotically stable, whenever

$$p \geq p_{\text{crit}}\left(1 - \frac{\mathcal{R}_V}{\mathcal{R}_0}\right), \tag{3.2}$$

where p_{crit} is the minimum proportion of the population that must be vacci-

nated to eradicate a disease with a vaccine that is not transmissible, i.e.,

$$p_{\text{crit}} = 1 - \frac{1}{\mathcal{R}_0}. \tag{3.3}$$

It is important to note that contact vaccination leads to a significant reduction in the threshold vaccination proportion p_{crit} even for $\mathcal{R}_V < 1$,in which case we expect the vaccine virus to fade from the population upon cessation of vaccination. This reduction of critical proportion is demonstrated in Figure 3.1 which compares the critical proportion under contact vaccination to p_{crit} (standard vaccination) for various fixed $\mathcal{R}_V$ values across a range of $\mathcal{R}_0$ values.

Below threshold (3.2), system (3.1) has a biologically meaningful endemic equilibrium. We demonstrate below that the DFE is, in fact, *globally* asymptotically stable if condition (3.2) holds and that the endemic equilibrium is globally asymptotically stable whenever it exists. These conclusions are also valid for models that incorporate latent periods (delays between the time of infection or vaccination and the onset of infectiousness); see the SEIVR model depicted in Figure 3.2. Much more generally, we show in this paper that these global stability results are valid for any staged-progression LAVV model (depicted generically in Figure 3).

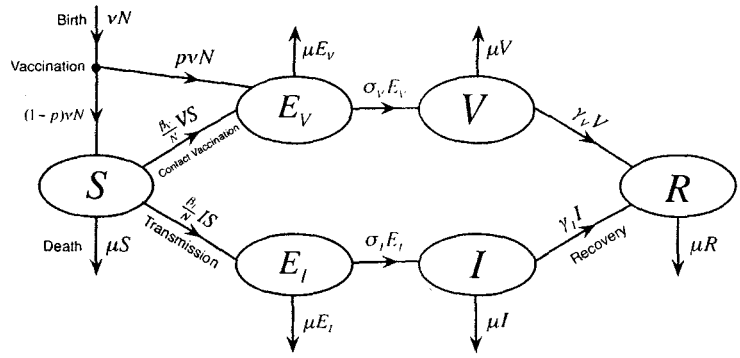

Figure 3.2: Flow diagram for the SEIVR model. The compartments E_V and E_I represent exposed classes of individuals who have been infected, respectively, by the vaccine and wild virus but are not yet infectious. The mean latent periods for the vaccine and wild virus are given by $\frac{1}{\sigma_V}$ and $\frac{1}{\sigma_I}$.

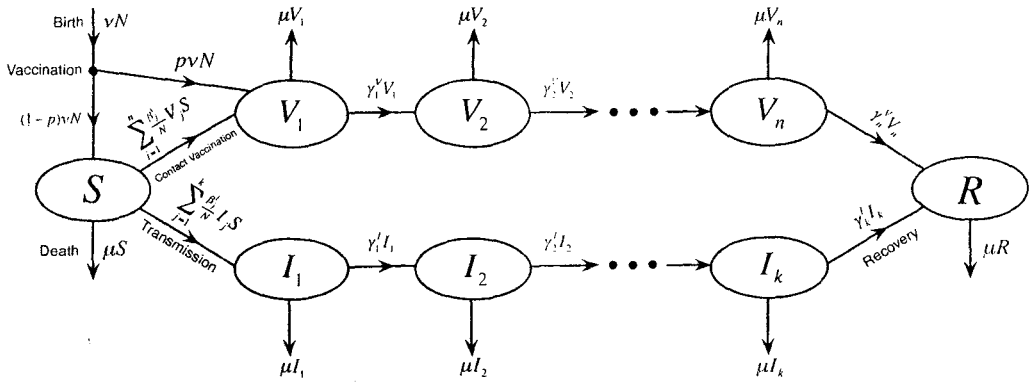

Figure 3.3: Flow diagram for the general staged progression $SI_1I_2\cdots I_kV_1V_2\cdots V_nR$ model, which includes an arbitrary number of stages of infection for both the wild and vaccine viruses.

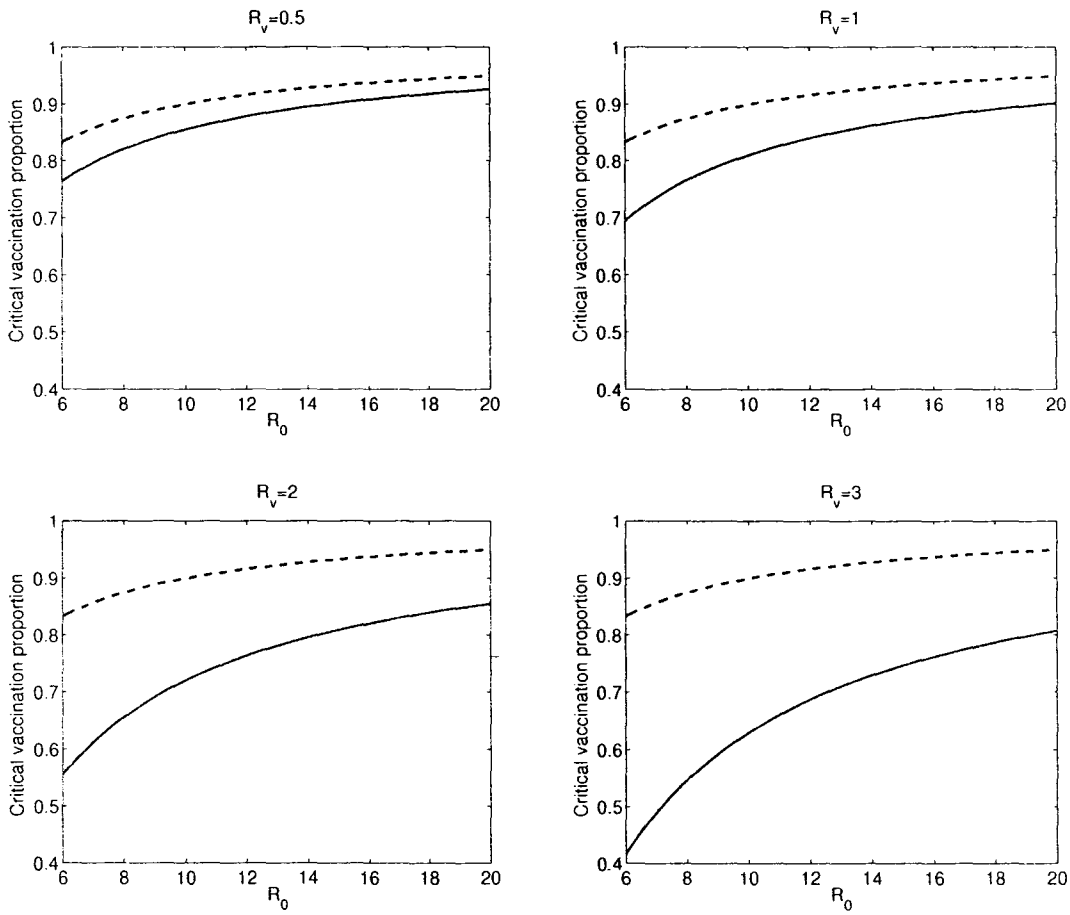

Figure 3.4: Critical vaccination proportion (3.2) as a function of wild virus basic reproduction number $\mathcal{R}_0$ for fixed values of vaccine virus basic reproduction number $\mathcal{R}_V$ (solid line). Also shown is the standard critical vaccination level p_{crit} (dashed line) corresponding to $\mathcal{R}_V = 0$. Contact vaccination leads to a significant reduction in the critical vaccination proportion even for $\mathcal{R}_V < 1$ and relatively high $\mathcal{R}_0$ values.

3.2.1 Global stability of generalized LAVV models

We show that for the very general class of LAVV models depicted in Figure 3.3, there is always a unique DFE and a critical vaccination threshold that is always given by Eq. (3.2). If $p \geq p_{\text{crit}}(1 - \frac{\mathcal{R}_V}{\mathcal{R}_0})$ then the DFE is globally asymptotically stable, while if $p < p_{\text{crit}}(1 - \frac{\mathcal{R}_V}{\mathcal{R}_0})$ there exists a unique globally asymptotically stable *endemic equilibrium*.

The General Staged Progression LAVV Model

We begin by formulating the general staged progression LAVV model depicted in Figure 3.3 as the following system of ODEs.

$$\frac{dS}{dt} = (1-p)\nu - \sum_{j=1}^{n} \beta_j^{\mathrm{V}} V_j S - \sum_{j=1}^{k} \beta_j^{\mathrm{I}} I_j S - \nu S \tag{3.4a}$$

$$\frac{dV_1}{dt} = p\nu + \sum_{j=1}^{n} \beta_j^{\mathrm{V}} V_j S - \left(\nu + \gamma_1^{\mathrm{V}}\right) V_1 \tag{3.4b}$$

$$\frac{dV_2}{dt} = \gamma_1^{\mathrm{V}} V_1 - \left(\nu + \gamma_2^{\mathrm{V}}\right) V_2 \tag{3.4c}$$

$$\vdots$$

$$\frac{dV_j}{dt} = \gamma_{j-1}^{\mathrm{V}} V_{j-1} - \left(\nu + \gamma_j^{\mathrm{V}}\right) V_j \tag{3.4d}$$

$$\vdots$$

$$\frac{dV_n}{dt} = \gamma_{n-1}^{\mathrm{V}} V_{n-1} - \left(\nu + \gamma_n^{\mathrm{V}}\right) V_n \tag{3.4e}$$

$$\frac{dI_1}{dt} = \sum_{j=1}^{k} \beta_j^{\mathrm{I}} I_j S - \left(\nu + \gamma_1^{\mathrm{I}}\right) I_1 \tag{3.4f}$$

$$\frac{dI_2}{dt} = \gamma_1^{\mathrm{I}} I_1 - \left(\nu + \gamma_2^{\mathrm{I}}\right) I_2 \tag{3.4g}$$

$$\vdots$$

$$\frac{dI_j}{dt} = \gamma_{j-1}^{\mathrm{I}} I_{j-1} - \left(\nu + \gamma_j^{\mathrm{I}}\right) I_j \tag{3.4h}$$

$$\vdots$$

$$\frac{dI_k}{dt} = \gamma_{k-1}^{\mathrm{I}} I_{k-1} - \left(\nu + \gamma_k^{\mathrm{I}}\right)) I_k \tag{3.4i}$$

$$\frac{dR}{dt} = \gamma_k^{\mathrm{I}} I_k + \gamma_n^{\mathrm{V}} V_n - \nu R \tag{3.4j}$$

In system (3.1), the variables V_j represent infected stages (latent if the transmission rate $\beta_j^{\mathrm{V}} = 0$ and infectious if $\beta_j^{\mathrm{V}} > 0$). Similarly, the I_j represent wild virus infected stages and β_j^{I} are the transmission rates in these stages. We denote the numbers of vaccine virus and wild virus infected classes by n and k, respectively. Without loss of generality, we assume V_n and I_k are the final vaccine and wild virus stages with nonzero infectivity (further classes with $\beta_j^{\mathrm{V}} = 0$ or $\beta_j^{\mathrm{I}} = 0$ could be absorbed into the removed class R). As in (3.1) the model (3.4) is written in terms of proportions, so only the *per capita* birth rate ν appears and not the *per capita* death rate μ . The parameters $\frac{1}{\gamma_j^{\mathrm{V}}}$ and $\frac{1}{\gamma_j^{\mathrm{I}}}$ represent the mean duration of the jth vaccine and wild virus infected stages respectively, and p is the proportion of newborns which are successfully vaccinated (after maternal antibodies have waned).

We denote the state of the system ( ) as

$$\mathbf{X} = (S, V_1, V_2, \ldots, V_n, I_1, I_2, \ldots, I_k, R) \tag{3.5}$$

and the biological meaningful set, as we are dealing with proportions, is defined as

$$\mathcal{B} = \{\mathbf{X} : \mathbf{X}_i \geq 0, \sum_i \mathbf{X}_i = 1\}. \tag{3.6}$$

The set $\mathcal{B}$ is positively invariant. From the form of the equations it is straightforwardly seen that if all initial states are non-negative, they remain non-negative for all positive time. Furthermore summing Eqs. (3.4a)-(3.4j) yields

the differential equation

$$\frac{d}{dt}\left(\sum_i \mathbf{X}_i\right) = \nu - \nu \sum_i \mathbf{X}_i \tag{3.7}$$

which has a single equilibrium at $\sum_i X_i = 1$. Since by definition any initial condition in $\mathcal{B}$ satisfies $\sum_i \mathbf{X}_i(0) = 1$, ( ) trivially implies that $\sum_i \mathbf{X}(t) = 1 \, \forall t > 0$. Thus, $\mathbf{X}(t) \in \mathcal{B} \quad \forall t \geq 0$ and the model(3.1) is biologically well posed.

Note that since Eqs. (3.1a)- (3.1f) are independent of R, we need only deal *directly* with this subsystem, ignoring Eq. (3.1g). Thus, it is convenient to express $\mathcal{B}$ as

$$\mathcal{B} = \{S, V_i, I_i : S, V_i, I_i \geq 0, \quad S + \sum_{i=1}^{n} V_i + \sum_{i=1}^{k} I_i \leq 1\} \tag{3.8}$$

where it is understood that $R = 1 - S - \sum_{i=1}^{n} V_i - \sum_{i=1}^{k} I_i$

Basic reproduction numbers

We calculate the basic reproduction numbers of the vaccine ($\mathcal{R}_V$) and wild virus ($\mathcal{R}_0$), defined to be the number of secondary transmissions of a single infectious individual in an otherwise fully susceptible population. From the definition, we see that each virus must be considered independently. If considering the vaccine virus we fix all wild virus classes to zero, and vice versa, and set vaccination to zero. Applying the next generation method [7, 31] to

the resulting system yields the reproduction numbers,

$$\mathcal{R}_{\mathrm{V}} = \left(\frac{\beta_1^{\mathrm{V}}}{(\nu + \gamma_1^{\mathrm{V}})} + \sum_{j=2}^{n} \frac{\beta_j^{\mathrm{V}}}{(\nu + \gamma_j^{\mathrm{V}})} \left(\prod_{i=1}^{j-1} \frac{\gamma_i^{\mathrm{V}}}{(\nu + \gamma_i^{\mathrm{V}})} \right) \right) \tag{3.9a}$$

$$\mathcal{R}_0 = \left(\frac{\beta_1^{\mathrm{I}}}{(\nu + \gamma_1^{\mathrm{I}})} + \sum_{j=2}^{k} \frac{\beta_j^{\mathrm{I}}}{(\nu + \gamma_j^{\mathrm{I}})} \left(\prod_{i=1}^{j-1} \frac{\gamma_i^{\mathrm{I}}}{(\nu + \gamma_i^{\mathrm{I}})} \right) \right) \tag{3.9b}$$

The next generation method provides a straightforward algorithm to obtain reproduction numbers by examining the stability of the system at the DFE. For staged progression models, reproduction numbers are worked out explicitly in [31], along with a complete discussion of the method.

Eqs. (3.9) can be also understood at a heuristic level. For example (for constant population) the term $\frac{\beta_j^{\mathrm{V}}}{(\nu+\gamma_j^{\mathrm{V}})}$ can be understood as the average number of people infected (in a fully susceptible population) by an individual in the jth class, while the product term $\prod_{i=1}^{j-1} \frac{\gamma_i^{\mathrm{V}}}{(\nu+\gamma_i^{\mathrm{V}})}$ represents the probability that an individual beginning in the first class will proceed to the jth class before dying. Summing over all classes gives the total average number of infections.

3.2.2 Equilibria

For system (3.1), we explicitly compute the *disease free equilibrium* (DFE, which always exists and is unique) and the *endemic equilibrium* (EE, which is unique whenever it exists).

We note that for any equilibrium $\mathbf{X}^*$ such that $(S^*, V_i^*, I_i^*) \geq 0\,, \forall i$ must

in fact lie in the biologically meaningful set $\mathcal{B}$. To see this observe that at equilibrium Eq. (3.1j) implies

$$R^* = \frac{1}{\nu}\left(\gamma_n^{\mathrm{V}} V_n^* + \gamma_k^{\mathrm{I}} I_k^*\right) . \tag{3.10}$$

The assumption that V_n^*, I_k^* are non-negative then implies that $R^* \geq 0$, and thus all states are non-negative. As previously shown by (3.7) at *any* equilibrium we must have

$$\sum_i X_i^* = S^* + R^* + \sum_{i=1}^{n} V_i^* + \sum_{i=1}^{k} I_i^* = 1 \tag{3.11}$$

implying that $\mathbf{X}^* \in \mathcal{B}$. We make use of this result in the computation of the *disease free* and *endemic* equilibrium.

The Disease Free Equilibrium

By definition, the DFE has $I_j^* = 0$ for all j, and we notice from (3.1b) that at equilibrium we must have

$$V_j^* = \frac{\gamma_{j-1}^{\mathrm{V}}}{(\nu + \gamma_j^{\mathrm{V}})} V_{j-1}^* . \qquad j \geq 2 . \tag{3.12}$$

Summing Eqs. (3.1a) and (3.1b) at equilibrium yields the relation

$$S^* = 1 - \frac{(\nu + \gamma_1^{\mathrm{V}})}{\nu} V_1^* . \tag{3.13}$$

Expressing V_j^* in terms of V_1^* via Eqs. (12), (3.9) and substituting (3.1a) into (3.4b) at equilibrium yields the quadratic equation

$$\frac{(\nu+\gamma_1^V)}{\nu}V_1^{*2} - \left(1-\frac{1}{\mathcal{R}_V}\right)V_1^* - \frac{p\nu}{\mathcal{R}_V(\nu+\gamma_1^V)}. \tag{3.14}$$

We compute the unique positive solution of (3.14) yielding the DFE.

$$S^* = \left(1-\frac{1}{2}(1-\frac{1}{\mathcal{R}_V}) - \sqrt{\left(\frac{1}{2}(1-\frac{1}{\mathcal{R}_V})\right)^2+\frac{p}{\mathcal{R}_V}}\right) \tag{3.15a}$$

$$V_1^* = \frac{\nu}{(\nu+\gamma_1^V)}\left(\frac{1}{2}(1-\frac{1}{\mathcal{R}_V}) + \sqrt{\left(\frac{1}{2}(1-\frac{1}{\mathcal{R}_V})\right)^2+\frac{p}{\mathcal{R}_V}}\right) \tag{3.15b}$$

$$V_j^* = \frac{\nu}{(\nu+\gamma_1^V)}\left(\prod_{i=2}^{j}\frac{\gamma_{i-1}^V}{(\nu+\gamma_i^V)}\right)\left(\frac{1}{2}(1-\frac{1}{\mathcal{R}_V}) + \sqrt{\left(\frac{1}{2}(1-\frac{1}{\mathcal{R}_V})\right)^2+\frac{p}{\mathcal{R}_V}}\right) \tag{3.15c}$$

$$I_j^* = 0 \tag{3.15d}$$

It should be noted that the equilibrium number of susceptibles, S^*, depends only on the reproduction numbers $\mathcal{R}_0$ and $\mathcal{R}_V$, and not on the durations of any of the stages. The non-negativity of the equilibrium (established in Appendix A of [32]) implies that the equilibrium lies in the biologically meaningful set $\mathcal{B}$.

Endemic Equilibrium

For $p < p_{\text{crit}}(1 - \frac{\mathcal{R}_V}{\mathcal{R}_0})$ there exists a unique endemic equilibrium. To see this, we first note that (3.12) holds, as does the analogous relationship for the infected classes,

$$I_j^* = \frac{\gamma_{j-1}^I}{(\nu + \gamma_j^I)} I_{j-1}^*, \qquad j \geq 2. \tag{3.16}$$

Applying Eqs. (3.16) and (3.9) to (3.11) at equilibrium yields

$$\left(\nu + \gamma_1^I\right)\left(1 - \mathcal{R}_0 S^*\right) = 0, \tag{3.17}$$

which is equivalent to

$$S^* = \frac{1}{\mathcal{R}_0}. \tag{3.18}$$

Similarly, applying (3.12), (3.9) and (3.) to Eq. (3.11b) yields

$$V_1^* = \frac{p\nu\mathcal{R}_0}{(\nu + \gamma_1^I)(\mathcal{R}_0 - \mathcal{R}_V)} \tag{3.19}$$

which is positive under the attenuation condition that $\mathcal{R}_V < \mathcal{R}_0$. Substituting expression (3.19) into (3.11) at equilibrium and again using (3.12), (3.9) and (3.16) yields

$$I_1^* = \frac{\nu}{(\nu + \gamma_1^I)}\left((1 - \frac{1}{\mathcal{R}_0}) - p\left(1 + \frac{\mathcal{R}_V}{(\mathcal{R}_0 - \mathcal{R}_V)}\right)\right) \tag{3.20}$$

We see that ${I_1}^* > 0$ if and only if $p < (1 - \frac{1}{\mathcal{R}_0})(1 - \frac{\mathcal{R}_V}{\mathcal{R}_0})$, and the *endemic equilibrium* may be expressed as

$$S^* = \frac{1}{\mathcal{R}_0} \tag{3.21a}$$

$$V_1^* = \left(\frac{p\nu\mathcal{R}_0}{(\nu + \gamma_1^V)(\mathcal{R}_0 - \mathcal{R}_V)}\right) \tag{3.21b}$$

$$V_j^* = \left(\frac{p\nu\mathcal{R}_0}{(\nu + \gamma_1^V)(\mathcal{R}_0 - \mathcal{R}_V)}\right)\left(\prod_{i=2}^{j}\frac{\gamma_{i-1}^V}{(\nu + \gamma_i^V)}\right) \tag{3.21c}$$

$$j = 2, \ldots, n$$

$${I_1}^* = \left(\frac{\nu}{(\nu + \gamma_1^I)}\right)\left((1 - \frac{1}{\mathcal{R}_0}) - p\left(1 + \frac{\mathcal{R}_V}{(\mathcal{R}_0 - \mathcal{R}_V)}\right)\right) \tag{3.21d}$$

$${I_j}^* = \left(\frac{\nu}{(\nu + \gamma_1^I)}\right)\left(\prod_{i=2}^{j}\frac{\gamma_{i-1}^I}{(\nu + \gamma_i^I)}\right)\left((1 - \frac{1}{\mathcal{R}_0}) - p\left(1 + \frac{\mathcal{R}_V}{(\mathcal{R}_0 - \mathcal{R}_V)}\right)\right) \tag{3.21e}$$

$$j = 2, \ldots, k$$

Again, the fact that the equilibrium is nonnegative implies that it lies in the biologically meaningful state region $\mathcal{B}$.

3.2.3 Global Stability Conditions

We use Lyapunov's direct method [23] to establish that the DFE is globally asymptotically stable if $p \geq p_{\text{crit}}(1 - \frac{\mathcal{R}_V}{\mathcal{R}_0})$ and that the endemic equilibrium is asymptotically stable if $p < p_{\text{crit}}(1 - \frac{\mathcal{R}_V}{\mathcal{R}_0})$.

The Lyapunov functions we construct are related to those used by Guo

and Li [15] to prove global stability in a standard epidemiological staged progression model. The Guo-Li functions are in turn generalizations of Lyapunov functions recently developed to prove global stability for a variety of epidemiological and ecological models [18, 19, 20, 21]. The primary reason that these methods work for a wide range of high-dimensional ecological and epidemiological models is that they do not rely on explicit equilibrium expressions. Instead, we only require implicit relationships among the parameters and equilibria (which are straightforwardly derived directly from the differential equations) and the positive invariance of the positive cone with respect to the dynamical system.

Global Stability of the Disease Free Equilibrium

To establish the global asymptotic stability of the DFE (3.15) when $p \geq p_{\text{crit}}(1 - \frac{\mathcal{R}_V}{\mathcal{R}_0})$ we first note that this condition is equivalent to the condition $S^* \leq \frac{1}{\mathcal{R}_0}$ (Appendix 3.7). We then proceed to construct a Lyapunov function of the form

$$L_{\text{DFE}} = L^1_{\text{DFE}} + L^2_{\text{DFE}} \tag{3.22a}$$

$$L^1_{\text{DFE}} = I_1 + \sum_{j=2}^{k} a_j I_j \tag{3.22b}$$

$$L^2_{\text{DFE}} = (S - S^* \ln(S)) + (V_1 - V_1^* \ln(V_1)) + \sum_{j=2}^{n} b_j \left(V_j - V_j^* \ln(V_j)\right) \tag{3.22c}$$

where a_j, b_j are appropriately chosen positive coefficients and $*$ denotes the equilibrium value at the DFE. We note that L_{DFE} has a global minimum (with respect to the positive cone) located at the DFE which we denote as $E^0 = (S^*, V_1^* \dots V_k^*, 0, \dots 0)$ and furthermore that for any variable P,

$$\frac{\partial}{\partial P}\left(P - P^* \ln\left(P\right)\right) = 1 - \frac{P^*}{P}. \tag{3.23}$$

Construction of L^1_{DFE}

We observe that Eqs. (3.11)–(3.15) can be written in the form

$$\frac{d}{dt}\begin{pmatrix} I_1 \\ I_2 \\ \vdots \\ I_k \end{pmatrix} = \begin{pmatrix} \sum_{j=1}^k \beta_j^1 I_j S \\ 0 \\ \vdots \\ 0 \end{pmatrix} - \mathcal{V}\begin{pmatrix} I_1 \\ I_2 \\ \vdots \\ I_k \end{pmatrix}, \tag{3.24}$$

where the $k \times k$ matrix $\mathcal{V}$ is given by

$$\mathcal{V} = \begin{pmatrix} -(\nu + \gamma_1^{\text{I}}) & & & & \\ \gamma_1^{\text{I}} & -(\nu + \gamma_2^{\text{I}}) & & & \\ & \gamma_2^{\text{I}} & -(\nu + \gamma_3^{\text{I}}) & & \\ & & \ddots & \ddots & \\ & & & \gamma_{k-1}^{\text{I}} & -(\nu + \gamma_k^{\text{I}}) \end{pmatrix}. \tag{3.25}$$

The matrix $\mathcal{V}$ has a non-negative inverse which can be computed directly as

$$\mathcal{V}^{-1} = \begin{pmatrix} \frac{1}{(\nu+\gamma_1^{\mathrm{I}})} & & \\ \frac{\gamma_1^{\mathrm{I}}}{(\nu+\gamma_1^{\mathrm{I}})(\nu+\gamma_2^{\mathrm{I}})} & \frac{1}{(\nu+\gamma_2^{\mathrm{I}})} & \\ \frac{\gamma_1^{\mathrm{I}}\gamma_2^{\mathrm{I}}}{(\mu+\gamma_1^{\mathrm{I}})(\nu+\gamma_2^{\mathrm{I}})(\nu+\gamma_3^{\mathrm{I}})} & \frac{\gamma_2^{\mathrm{I}}}{(\nu+\gamma_2^{\mathrm{I}})(\nu+\gamma_3^{\mathrm{I}})} & \frac{1}{(\nu+\gamma_3^{\mathrm{I}})} \\ \vdots & \vdots & \vdots \end{pmatrix} \ddots \tag{3.26}$$

Furthermore, $\mathcal{R}_0$ can be expressed in a straightforward manner [7, 31] in terms of $\mathcal{V}$ as

$$\mathcal{R}_0 = \begin{pmatrix} \beta_1^{\mathrm{I}} & \beta_2^{\mathrm{I}} & \dots & \beta_k^{\mathrm{I}} \end{pmatrix} \mathcal{V}^{-1} \begin{pmatrix} 1 \\ 0 \\ \vdots \\ 0 \end{pmatrix}. \tag{3.27}$$

Motivated by (3.24) and (3.27), we choose the coefficients a_j as

$$\begin{pmatrix} 1 & a_2 & \dots & a_k \end{pmatrix} = \frac{1}{\mathcal{R}_0} \begin{pmatrix} \beta_1^{\mathrm{I}} & \beta_2^{\mathrm{I}} & \dots & \beta_k^{\mathrm{I}} \end{pmatrix} \mathcal{V}^{-1}, \tag{3.28}$$

where we note that the leading coefficient is equal to 1 by construction (Eq. (3.27)).

It then follows from (3.22b), (3.24), ( ), and (3.28) that

$$\frac{d}{dt}L^1_{\text{DFE}} = \begin{pmatrix} 1 & a_2 & \dots & a_k \end{pmatrix} \frac{d}{dt} \begin{pmatrix} I_1 \\ I_2 \\ \vdots \\ I_k \end{pmatrix} = (S - \frac{1}{\mathcal{R}_0}) \sum_{j=1}^{k} \beta^1_j I_j \,. \qquad (3.29)$$

Construction of L^2_{DFE}

We first write obtain the required implicit equilibrium expressions among the state variables at S and $V_1, \dots, V_n$, namely

$$(1-p)\nu = \sum_{j=1}^{n} \beta^{\text{V}}_j V^*_j S^* + \nu S^* \qquad (3.30a)$$

$$\sum_{j=1}^{n} \beta^{\text{V}}_j V^*_j = (\gamma^{\text{V}}_1 + \nu) V^*_1 - p\nu \qquad (3.30b)$$

$$\frac{\gamma^{\text{V}}_{j-1} V^*_{j-1}}{(\nu + \gamma^{\text{V}}_j)} = V^*_j \,. \qquad j = 2, \dots, n. \qquad (3.30c)$$

From expressions (3.22c) and (3.23) we see that

$$\frac{d}{dt}L^2_{\text{DFE}} = (1 - \frac{S^*}{S})\frac{dS}{dt} + (1 - \frac{V^*_1}{V_1})\frac{dV_1}{dt} + \sum_{j=2}^{n} b_j (1 - \frac{V^*_j}{V_j})\frac{dV_j}{dt} \,. \qquad (3.31)$$

We select the coefficients b_j using the same inductive algorithm presented by Guo and Li [15], which yields

$$b_n = \frac{\beta_n^{\mathrm{V}} S^*}{(\nu + \gamma_n^{\mathrm{V}})} \tag{3.32a}$$

$$b_j = \frac{b_{j+1}\gamma_j^{\mathrm{V}} + \beta_j^{\mathrm{V}} S^*}{(\nu + \gamma_j^{\mathrm{V}})}, \qquad j = 2, \ldots, n-1. \tag{3.32b}$$

We note that the definition as V_n as the final class with nonzero vaccine virus infectivity, $\beta_n^{\mathrm{V}} > 0$, ensures that $b_j > 0$ for all j, and that recurrence relation (3.32) can be straightforwardly solved [15] to yield

$$b_j = \frac{\sum_{i=j}^{n} \beta_i^{\mathrm{V}} V_i^* S^*}{(\nu + \gamma_j^{\mathrm{V}}) V_j^*}. \qquad j = 2, \ldots, n. \tag{3.33}$$

We compute the first term of (3.31) as

$$\begin{aligned}
\left(1-\frac{S}{S^*}\right)\frac{dS}{dt} &= (1-p)\nu - \sum_{j=1}^{n}\beta_j^{\mathrm{V}}V_jS - \sum_{j=1}^{k}\beta_j^{\mathrm{I}}I_jS - \nu S \\
&\quad - (1-p)\nu\frac{S^*}{S} + \sum_{j=1}^{n}\beta_j^{\mathrm{V}}V_jS^* + \sum_{j=1}^{k}\beta_j^{\mathrm{I}}I_jS^* + \nu S^* \\
&= \sum\beta_j^{\mathrm{V}}V_j^*S^* + \nu S^* - \sum_{j=1}^{n}\beta_j^{\mathrm{V}}V_jS - \sum_{j=1}^{k}\beta_j^{\mathrm{I}}I_jS - \nu S \\
&\quad - \sum_{j=1}^{n}\beta_j^{\mathrm{V}}V_j^*\frac{S^{*2}}{S} - \nu\frac{S^{*2}}{S} + \sum_{j=1}^{n}\beta_j^{\mathrm{V}}V_jS^* + \sum_{j=1}^{k}\beta_j^{\mathrm{I}}I_jS^* + \nu S^* \\
&= \nu S^*\left(2-\frac{S}{S^*}-\frac{S^*}{S}\right) - \sum_{j=1}^{k}\beta_j^{\mathrm{I}}I_jS + \sum_{j=1}^{k}\beta_j^{\mathrm{I}}I_jS^* \\
&\quad - \sum_{j=1}^{n}\beta_j^{\mathrm{V}}V_jS + \sum_{j=1}^{n}\beta_j^{\mathrm{V}}V_jS^* + \sum_{j=1}^{n}\beta_j^{\mathrm{V}}V_j^*S^* - \sum_{j=1}^{n}\beta_j^{\mathrm{V}}\frac{S^{*2}}{S} \\
&\leq -\sum_{j=1}^{k}\beta_j^{\mathrm{I}}I_jS + \sum_{j=1}^{k}\beta_j^{\mathrm{I}}I_jS^* - \sum_{j=1}^{n}\beta_j^{\mathrm{V}}V_jS + \sum_{j=1}^{n}\beta_j^{\mathrm{V}}V_jS^* \\
&\quad + \sum_{j=1}^{n}\beta_j^{\mathrm{V}}V_j^*S^* - \sum_{j=1}^{n}\beta_j^{\mathrm{V}}\frac{S^{*2}}{S}.
\end{aligned} \tag{3.34}$$

In Eq. (3.34) we substitute for $(1-p)\nu$ using (3.30a) and in the final inequality we use the fact that $\left(2-\frac{S}{S^*}-\frac{S^*}{S}\right) \leq 0$ with equality only if $S = S^*$. This inequality is just a corollary of the fact that the arithmetic mean is always greater than or equal to the geometric mean (Appendix 3.6).

Computing the second term of (3.31), using (3.4) and (3.30b), we find

$$\begin{aligned}\left(1-\frac{V_1^*}{V_1}\right)\frac{d}{dt}V_1 &= p\nu - p\nu\frac{V_1^*}{V_1} + \sum_{j=1}^{n}\beta_j^{\mathrm{V}}V_jS - \left(\nu+\gamma_1^{\mathrm{V}}\right)V_1 \\ &\quad - \sum_{j=1}^{n}\beta_j^{\mathrm{V}}V_jS\frac{V_1^*}{V_1} + \left(\nu+\gamma_1^{\mathrm{V}}\right)V_1^* \\ &= 2p\nu - p\nu\frac{V_1^*}{V_1} + \sum_{j=1}^{n}\beta_j^{\mathrm{V}}V_jS - \left(\nu+\gamma_1^{\mathrm{V}}\right)V_1 \\ &\quad - \sum_{j=1}^{n}\beta_j^{\mathrm{V}}V_jS\frac{V_1^*}{V_1} + \sum_{j=1}^{n}\beta_j^{\mathrm{V}}V_j^*S^*.\end{aligned} \tag{3.35}$$

Now we proceed as in [15] to make the inductive choice of the coefficients b_j clear. For $j \geq 2$,

$$\begin{aligned}b_j\left(1-\frac{V_j^*}{V_j}\right)\frac{d}{dt}V_j &= b_j\gamma_{j-1}^{\mathrm{V}}V_{j-1} - b_j\left(\nu+\gamma_j^{\mathrm{V}}\right)V_j \\ &\quad - b_j\gamma_{j-1}^{\mathrm{V}}V_{j-1}\frac{V_j^*}{V_j} + b_j\left(\nu+\gamma_j^{\mathrm{V}}\right)V_j^*.\end{aligned} \tag{3.36}$$

Using the choice of the coefficients b_j ( ), we find

$$\begin{aligned}&\sum_{j=1}^{n}\beta_j^{\mathrm{V}}V_jS^* - \left(\nu+\gamma_1^{\mathrm{V}}\right)V_1 + \sum_{j=2}^{n}b_j\gamma_{j-1}^{\mathrm{V}}V_{j-1} - b_j\left(\nu+\gamma_j^{\mathrm{V}}\right)V_j \\ &\quad = \left(\beta_1^{\mathrm{V}}S^* - \left(\nu+\gamma_1^{\mathrm{V}}\right) + b_2\gamma_1^{\mathrm{V}}\right)V_1 + \left(\beta_n^{\mathrm{V}}S^* - b_n\left(\nu+\gamma_n^{\mathrm{V}}\right)\right)V_n \\ &\qquad + \sum_{j=2}^{n-1}\left(\beta_j^{\mathrm{V}}S^* + b_{j+1}\gamma_j^{\mathrm{V}} - b_j\left(\nu+\gamma_j^{\mathrm{V}}\right)\right)V_j \\ &\quad = \left(\beta_1^{\mathrm{V}}S^* - \left(\nu+\gamma_1^{\mathrm{V}}\right) + b_2\gamma_1^{\mathrm{V}}\right)V_1.\end{aligned} \tag{3.37}$$

Eq. (3.37) may be further simplified by substituting from Eq. (3.33) for b_2 and employing (3.30b) and (3.30c). In this way we find

$$\begin{aligned}
&\left(\beta_1^{\mathrm{V}} S^* - \left(\nu + \gamma_1^{\mathrm{V}}\right) + b_2 \gamma_1^{\mathrm{V}}\right) V_1 \\
&\quad = \left(\beta_1^{\mathrm{V}} S^* - \left(\nu + \gamma_1^{\mathrm{V}}\right) + \frac{\sum_{j=2}^{n} \beta_j^{\mathrm{V}} V_j^* S^*}{\left(\nu + \gamma_2^{\mathrm{V}}\right) V_2^*} \gamma_1^{\mathrm{V}}\right) V_1 \\
&\quad = \left(-\left(\nu + \gamma_1^{\mathrm{V}}\right) V_1^* + \sum_{j=1}^{n} \beta_j^{\mathrm{V}} V_j^* S^*\right) \frac{V_1}{V_1^*} \\
&\quad = -p\nu \frac{V_1}{V_1^*} .
\end{aligned} \tag{3.38}$$

Therefore, collecting terms from (3.37), (3.38), (3.35) and (3.31), we see that

$$\begin{aligned}
\frac{d}{dt}L^2_{\mathrm{DFE}} &\leq \left(\sum_{j=1}^{k}\beta_j^{\mathrm{I}}I_jS^* - \sum_{j=1}^{k}\beta_j^{\mathrm{I}}I_jS\right) + p\nu\left(2 - \frac{V_1^*}{V_1} - \frac{V_1}{V_1^*}\right) \\
&\quad + \left(-\sum_{j=1}^{n}\beta_j^{\mathrm{V}}V_j^*\frac{S^{*2}}{S} - \sum_{j=1}^{n}\beta_j^{\mathrm{V}}V_jS\frac{V_1^*}{V_1} - \sum_{j=2}^{n}\frac{b_j\gamma_{j-1}^{\mathrm{V}}V_{j-1}V_j^*}{V_j}\right) \\
&\quad + \left(\sum_{j=2}^{n}b_j\left(\nu+\gamma_j^{\mathrm{V}}\right)V_j^* + 2\sum_{j=1}^{n}\beta_j^{\mathrm{V}}V_j^*S^*\right) \\
&\leq \underbrace{\left(\sum_{j=1}^{k}\beta_j^{\mathrm{I}}I_jS^* - \sum_{j=1}^{k}\beta_j^{\mathrm{I}}I_jS\right)}_{F} \\
&\quad + \underbrace{\left(-\sum_{j=1}^{n}\beta_j^{\mathrm{V}}V_j^*\frac{S^{*2}}{S} - \sum_{j=1}^{n}\beta_j^{\mathrm{V}}V_jS\frac{V_1^*}{V_1} - \sum_{j=2}^{n}\frac{b_j\gamma_{j-1}^{\mathrm{V}}V_{j-1}V_j^*}{V_j}\right)}_{G} \\
&\quad + \underbrace{\left(\sum_{j=1}^{n}b_j\left(\nu+\gamma_j^{\mathrm{V}}\right)V_j^* + 2\sum_{j=2}^{n}\beta_j^{\mathrm{V}}V_j^*S^*\right)}_{H},
\end{aligned} \tag{3.39}$$

with equality if and only if $S = S^*$ and $V_1 = V_1^*$. The terms G and H may be simplified to show $G + H \leq 0$, precisely as in [15]. We include the argument here for the sake of completeness. Using the solution of the inductive relationship for the terms $b_j\left(\nu+\gamma_j^{\mathrm{V}}\right)V_j^*$ (3.33) yields

$$H = \sum_{j=2}^{n}b_j\left(\nu+\gamma_j^{\mathrm{V}}\right)V_j^* + 2\sum_{j=1}^{n}\beta_j^{\mathrm{V}}V_j^*S^* = \sum_{j=1}^{n}(j+1)\beta_j^{\mathrm{V}}V_j^*S^*. \tag{3.40}$$

Substituting for b_j in terms of (3.33), applying the equilibrium relationship (3.36c) and exchanging the order of summation, yields

$$\begin{aligned}\sum_{j=2}^{n}\frac{b_j\gamma_{j-1}^{\mathrm{V}}V_{j-1}V_j^*}{V_j} &= \sum_{j=2}^{n}\sum_{r=j}^{n}\beta_r^{\mathrm{V}}V_r^*S^*\frac{\gamma_{j-1}^{\mathrm{V}}V_{j-1}}{\left(\nu+\gamma_j^{\mathrm{V}}\right)V_j} \\ &= \sum_{j=2}^{n}\sum_{r=j}^{n}\beta_r^{\mathrm{V}}V_r^*S^*\frac{V_j^*V_{j-1}}{V_jV_{j-1}^*} = \sum_{j=2}^{n}\beta_j^{\mathrm{V}}V_j^*S^*\sum_{r=2}^{j}\frac{V_r^*V_{r-1}^*}{V_rV_{r-1}^*}.\end{aligned} \tag{3.41}$$

Using (3.33) and (3.41) yields the desired result

$$\begin{aligned}G+H &= \beta_1^{\mathrm{V}}V_1^*S^*(2-\frac{S^*}{S}-\frac{S}{S^*}) \\ &\quad+\sum_{j=2}^{n}\beta_j^{\mathrm{V}}V_j^*S^*\left((j+1)-\frac{S^*}{S}-\frac{SV_jV_1^*}{S^*V_j^*V_1}-\sum_{r=2}^{j}\frac{V_r^*V_{r-1}}{V_rV_{r-1}^*}\right) \\ &\leq 0,\end{aligned} \tag{3.42}$$

with equality if and only if $S = S^*$, $V_1 = V_1^*, \ldots, V_j = V_j^*$, since the arithmetic mean is always greater than the geometric mean (Appendix 3.6).

Combining (3.29), (3.39) and (3.42) yields

$$\frac{d}{dt}L_{\mathrm{DFE}} = \frac{d}{dt}L_{\mathrm{DFE}}^1 + \frac{d}{dt}L_{\mathrm{DFE}}^2 \leq \left(S^*-\frac{1}{\mathcal{R}_0}\right)\sum_{j=1}^{k}\beta_j^{\mathrm{I}}I_jS \tag{3.43}$$

Applying the result of Appendix 3.7, which states

$$S^* \leq \frac{1}{\mathcal{R}_0} \iff p \geq p_{\mathrm{crit}}\left(1-\frac{\mathcal{R}_{\mathrm{V}}}{\mathcal{R}_0}\right), \tag{3.44}$$

we obtain the desired result

$$p \geq p_{\text{crit}} \left(1 - \frac{\mathcal{R}_V}{\mathcal{R}_0}\right) \implies \frac{d}{dt} L_{\text{DFE}} \leq 0 \,, \tag{3.45}$$

with equality in Eq. (3.45) along a subset of $\mathcal{K} = \{(S, V_1, \ldots V_n, I_1 \ldots, I_k) : S = S^*, V_1 = V_1^*, \ldots, V_j = V_j^*\}$, containing the first $n+1$ coordinates of the DFE, $\mathbf{X}^0$. Notice that if $S^* = \frac{1}{\mathcal{R}_0}$ then equality in (3.45) holds everywhere in $\mathcal{K}$. However, it is evident from (3.4) that $\mathbf{X}^0$ is the only invariant subset of $\mathcal{K}$. Hence, the LaSalle Invariance Principle [23, 24] guarantees that $\mathbf{X}^0$ is globally asymptotically stable, completing the proof.

Global Stability of the Endemic Equilibrium

We employ a Lyapunov function of the standard form to prove that the endemic equilibrium (3.21) is globally asymptotically stable whenever it exists, i.e., if $p < p_{\text{crit}}(1 - \frac{\mathcal{R}_V}{\mathcal{R}_0})$. The Lyapunov function is

$$\begin{aligned} L_{\text{EE}} = &(S - S^* \ln(S)) + (I_1 - I_1{}^* \ln(I_1)) + (V_1 - V_1^* \ln(V_1)) \\ &+ \sum_{j=2}^{n} c_j \left(V_j - V_j^* \ln(V_j)\right) + \sum_{j=2}^{k} d_j \left(I_j - I_j{}^* \ln(I_j)\right) \,, \end{aligned} \tag{3.46}$$

where $*$ denotes the value at the endemic equilibrium (3.24). Again we choose the a_j, b_j by the inductive algorithm presented in [15], such that

$$c_n = \frac{\beta_n^{\mathrm{V}} S^*}{(\nu + \gamma_n^{\mathrm{V}})} \tag{3.47a}$$

$$c_j = \frac{c_{j+1}\gamma_j^{\mathrm{V}} + \beta_j^{\mathrm{V}} S^*}{(\nu + \gamma_j^{\mathrm{V}})} \quad j = 2 \ldots n-1 \tag{3.47b}$$

$$d_k = \frac{\beta_k^{\mathrm{I}} S^*}{(\nu + \gamma_k^{\mathrm{I}})} \tag{3.47c}$$

$$d_j = \frac{d_{j+1}\gamma_j^{\mathrm{I}} + \beta_j^{\mathrm{I}} S^*}{(\nu + \gamma_j^{\mathrm{I}})} \quad j = 2 \ldots k-1 \tag{3.47d}$$

Much of the analysis is identical to that of §3.2.3 of this paper and §5 of [15], so we highlight only the differences.

The equilibrium relationships, (3.30b) and (3.30c), still hold for the endemic equilibrium as they did for the DFE. However, Eq. (3.30a) is now replaced by the expression

$$(1-p)\nu = \sum_{j=1}^{n} \beta_j^{\mathrm{V}} V_j^* S^* + \sum_{j=1}^{k} \beta_j^{\mathrm{I}} I_j^* S^* + \nu S^* \tag{3.48}$$

and we now have the equilibrium relationships

$$\sum_{j=1}^{k} \beta_j^{\mathrm{I}} I_j^* S^* = \left(\nu + \gamma_1^{\mathrm{I}}\right) I_1^* \tag{3.49a}$$

$$\frac{\gamma_{j-1}^{\mathrm{I}} I_{j-1}^*}{(\nu + \gamma_j^{\mathrm{I}})} = I_j^* . \tag{3.49b}$$

We compute the first term of $\frac{d}{dt}L_{\text{EE}}$ analogously to (3.31), employing (3.48).

$$\begin{aligned}
\frac{\partial L_{\text{EE}}}{\partial S}\frac{d}{dt}S =& \left(1-\frac{S^*}{S}\right)\frac{dS}{dt} \\
=& \nu S^*\left(2-\frac{S}{S^*}-\frac{S^*}{S}\right) \\
&+\left(-\sum_{j=1}^{n}\beta_j^{\text{V}}V_jS+\sum_{j=1}^{n}\beta_j^{\text{V}}V_jS^*+\sum_{j=1}^{n}\beta_j^{\text{V}}V_j^*S^*-\sum_{j=1}^{n}\beta_j^{\text{V}}V_j^*\frac{S^{*2}}{S}\right) \\
&+\left(-\sum_{j=1}^{k}\beta_j^{\text{I}}I_jS+\sum_{j=1}^{k}\beta_j^{\text{I}}I_jS^*+\sum_{j=1}^{k}\beta_j^{\text{I}}I_j^*S^*-\sum_{j=1}^{k}\beta_j^{\text{I}}I_j^*\frac{S^{*2}}{S}\right) \\
\leq& \underbrace{\left(-\sum_{j=1}^{n}\beta_j^{\text{V}}V_jS+\sum_{j=1}^{n}\beta_j^{\text{V}}V_jS^*+\sum_{j=1}^{n}\beta_j^{\text{V}}V_j^*S^*-\sum_{j=1}^{n}\beta_j^{\text{V}}V_j^*\frac{S^{*2}}{S}\right)}_{A_{\text{V}}} \\
&+\underbrace{\left(-\sum_{j=1}^{k}\beta_j^{\text{I}}I_jS+\sum_{j=1}^{k}\beta_j^{\text{I}}I_jS^*+\sum_{j=1}^{k}\beta_j^{\text{I}}I_j^*S^*-\sum_{j=1}^{k}\beta_j^{\text{I}}I_j^*\frac{S^{*2}}{S}\right)}_{A_{\text{I}}}
\end{aligned} \tag{3.50}$$

with equality only when $S = S^*$. We now can split our calculations into

$$\begin{aligned}
\frac{d}{dt}L_{\text{EE}} \leq& \left(A_{\text{V}}+\left(1-\frac{V_1^*}{V_1}\right)\frac{d}{dt}V_1+\sum_{j=2}^{n}c_j\left(1-\frac{V_j}{V_j^*}\right)\frac{d}{dt}V_j\right) \\
&+\left(A_{\text{I}}+\left(1-\frac{I_1^*}{I_1}\right)\frac{d}{dt}I_1+\sum_{j=2}^{k}d_j\left(1-\frac{I_j}{I_j^*}\right)\frac{d}{dt}I_j\right)
\end{aligned} \tag{3.51}$$

The first term of (3.51) is exactly that computed in Eqs. (3.34)–(3.38), while the second term is exactly that computed in Eqs. (25)–(33) of [15]. We

therefore conclude that

$$\frac{d}{dt}L_{\text{END}} \leq 0, \tag{3.52}$$

with equality if and only if $S = S^*, V_1 = V_1^*, \ldots, V_j = V_j^*, I_1 = I_1^*, \ldots, I_j = I_j^*$. This confirms that the endemic equilibrium (3.21) is globally asymptotically stable when it exists.

3.2.4 Disease and Vaccine-Induced Mortality

The model (3.1) does not take into account the effects of disease or vaccine induced mortality. Using a related model, we take these factors into account. We demonstrate that inclusion of these effects does not change the qualitative results (stability thresholds). The staged-progression model we consider may be phrased in the following manner,

$$\frac{dS}{dt} = (1-p)B - \sum_{j=1}^{n}\beta_j^{\text{V}}V_jS - \sum_{j=1}^{k}\beta_j^{\text{I}}I_jS - \mu S \tag{3.53a}$$

$$\frac{dV_1}{dt} = pB + \sum_{j=1}^{n}\beta_j^{\text{V}}V_jS - \left(\mu + \gamma_1^{\text{V}} + \varepsilon_1^{\text{V}}\right)V_1 \tag{3.53b}$$

$$\frac{dV_2}{dt} = \gamma_1^{\text{V}}V_1 - \left(\mu + \gamma_2^{\text{V}} + \varepsilon_2^{\text{V}}\right)V_2 \tag{3.53c}$$

$$\vdots$$

$$\frac{dV_j}{dt} = \gamma_{j-1}^{\text{V}}V_{j-1} - \left(\mu + \gamma_j^{\text{V}} + \varepsilon_j^{\text{V}}\right)V_j \tag{3.53d}$$

$$\vdots$$

$$\frac{dV_n}{dt} = \gamma_{n-1}^{\text{V}}V_{n-1} - \left(\mu + \gamma_n^{\text{V}} + \varepsilon_n^{\text{V}}\right)V_n \tag{3.53e}$$

$$\frac{dI_1}{dt} = \sum_{j=1}^{k} \beta_j^{\mathrm{I}} I_j S - \left(\mu + \gamma_1^{\mathrm{I}} + \varepsilon_1^{\mathrm{I}}\right) I_1 \tag{3.53f}$$

$$\frac{dI_2}{dt} = \gamma_1^{\mathrm{I}} I_1 - \left(\mu + \gamma_2^{\mathrm{I}} + \varepsilon_2^{\mathrm{I}}\right) I_2 \tag{3.53g}$$

$$\vdots$$

$$\frac{dI_j}{dt} = \gamma_{j-1}^{\mathrm{I}} I_{j-1} - \left(\mu + \gamma_j^{\mathrm{I}} + \varepsilon_j^{\mathrm{I}}\right) I_j \tag{3.53h}$$

$$\vdots$$

$$\frac{dI_k}{dt} = \gamma_{k-1}^{\mathrm{I}} I_{k-1} - \left(\mu + \gamma_k^{\mathrm{I}} + \varepsilon_k^{\mathrm{I}}\right)) I_k \tag{3.53i}$$

$$\frac{dR}{dt} = \gamma_k^{\mathrm{I}} I_k + \gamma_n^{\mathrm{V}} V_n - \mu R \tag{3.53j}$$

In contrast to (3.4) the system (3.5) is phrased in terms of total population N rather than proportions. The total birth rate is give by B, $\varepsilon_j^{\mathrm{V}}$ and $\varepsilon_j^{\mathrm{I}}$ represent the vaccine and wild virus-induced death rates in each stage, while μ is the *per capita* natural death rate. The terms $\beta_j^{\mathrm{V}}, \beta_j^{\mathrm{I}}$ represent the total transmission rate of vaccine and wild virus in each stage. Note that this model assumes pseudo-mass action incidence β as opposed to standard incidence $\frac{\beta}{N}$. The previous LAVV models considered assumed standard incidence. Other parameters are as defined in (3.4).

The motivation for our departure from using proportional models is strictly mathematical in nature. As demonstrated in [16] for the proportional version of the standard SIR model with disease-induced mortality, inclusion of disease induced mortality results in quadratic terms not present in the original proportional model. Due to this fact, the form of Lyapunov functions used

to show stability in the absence of vaccine and disease-induced mortality can not be straightforwardly employed. However, the Lyapunov functions can be straightforwardly employed to the model written in terms of total population (3.53). In the absence of vaccine and disease induced mortality there is no difference between the models (3.53) and (3.1) after the latter is expressed in proportions.

Since the total birth rate is fixed, the model (3.53) will be valid over time periods for which the total birth rate is relatively stable. As previously noted the model (3.1) employs pseudo-mass action mixing as opposed to standard mass action mixing. This assumption is not biologically unrealistic, as pseudo-mass action mixing has been shown to successfully predict transitions in dynamics of childhood diseases [5, 11].

For system (3.53) the basic reproduction of the wild and vaccine virus are [15, 31]

$$\mathcal{R}_V = \frac{B}{\mu}\left(\frac{\beta_1^V}{(\mu+\gamma_1^V+\varepsilon_1^V)} + \sum_{j=2}^{n}\frac{\beta_j^V}{(\mu+\gamma_j^V+\varepsilon_j^V)}\left(\prod_{i=1}^{j-1}\frac{\gamma_i^V}{(\mu+\gamma_i^V+\varepsilon_i^V)}\right)\right) \tag{3.54a}$$

$$\mathcal{R}_0 = \frac{B}{\mu}\left(\frac{\beta_1^I}{(\mu+\gamma_1^I+\varepsilon_1^I)} + \sum_{j=2}^{k}\frac{\beta_j^I}{(\mu+\gamma_j^I+\varepsilon_j^I)}\left(\prod_{i=1}^{j-1}\frac{\gamma_i^I}{(\mu+\gamma_i^I+\varepsilon_i^I)}\right)\right). \tag{3.54b}$$

Straightforward computation establishes that system (3.53) has a unique

DFE given by

$$S^* = \frac{B}{\mu}\left(1 - \frac{1}{2}(1 - \frac{1}{\mathcal{R}_V}) - \sqrt{\left(\frac{1}{2}(1 - \frac{1}{\mathcal{R}_V})\right)^2 + \frac{p}{\mathcal{R}_V}}\right) \tag{3.55a}$$

$$V_1^* = \frac{B}{(\mu + \gamma_1^V + \varepsilon_1^V))}\left(\frac{1}{2}(1 - \frac{1}{\mathcal{R}_V}) + \sqrt{\left(\frac{1}{2}(1 - \frac{1}{\mathcal{R}_V})\right)^2 + \frac{p}{\mathcal{R}_V}}\right) \tag{3.55b}$$

$$V_j^* = \frac{B}{(\mu + \gamma_1^V + \varepsilon_1^V)}\left(\prod_{i=2}^{j}\frac{\gamma_{i-1}^V}{(\mu + \gamma_i^V + \varepsilon_i^V)}\right)\left(\frac{1}{2}(1 - \frac{1}{\mathcal{R}_V}) + \sqrt{\left(\frac{1}{2}(1 - \frac{1}{\mathcal{R}_V})\right)^2 + \frac{p}{\mathcal{R}_V}}\right), \tag{3.55c}$$

$$I_j^* = 0 \tag{3.55d}$$

and a unique *endemic equilibrium* given by

$$S^* = \frac{B}{\mu\mathcal{R}_0} \tag{3.56a}$$

$$V_1^* = \left(\frac{pB\mathcal{R}_0}{(\mu + \gamma_1^V + \varepsilon_1^V)(\mathcal{R}_0 - \mathcal{R}_V)}\right) \tag{3.56b}$$

$$V_j^* = \left(\frac{pB\mathcal{R}_0}{(\mu + \gamma_1^V + \varepsilon_1^V)(\mathcal{R}_0 - \mathcal{R}_V)}\right)\left(\prod_{i=2}^{j}\frac{\gamma_{i-1}^V}{(\mu + \gamma_i^V + \varepsilon_i^V)}\right) \tag{3.56c}$$

$j = 2, \ldots, n$

$$I_1^* = \left(\frac{B}{(\mu + \gamma_1^I + \varepsilon_1^I)}\right)\left((1 - \frac{1}{\mathcal{R}_0}) - p\left(1 + \frac{\mathcal{R}_V}{(\mathcal{R}_0 - \mathcal{R}_V)}\right)\right) \tag{3.56d}$$

$$I_j^* = \left(\frac{B}{(\mu + \gamma_1^I + \varepsilon_1^I)}\right)\left(\prod_{i=2}^{j}\frac{\gamma_{i-1}^I}{(\mu + \gamma_i^I + \varepsilon_i^I)}\right)\left((1 - \frac{1}{\mathcal{R}_0}) - p\left(1 + \frac{\mathcal{R}_V}{(\mathcal{R}_0 - \mathcal{R}_V)}\right)\right) \tag{3.56e}$$

$j = 2, \ldots, k$

By employing Lyapunov function analogous to those used to show global stability of the DFE and EE for the LAVV model (3.4), it is seen that the EE is globally asymptotically stable whenever $p < p_{\text{crit}}(1 - \frac{\mathcal{R}_V}{\mathcal{R}_0})$ while the DFE is globally asymptotically stable whenever $p \geq p_{\text{crit}}(1 - \frac{\mathcal{R}_V}{\mathcal{R}_0})$. The computations follow exactly from the stability proofs for system (3.4), therefore we don't repeat them here.

We see that incorporating vaccine and wild virus induced death rates, the stability threshold for wild virus eradication remains the same, specified by the reproduction numbers of the vaccine and wild virus.

3.2.5 Realistically distributed stage durations

An important feature of the general staged progression model that we have considered (3.4) is that any of the stages of infection can have durations that are distributed realistically (as opposed to exponentially). To illustrate this, we highlight the most important special case of (3.4), which is specified by

$$\gamma_j^V = n\sigma^V \qquad j = 1, \ldots, n \tag{3.57a}$$

$$\gamma_j^V = (m-n)\gamma^V \qquad j = n+1, \ldots, m \tag{3.57b}$$

$$\gamma_j^I = l\sigma^I \qquad j = 1, \ldots, l \tag{3.57c}$$

$$\gamma_j^I = (k-l)\gamma^I \qquad j = l+1, \ldots, k \tag{3.57d}$$

$$\beta_j^{\mathrm{V}} = 0 \qquad j = 1, \ldots, n \tag{3.57e}$$

$$\beta_j^{\mathrm{V}} = \beta^{\mathrm{V}} \qquad j = n+1, \ldots, m \tag{3.57f}$$

$$\beta_j^{\mathrm{I}} = 0 \qquad j = 1, \ldots, l \tag{3.57g}$$

$$\beta_j^{\mathrm{I}} = \beta^{\mathrm{I}} \qquad j = l+1, \ldots, k \tag{3.57h}$$

Here, Eqs. (3.57e) and (3.57g) define the first n vaccine virus compartments and l wild virus compartments to be latent. With these parameter relationships, the differential equations (3.4) model the situation where there is a single latent and infectious stage for each of the wild and vaccine viruses, but the stage durations are distributed according to Erlang distributions. The Erlang distribution is a special case of a Gamma distribution, namely

$$\mathrm{Gamma}\left(n, \frac{T}{n}\right), \tag{3.58}$$

where n is a positive integer specifying the shape of the distribution and T is the mean of the distribution (for the parameter choices indicated in Eq. (3.57), the means are $T = 1/\sigma^{\mathrm{V}}$, $1/\gamma^{\mathrm{V}}$, $1/\sigma^{\mathrm{I}}$ and $1/\gamma^{\mathrm{I}}$). The distribution $\mathrm{Gamma}(n, \frac{T}{n})$ has a probability density given by

$$g\left(x; n, \frac{T}{n}\right) = \frac{(n/T)^n}{\Gamma(n)} x^{n-1} e^{-nx/T}. \tag{3.59}$$

The Erlang distribution is representative of realistic latent and infectious periods, as it may be narrowly focused about the mean [3, 14, 25, 26, 32].

The extreme limits are the exponential distribution ($n = 1$) and the delta distribution ($n \to \infty$). Figure 3.5 shows the *probability density* for Erlang distributions with shape parameter ranging from 1 to 1000.

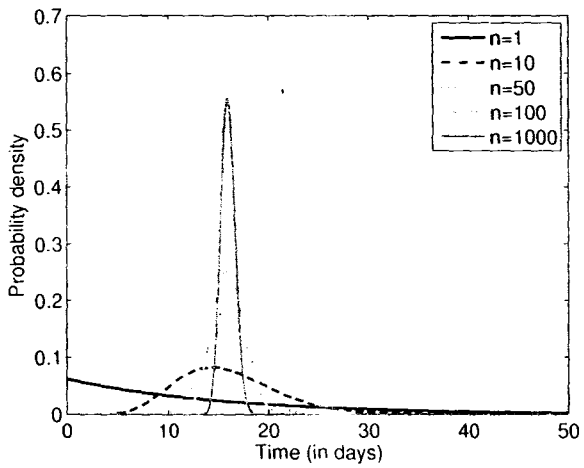

Figure 3.5: Probability density for an Erlang distribution of Gamma($n, \frac{16}{n}$), with mean 16 days and shape parameter n ranging from 1 (exponential) to 1000. As the shape parameter is increased the distribution becomes more closely focused about the mean.

While Eq. (3.57) specifies the parameter conditions that yield an SEIR model with Erlang distributed latent and infectious periods, the same approach can be applied to any stage of an arbitrary staged progression model. Consequently, our results are valid for the very general situation in which there are an arbitrary number of infectious stages for the wild and/or the vaccine virus, and where each stage has an Erlang distributed duration. Thus, regardless of how complex the sequence of infected stages are, the threshold for eradication is given by Eq. (3.2) and depends only upon the reproduction

numbers $\mathcal{R}_V$ and $\mathcal{R}_0$.

3.3 Contact Vaccination within a Pulse Vaccination Campaign

Contact vaccination within a pulse vaccination campaign may be described by the following equations, where the time interval between vaccination pulses is T. The underlying structure is based upon the standard (SIR) model [2].

$$\frac{dS}{dt} = \nu - \beta^{I}(t)IS - \beta^{V}(t)VS - \nu S - p_{\text{pulse}} \sum_{n} S(nT^{-})\delta(t - nT) \quad (3.60a)$$

$$\frac{dV}{dt} = p_{\text{pulse}} \sum_{n} S(nT^{-})\delta(t - nT) + \beta^{V}(t)VS - (\nu + \gamma^{V})V \quad (3.60b)$$

$$\frac{dI}{dt} = \beta^{I}(t)IS - (\nu + \gamma^{I})I \quad (3.60c)$$

$$\frac{dR}{dt} = \gamma^{I}I + \gamma^{V}V - \nu R \quad (3.60d)$$

Here, we use the notation

$$S(nT^{-}) = \lim_{\varepsilon \to 0^{+}} S(nT - \varepsilon)\,. \quad (3.60e)$$

and we assume

$$\beta^{V}(t+T) = \beta^{V}(t) \tag{3.60f}$$

$$\beta^{I}(t+T) = \beta^{I}(t)\,. \tag{3.60g}$$

Here, we ignore wild virus and vaccine virus specific death and express the model in terms of proportions. The parameter p_{pulse} is the pulse vaccination proportion, i.e., the proportion of susceptibles who are vaccinated during each vaccination pulse. Other quantities in (3.60) have the same meanings that they do in systems (3.1) and (3.1). For the sake of generality, we allow the vaccine virus transmission rate $\beta^{V}(t)$ and the wild virus transmission rate $\beta^{I}(t)$ to be time-dependent. However, we assume that the transmission rates are continuous functions of time and T-periodic. In practice, the pulse interval T will always be a multiple of one year, so we are including the possibility of any seasonal changes in transmission rates for any realistic pulse interval.

3.3.1 Existence of the Disease Free T-Periodic Solution

We prove in this subsection that for the system given by (3.60) a biologically meaningful T-periodic *disease free solution* (DFS) always exists. The stability of this solution, and the existence of multiple T-periodic disease free solutions, will be discussed in subsequent subsections.

Existence is shown in the following manner. Firstly, we enforce the disease

free condition, $I \equiv 0$, so Eq. (3.60c) is automatically satisfied and we are left with the reduced system

$$\frac{dS}{dt} = \nu - \beta^{\mathrm{V}}(t)VS - \nu S - p_{\mathrm{pulse}} \sum_n S(nT^-)\delta(t - nT) \tag{3.61a}$$

$$\frac{dV}{dt} = p_{\mathrm{pulse}} \sum_n S(nT^-)\delta(t - nT) + \beta^{\mathrm{V}}(t)VS - (\nu + \gamma^{\mathrm{V}})V\,. \tag{3.61b}$$

Eq. (3.61) is two dimensional and non-autonomous. Nevertheless, existence of a T-periodic solution may be shown by exploiting the theory of impulsive differential equations. We proceed by applying the methods described in [4]. The necessary definitions and notation (as in [4]) are summarized in Appendix 3.8 for reference.

We note that our system (3.61) can be rewritten in the form of Eq. (3.95) in Appendix 3.8 as

$$\left.\begin{aligned} \frac{dS}{dt} &= \nu - \beta^{\mathrm{V}}(t)VS - \nu S \\ \frac{dV}{dt} &= \beta^{\mathrm{V}}(t)VS - (\nu + \gamma^{\mathrm{V}})V \end{aligned}\right\} = g(t,x) \qquad t \neq kT \tag{3.62}$$

$$\begin{pmatrix} \Delta S \\ \Delta V \end{pmatrix} = (P - \mathcal{I}) \begin{pmatrix} S \\ V \end{pmatrix} \qquad t = kT$$

where $\Delta X \equiv X(kT^+) - X(kT^-)$, $\mathcal{I}$ is the identity matrix and

$$P = \begin{pmatrix} 1 - p_{\text{pulse}} & 0 \\ p_{\text{pulse}} & 1 \end{pmatrix} \tag{3.63}$$

As we are dealing with proportions of the population, the biologically meaningful set is $\mathcal{B} = \{(S, V) : S \geq 0, V \geq 0, S + V \leq 1\}$.

By assumption, $\beta^V(t)$ in (3.62) is continuous. In addition, conditions 1 and 3 of Appendix 3.8 are satisfied directly by Eqs. (3.62) and (3.63) with $\Omega = \mathcal{B}$. The set $\mathcal{B}$ is canonical in the sense of Appendix 3.8: Firstly, $\mathcal{B}$ is compact (closed and bounded) and convex. Secondly, $\mathcal{B}$ is specified by three inequalities, which—together with their respective Jacobians—are

$$\Phi_1(x) = -S \leq 0 \qquad \frac{\partial \Phi_1}{\partial (S, V)} = \begin{bmatrix} -1 & 0 \end{bmatrix} \tag{3.64a}$$

$$\Phi_2(x) = -V \leq 0 \qquad \frac{\partial \Phi_2}{\partial (S, V)} = \begin{bmatrix} 0 & -1 \end{bmatrix} \tag{3.64b}$$

$$\Phi_3(x) = S + V - 1 \leq 0 \qquad \frac{\partial \Phi_3}{\partial (S, V)} = \begin{bmatrix} 1 & 1 \end{bmatrix} \tag{3.64c}$$

We next note that for $x \in \partial\mathcal{B}$

$$1 \in \alpha(x) \quad \text{if } S = 0 \tag{3.65a}$$

$$2 \in \alpha(x) \quad \text{if } V = 0 \tag{3.65b}$$

$$3 \in \alpha(x) \quad \text{if } S + V = 1 \tag{3.65c}$$

where $\alpha(x) = \{i : \Phi_i(x) = 0\}$, as defined in Appendix 3.8. This implies that for $i \in \alpha(x)$ and $x \in \partial\mathcal{B}$

$$\frac{\partial \Phi_1}{\partial x}(x)g(t,x) = -\nu \tag{3.66a}$$

$$\frac{\partial \Phi_2}{\partial x}(x)g(t,x) = 0 \tag{3.66b}$$

$$\frac{\partial \Phi_3}{\partial x}(x)g(t,x) = -\gamma^{\mathrm{V}}V \leq 0 \tag{3.66c}$$

Additionally

$$\Phi_i\left(P\begin{pmatrix} S \\ V \end{pmatrix}\right) \leq 0 \tag{3.67}$$

since P is a linear function whose matrix representation has non-negative entries and column sums equal to one (3.64) (hence P maps $\mathcal{B}$ to $\mathcal{B}$). From a biological perspective, P moves individuals from the susceptible to the vaccinated class but does not result in a net change in the number of individuals, hence maintaining the positive invariance of $\mathcal{B}$.

Therefore, by Theorem 1 of Appendix 3.8, the system (3.61)—and hence the original pulse vaccination system given by (3.60)—possesses a biologically meaningful T-periodic DFS.

3.3.2 Stability of the T-Periodic Disease Free Solution

Necessary Conditions

Having shown that a disease free T-periodic solution always exists, we now seek to discover under what conditions this solution is asymptotically stable. To this end we investigate the variational equation obtained from linearization of system (3.60) about the disease free T-periodic solution which we denote $\{S(t) = \widehat{S(t)}, V(t) = \widehat{V(t)}, I(t) = 0\}$. The variational equation that governs the growth and decay of small perturbations (s, v, i) about the DFS is given as follows, where $\dot{x}$ denotes the time derivative of x. For $t \neq kT$,

$$\begin{pmatrix} \dot{s} \\ \dot{v} \\ \dot{i} \end{pmatrix} = \begin{pmatrix} -\beta^{\mathrm{V}}(t)\widehat{V(t)} - \nu & -\beta^{\mathrm{V}}(t)\widehat{S(t)} & -\beta^{\mathrm{I}}(t)\widehat{S(t)} \\ \beta^{\mathrm{V}}(t)\widehat{V(t)} & \beta^{\mathrm{V}}(t)\widehat{S(t)} - (\nu + \gamma^{\mathrm{V}}) & 0 \\ 0 & 0 & \beta^{\mathrm{I}}(t)\widehat{S(t)} - (\nu + \gamma^{\mathrm{I}}) \end{pmatrix} \begin{pmatrix} s \\ v \\ i \end{pmatrix} \tag{3.68a}$$

while for $t = kT$,

$$\begin{pmatrix} s(kT) \\ v(kT) \\ i(kT) \end{pmatrix} = \begin{pmatrix} (1-p) & 0 & 0 \\ p & 1 & 0 \\ 0 & 0 & 1 \end{pmatrix} \begin{pmatrix} s(kT^-) \\ v(kT^-) \\ i(kT^-) \end{pmatrix}. \tag{3.68b}$$

The fundamental matrix solution $\Psi(t)$ of (3.68a) is defined to be

$$\Psi(t) = \begin{pmatrix} s_1 & s_2 & s_3 \\ v_1 & v_2 & v_3 \\ i_1 & i_2 & i_3 \end{pmatrix} \tag{3.69a}$$

$$\Psi(0) = \mathcal{I} \tag{3.69b}$$

where each column of (3.69a) is a solution of (3.68a). The stability of the T-periodic solution is determined by the eigenvalues of $\Psi(t)$ evaluated at time $t = T$. This result is explained by standard Floquet theory [26]. For any small perturbation from the DFS which we denote $\varepsilon_S^0, \varepsilon_V^0, \varepsilon_I^0$, the growth of the perturbation is given to first order in ε as

$$\begin{pmatrix} \varepsilon_S(T) \\ \varepsilon_V(T) \\ \varepsilon_I(T) \end{pmatrix} = \Psi(T) \begin{pmatrix} \varepsilon_S^0 \\ \varepsilon_V^0 \\ \varepsilon_I^0 \end{pmatrix} \tag{3.70}$$

Eq. (3.70) implies that

$$||\varepsilon(T)|| \leq ||\Psi(T)||\,||\varepsilon^0|| = \max_{i=1,2,3} |\lambda_i(\Psi(T))|\,||\varepsilon^0||, \tag{3.71}$$

where λ_i denotes an eigenvalue of $\Psi(T)$. Therefore, if all eigenvalues of $\Psi(T)$ have magnitude less than one, any perturbations will decay at least geometrically with every period T and the DFS will be (locally) asymptotically

stable.

Although there is no general method for constructing the fundamental matrix, much can still be said about it. It can be seen from (3.68a) that the equation for the perturbation $i(t)$ is decoupled from the rest of the system and thus can be explicitly solved as

$$i(t) = i(0)e^{\int_0^t \beta^1(r)\widehat{S(r)} - (\nu+\gamma^1)dr} . \tag{3.72}$$

As a result, we can slightly simplify the form of the fundamental matrix and write

$$\Psi(T) = \begin{pmatrix} \Psi_{11}(T) & \Psi_{12}(T) & \Psi_{13}(T) \\ \Psi_{21}(T) & \Psi_{22}(T) & \Psi_{23}(T) \\ 0 & 0 & e^{\int_0^T [\beta^1(t)\widehat{S(t)} - (\nu+\gamma^1)]\,dt} \end{pmatrix} . \tag{3.73}$$

Because the eigenvalues of block diagonal matrices are the eigenvalues of each of the blocks, the form of (3.73) implies that one of the eigenvalues of $\Psi(T)$ is

$$\lambda_3 = e^{[\int_0^T \beta^1(t)\widehat{S(t)}\,dt] - (\nu+\gamma^1)T} , \tag{3.74}$$

The T-periodic solution (DFS) will be local asymptotically stable if

$$\max_{i=1,2,3} |\lambda_i(\Psi(T))| < 1 , \tag{3.75}$$

and only if

$$\max_{i=1,2,3} |\lambda_i(\Psi(T))| \leq 1 . \tag{3.76}$$

Inserting (3.74) in (3.76) gives a necessary condition for stability,

$$|\lambda_3| \leq 1 \iff \int_0^T \beta^{\mathrm{I}}(t)\widehat{S(t)}\,dt \leq (\nu + \gamma^{\mathrm{I}})T\,. \tag{3.77}$$

A complete closed-form analytical expression for the Ψ_{ij} cannot in general be computed, so we will be forced to complete the stability analysis numerically. If condition (3.77) is satisfied then the stability of the DFS will be determined by the eigenvalues of the smaller matrix

$$\Psi_{\text{reduced}}(T) = \begin{pmatrix} \Psi_{11}(T) & \Psi_{12}(T) \\ \Psi_{21}(T) & \Psi_{22}(T) \end{pmatrix}. \tag{3.78}$$

$\Psi_{\text{reduced}}(T)$ may be thought of as the fundamental matrix solution of the variational equation (3.68a) restricted to the (S, V) plane. In the following sections we will numerically investigate the eigenvalues of this matrix to determine the stability of the DFS.

It is enlightening to note that if the transmission rate $\beta^{\mathrm{I}}(t) = \beta^{\mathrm{I}}$, a constant, then expression (3.77) simplifies to the ubiquitous condition [8, 29, 30]

$$\frac{1}{T}\int_0^T \widehat{S(t)}\,dt \leq \frac{\gamma^{\mathrm{I}} + \nu}{\beta^{\mathrm{I}}} = \frac{1}{\mathcal{R}_0}\,, \tag{3.79}$$

which states that the average proportion of the population that is susceptible (over a pulse interval T) must be kept below the threshold level $\frac{1}{\mathcal{R}_0}$. The general necessary condition (3.77) is different only in that the average of

$\widehat{S(t)}$ is weighted by the oscillation in transmission rate.

Sufficient conditions for Stability

For the remainder of our analysis, we focus on the case of constant transmission: $\beta^{\mathrm{V}}(t) = \beta^{\mathrm{V}}$, $\beta^{\mathrm{I}}(t) = \beta^{\mathrm{I}}$. The T-periodic DFS will be asymptotically stable whenever

$$\frac{1}{T}\int_0^T \widehat{S(t)}dt < \frac{1}{\mathcal{R}_0} \tag{3.80a}$$

$$\max_{i=1,2} |\lambda_i(\Psi_{\text{reduced}}(T))| < 1 \tag{3.80b}$$

In Eq. (3.80b) λ_i denotes the floquet multipliers, eigenvalues of $\Psi_{\text{reduced}}(T)$, where $\Psi_{\text{reduced}}(t)$ is fundamental matrix solution of the variational equation about the T-periodic DFS $(\widehat{S(t)}, \widehat{V(t)})$. The variational equation is given by

$$\begin{pmatrix} \dot{s} \\ \dot{v} \end{pmatrix} = \begin{pmatrix} -\beta^{\mathrm{V}}\widehat{V(t)} - \nu & -\beta^{\mathrm{V}}\widehat{S(t)} \\ \beta^{\mathrm{V}}\widehat{V(t)} & \beta^{\mathrm{V}}\widehat{S(t)} - (\nu + \gamma^{\mathrm{V}}) \end{pmatrix} \begin{pmatrix} s \\ v \end{pmatrix} \quad t \neq kT \tag{3.81a}$$

$$s(kT) = (1 - p_{\text{pulse}})\, s(kT^-) \tag{3.81b}$$

$$v(kT) = v(kT^-) + p_{\text{pulse}}\, s(kT^-) \tag{3.81c}$$

$$s(kT^-) = \lim_{\varepsilon \to 0^+} s(kT - \varepsilon) \tag{3.81d}$$

As there is no general analytical method for computing the fundamental matrix solution of the non-autonomous equation (3.81) we compute the eigenvalues of $\Psi_{\text{reduced}}(T)$ numerically. We define a non-linear map as the integration $\int_0^T$ of system (3.61) using a fourth-order Runge Kutta scheme with stepsize of $\frac{1}{2}$ day. The T periodic DFS is the fixed point of this map. Beginning from a known solution ($\mathcal{R}_V = 0$) or one obtained numerically from successive integrations of the map, we use the bifurcation and continuation analysis software CONTENT 1.5 [22] to numerically continue the T periodic DFS as a function of the system parameters and compute the Floquet multipliers (3.805). We subsequently investigate global stability via simulation in MATLAB, using a fourth order adaptive stepsize routine.

So far, we have focused on the T-periodic DFS that we know exists. Our analysis does not rule out the possibility of multiple coexisting period-T or period-kT disease free solutions, or more complicated dynamics. We address these issues in our numerical analysis in the next subsection.

Uniqueness of Disease Free Solutions

Pulse vaccination without transmission of vaccine virus ($\mathcal{R}_V = 0$) has been well studied. In this case there exists a *unique* T-periodic DFS which can be computed straightforwardly. Furthermore, for a given vaccination proportion of susceptibles (p_{pulse} in (3.60)) there exists a maximum pulsing period $T_{\max}$ for which this DFS is globally asymptotically stable [10, 30, 29]. The fundamental idea that local stability of the T-periodic DFS in fact implies global

stability has been extended to SEIR type models with Gamma distributed latent and infectious periods [8, 9].

In the numerical analysis we now describe, we considered vaccine virus in the fairly large range $0 < \mathcal{R}_V \leq 7$. The birth rate was fixed at $\nu = 0.02\,\mathrm{yr}^{-1}$ and the vaccine virus infectious period was taken to be $\frac{1}{\gamma_V} = 16\,\mathrm{days}$, roughly corresponding to wild poliovirus [2]. For $\mathcal{R}_V \leq 5$ and $T = 1, 2, 3$ years, the T-periodic DFS was computed via continuation in CONTENT 1.5, and found to be always locally stable in the (S, V) plane (3.8(b)). Subsequent simulations indicated that the computed DFS is likely the unique stable DFS in this parameter range. For $T = 6$ years, the same results hold for $0 < \mathcal{R}_V \leq 4$, with a seemingly unique DFS that is locally asymptotically stable in the (S, V) plane. (We note that in their continuous OPV vaccination models, Eichner and Hadeler [12] considered $\mathcal{R}_0 = 12$ and $\mathcal{R}_V = 3$.)

For higher $\mathcal{R}_V$, holding $\mathcal{R}_V$ fixed and varying the pulsing proportion ($0 \leq p_{\mathrm{pulse}} \leq 1$) we observe a sequence of limit point bifurcations resulting in bistability and hysteresis. As a two-parameter bifurcation in $(p_{\mathrm{pulse}}, \mathcal{R}_V)$ space, this is manifested as a cusp bifurcation starting at $\mathcal{R}_V > 4$. Figure 3.9 shows the coexisting stable and unstable DFS in (S, V) space for $T = 6$, $\mathcal{R}_V = 7$. The bifurcation parameter is the pulse vaccination proportion p_{pulse} while the vertical axis gives the proportion of the susceptible population immediately before the vaccination pulse, which we denote $S(T^-)$. The solid line denotes stable solution branches in (S, V) space, while the dashed lines denote unstable branches.

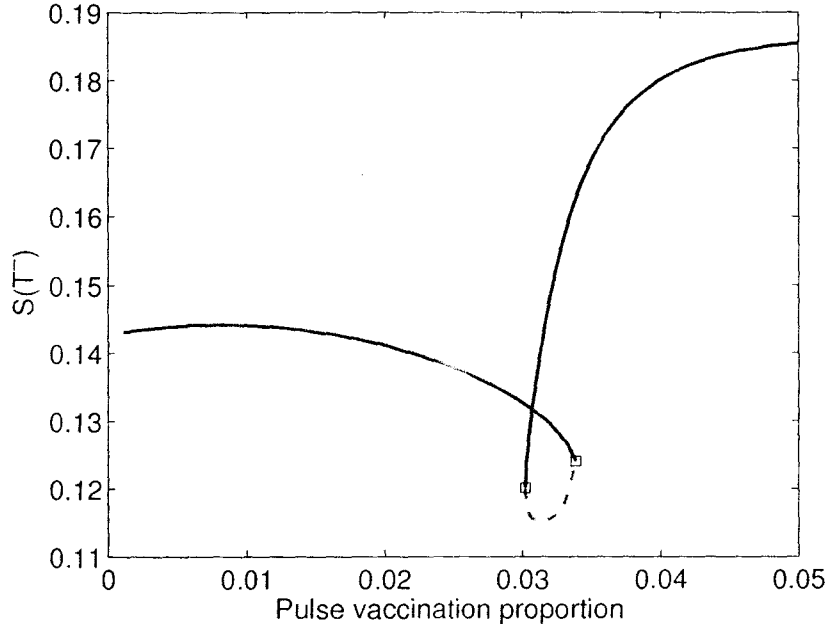

Figure 3.6: Bifurcation diagram for the $T = 6$ periodic *disease free solution* in the (S, V) plane ($\mathcal{R}_V = 7$, $\frac{1}{\gamma_V} = 16$ days, $\nu = 0.02$). The bifurcation parameter is p_{pulse}, the pulse vaccination proportion, while the dependent parameter is $S(T^-)$, the proportion of susceptibles immediately before the vaccination pulse. The (S, V) stable solution branches are shown with solid lines, unstable branches with dashed lines. Black rectangles indicate the location of the limit point bifurcations. The system exhibits bistability and hysteresis in the narrow range $0.030 < p_{\text{pulse}} < 0.035$.

There are two coexisting (S, V) stable DFSs in a narrow range of the proportion of susceptibles vaccinated ($0.030 \leq p_{\text{pulse}} \leq 0.035$). For smaller $\mathcal{R}_V$ this window is even narrower and closer to zero. The significance of the two coexisting DFSs is negligible in practice. These coexisting solutions are asymptotically stable in the (S, V) plane; however, to be stable in the full (S, V, I) space (3.60), condition (3.79) must also be satisfied. For the range of p_{pulse} where there is bistability, computing the average level of susceptibles for each DFS over the pulsing period T, and enforcing the stability condition (3.79), we find numerically that

$$\frac{1}{T}\int_0^T \widehat{S(t)}\, dt \leq \frac{1}{\mathcal{R}_0} \iff \mathcal{R}_V \approx \mathcal{R}_0 \tag{3.82}$$

So, the coexisting (S, V) stable DFSs will be stable in the full (S, V, I) space only if $\mathcal{R}_V \approx \mathcal{R}_0$. Result (3.82) may be intuitively obvious as the parameter range of bistability occurs when p_{pulse} is very close to zero. For example, if a single vaccinated person were introduced into a population with no other vaccination, the wild virus could only be eradicated if $\mathcal{R}_V > \mathcal{R}_0$. This is to say that the vaccine virus must out-compete the wild virus. Similarly for only a small amount of vaccination, the vaccine virus must remain almost as competitive as the wild virus in order to achieve eradication.

The attenuation process results in vaccine virus reproduction numbers $\mathcal{R}_V$ that are significantly lower than the wild virus $\mathcal{R}_0$; hence, we expect the coexisting DFS to be unstable in the full sense of the model (3.60) for all

realistic parameters. Furthermore, no bifurcations– cusp or otherwise – were detected for $T = 1, 2, 3$ years. Thus, we find that for realistic epidemiological parameters the full epidemiological system exhibits at most one asymptotically stable DFS.

3.4 Control of Wild Virus Spread

We now consider the control implications of the combination of pulse vaccination and contact vaccination, which we will abbreviate to "PC vaccination" for convenience. We analyze our model ( ) with two comparisons in mind, both related to the ability of contact vaccination to help control wild virus spread.

3.4.1 Definitions and Terminology

PC versus standard pulse vaccination

Firstly, we wish to compare the efficacy of PC vaccination to that of standard pulse vaccination (i.e., pulse vaccination in the absence of vaccine virus transmission). This comparison may be achieved straightforwardly by examining $p_{\text{pulse,crit}}$, the threshold level of the pulse vaccination parameter p_{pulse} required for asymptotic stability of the DFS (note that $p_{\text{pulse,crit}}$ depends on the pulse interval T).

For convenience, we define a normalized critical pulse proportion as

$$\widehat{p}_{\text{pulse,crit}}(\mathcal{R}_{\text{V}}, \mathcal{R}_0) = \frac{p_{\text{pulse,crit}}(\mathcal{R}_{\text{V}}, \mathcal{R}_0)}{p_{\text{pulse,crit}}(0, \mathcal{R}_0)}, \tag{3.83}$$

which represents the value of $p_{\text{pulse,crit}}$ normalized by the value of $p_{\text{pulse,crit}}$ in the absence of contact vaccination ($\mathcal{R}_{\text{V}} = 0$). Therefore, definition (3.83) gives the critical pulse vaccination proportion as a proportion of the critical value under standard pulse vaccination.

PC versus CC vaccination

Secondly, we wish to answer whether—in the presence of contact vaccination—pulse vaccination campaigns (i.e., PC vaccination) will be more or less effective in controlling wild virus spread than continuous vaccination campaigns (i.e., CC vaccination). This second question is not as straightforward to answer, as there are many ways to compare the continuous (3.4) and pulse (3.66) vaccination models.

One relevant measure of comparison is the critical effective pulse vaccination proportion $p_{\text{eff,crit}}$ required to ensure stability of the DFS. We define the effective pulse vaccination proportion to be the number of successful vaccinations per pulsing period as a proportion of births over that same period,

$$p_{\text{eff}} = \frac{\text{vaccinations per pulse interval } T}{\nu T} \tag{3.84}$$

Definition (3.84) is natural since in the case of continuous vaccination it re-

duces to the standard parameter p, the proportion of newborns vaccinated. Thus, for continuous vaccination $p_{\text{eff,crit}}$ can be computed analytically, while for pulse vaccination we compute it numerically. The critical values for continuous and pulse vaccination are given, respectively, by

$$p_{\text{eff,crit}}(\mathcal{R}_V, \mathcal{R}_0) = p_{\text{crit}}\left(1 - \frac{\mathcal{R}_V}{\mathcal{R}_0}\right) \qquad \text{continuous} \qquad (3.85a)$$

$$p_{\text{eff,crit}}(\mathcal{R}_V, \mathcal{R}_0) = \frac{p_{\text{pulse,crit}}\, S(T^-)}{\nu T} \qquad \text{pulse} \qquad (3.85b)$$

In Eq. (3.85b), $S(T^-)$ is the proportion of the population that is susceptible immediately before the vaccination pulse (in the T-periodic DFS with $p_{\text{pulse}} = p_{\text{pulse,crit}}$).

In the absence of contact vaccination ($\mathcal{R}_V = 0$) the value of $p_{\text{eff,crit}}$ is in fact equivalent for both continuous and pulse vaccination, independent of the vaccination period T [8, 29]. This fact is illustrated in Figure 3.7a which shows $p_{\text{eff,crit}}$ for $\mathcal{R}_V = 0$ as a function of $\mathcal{R}_0$ for pulsing periods of $T = 1, 2, 3, 6$ years. The result is a single curve $p_{\text{crit}} = (1 - \frac{1}{\mathcal{R}_0})$ as predicted by Eq. (3.85a).

Due to this equality it is useful to define normalized quantities to compare CC and PC vaccination programs. We normalize by the value p_{crit}, the value of $p_{\text{eff,crit}}$ when $\mathcal{R}_V = 0$. We define $\widehat{p}_{\text{eff,crit}}$ to be the normalized critical effective vaccination proportion which can be expressed for continuous and

pulse vaccination programs respectively as

$$\widehat{p}_{\text{eff,crit}}(\mathcal{R}_V, \mathcal{R}_0) = 1 - \frac{\mathcal{R}_V}{\mathcal{R}_0} \qquad \text{continuous} \qquad (3.86a)$$

$$\widehat{p}_{\text{eff,crit}}(\mathcal{R}_V, \mathcal{R}_0) = \frac{p_{\text{eff,crit}}(\mathcal{R}_V, \mathcal{R}_0)}{p_{\text{eff,crit}}(0, \mathcal{R}_0)} \qquad \text{pulse} \qquad (3.86b)$$

$$p_{\text{eff,crit}}(0, \mathcal{R}_0) = p_{\text{crit}} \qquad (3.86c)$$

3.4.2 Numerical Results

PC versus CC

Figures 3.8(a)-(d) show the normalized critical effective vaccination proportion $\widehat{p}_{\text{eff,crit}}$ as a function of $\mathcal{R}_V$ for wild viruses with $\mathcal{R}_0 = 6, 9, 14, 16$. Vaccine virus reproduction numbers are considered in the range $0 \leq \mathcal{R}_V \leq 4$. The solid line in each figure represents $\widehat{p}_{\text{eff,crit}}$ for continuous vaccination given by the analytical expression (3.86a).

It is apparent that continuous vaccination gives a lower bound for $\widehat{p}_{\text{eff,crit}}$. Furthermore, we see that for the pulse vaccination strategies $\widehat{p}_{\text{eff,crit}}$ increases as both the pulsing period and $\mathcal{R}_0$ are increased. However, for annual pulsing, $\widehat{p}_{\text{eff,crit}}$ differs negligibly from the threshold (3.86a) for continuous vaccination. The two curves are indistinguishable for $\mathcal{R}_0 = 6$, and even for $\mathcal{R}_0 = 16$, $\widehat{p}_{\text{eff,crit}}$ values differ by less than 4%. For biennial pulses there is little difference between the pulse and the continuous vaccination value of $\widehat{p}_{\text{eff,crit}}$, especially for lower $\mathcal{R}_0$ values. For $\mathcal{R}_0 = 16$, the biennial pulse and continuous vaccination curves differ maximally by less than 6%. For $T = 6$, the pulse and continuous

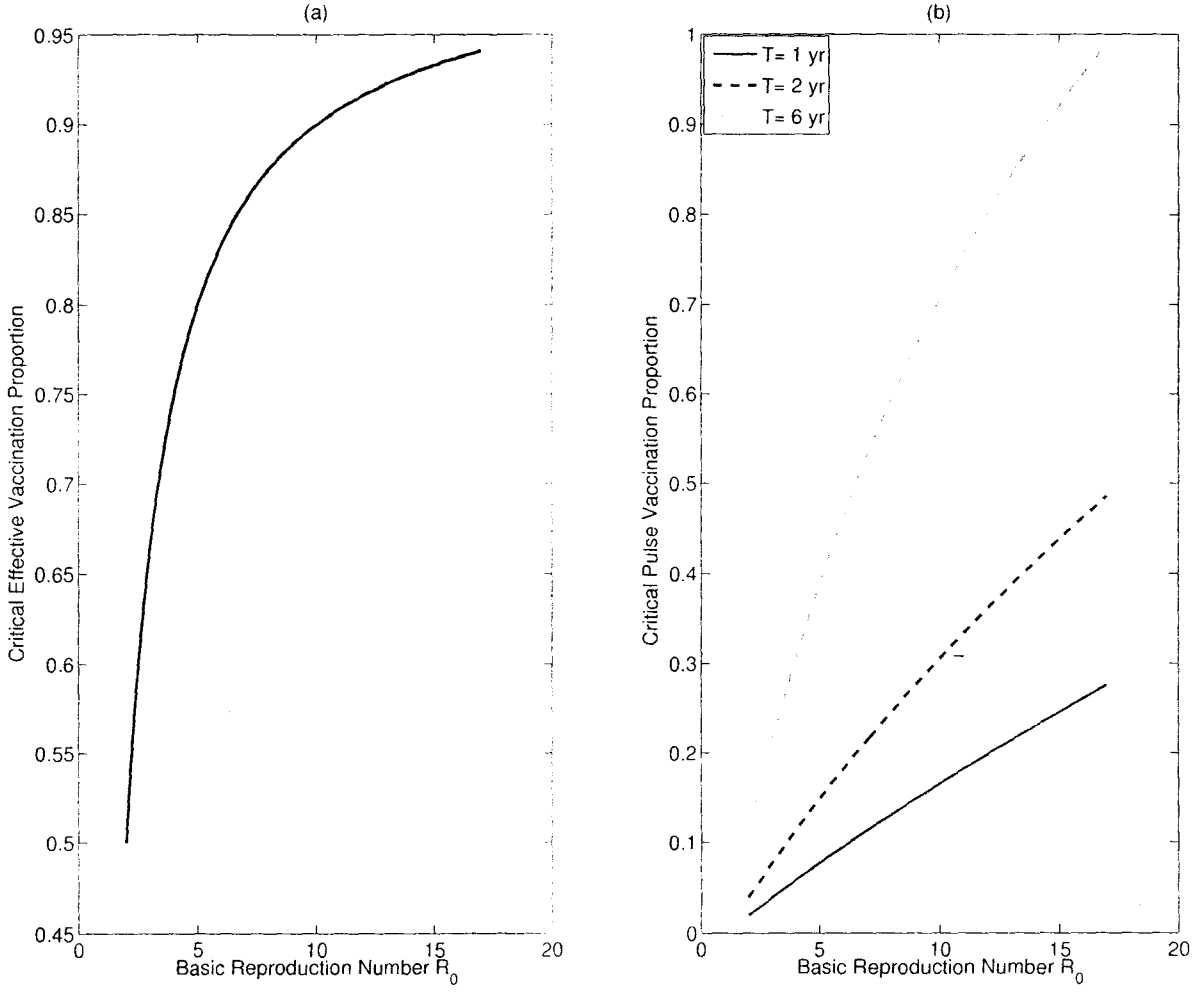

Figure 3.7: (a) Critical effective vaccination proportion $p_{\text{eff,crit}}$ in the absence of contact vaccination ($\mathcal{R}_V = 0$) as a function of wild virus reproduction basic reproduction number $\mathcal{R}_0$. For continuous vaccination as well as pulse vaccination the curve is given by $p_{\text{eff,crit}} = p_{\text{crit}} = (1 - \frac{1}{\mathcal{R}_0})$ independent of the pulsing period T. (b) Critical pulse vaccination proportion $p_{\text{pulse,crit}}$ in the absence of contact vaccination $\mathcal{R}_V = 0$ as a function of wild virus basic reproduction number $\mathcal{R}_0$. Pulsing periods of $T = 1, 2, 6$ years are considered. $p_{\text{pulse,crit}}$ increases non-linearly with $\mathcal{R}_0$. Note that higher T and $\mathcal{R}_0$ values necessitate vaccination of nearly all susceptibles. However, for annual and biennial pulses $p_{\text{pulse,crit}}$ remains in a realistic range

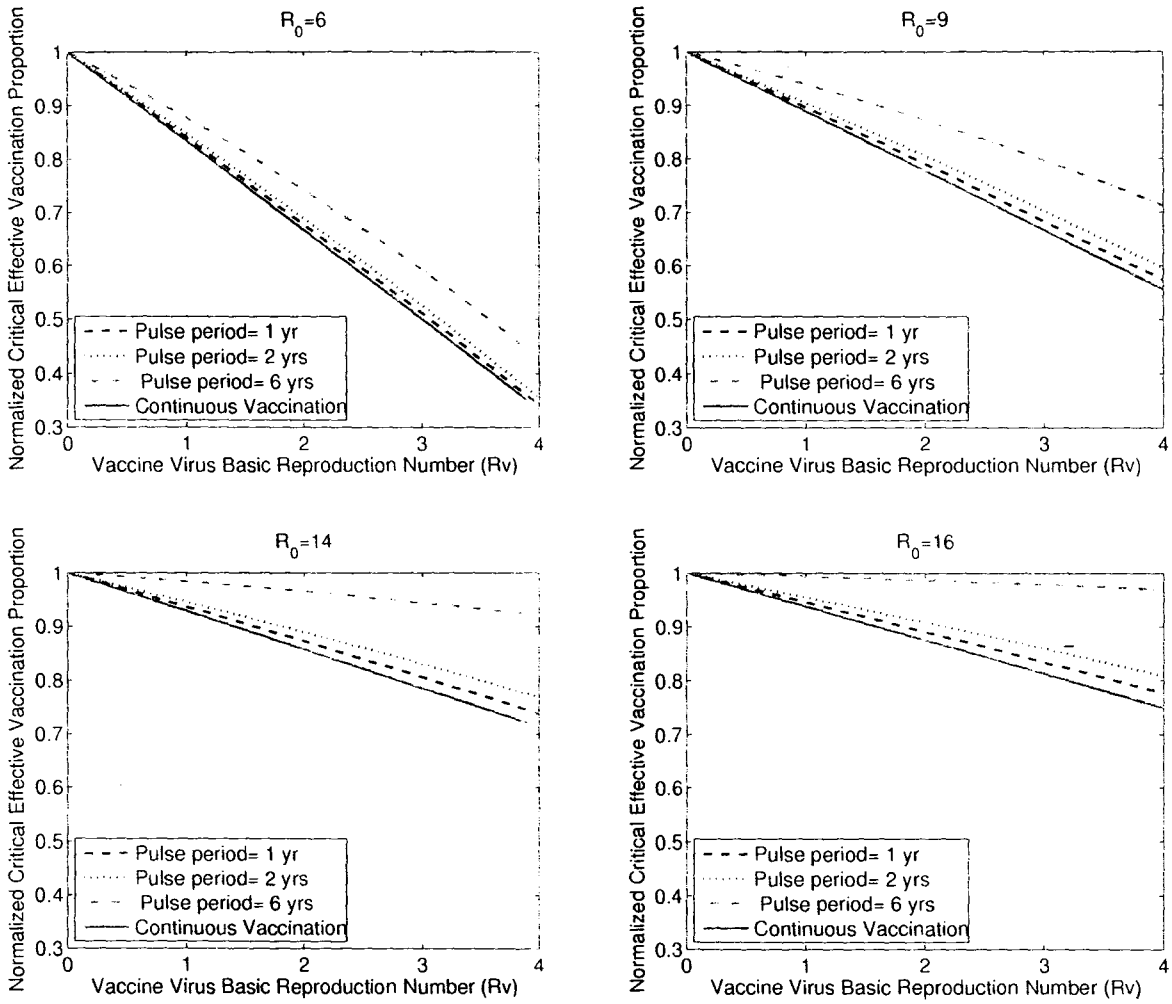

Figure 3.8: Normalized critical effective vaccination proportion $\widehat{p}_{\text{eff,crit}}$ (3.80b) as a function of vaccine virus basic reproduction number $\mathcal{R}_V$ for pulse and continuous vaccination campaigns across range of wild virus basic reproduction values $\mathcal{R}_0$. Continuous vaccination is optimal in the sense of $p_{\text{eff,crit}}$ given by Eq. (3.80a). As the period of vaccination T and $\mathcal{R}_0$ are increased $\widehat{p}_{\text{eff,crit}}$ increases. For relatively long vaccination periods and high values of $\mathcal{R}_0$ there is little advantage as compared to standard vaccination, however for annual vaccine pulses there remains a significant advantage and negligible difference with the continuous vaccination curve.

vaccination results are similar for lower values of $\mathcal{R}_0$, but the values of $\widehat{p}_{\text{eff,crit}}$ deviate greatly for higher $\mathcal{R}_0$ values. For $\mathcal{R}_0 = 16$ with $T = 6$, $\widehat{p}_{\text{eff,crit}}$ remains above 95% for $\mathcal{R}_V = 4$, while for continuous vaccination it has dropped to 80%.

From an epidemiological standpoint, the increase in $\widehat{p}_{\text{eff,crit}}$ with pulsing period T and $\mathcal{R}_0$ in Figure 3.8 can be explained in a relatively straightforward manner. As the pulsing period T and $\mathcal{R}_0$ are increased, the number of individuals that must be vaccinated in each pulse must also increase to keep the susceptible population below threshold level. Although pulse vaccination creates individuals infected with vaccine virus who can cause secondary immunizations, it is at the same time removing members from the susceptible class, depleting the reservoir of individuals for the newly immunized individuals to vaccinate by contact. Therefore although there is a larger pool of vaccine infectious individuals, each one is passing on the virus to fewer individuals.

Thus, continuous vaccination is — from the point of view of contact vaccination — an optimal strategy, in that removing susceptibles continuously maximizes the benefit of contact vaccination. We stress that we say optimal only in the sense of contact immunization, as there are a variety of other reasons why pulse vaccination as an overall strategy may be superior to continuous vaccination [28, 32].

PC versus standard pulse vaccination

It is useful to note that if $S(T^-)$ is independent of $\mathcal{R}_V$ then Eqs. (3.85) and (3.86) straightforwardly imply that $\widehat{p}_{\text{pulse,crit}} = \widehat{p}_{\text{eff,crit}}$. For the parameter values considered in this work, we have seen that $S(T^-)$ depends extremely weakly on $\mathcal{R}_V$. Consequently, graphs that we have drawn as a function of $\widehat{p}_{\text{eff,crit}}$ differ negligibly from the corresponding graphs as a function of $\widehat{p}_{\text{pulse,crit}}$; this equivalence is illustrated in Figure 3.9 which shows $\widehat{p}_{\text{pulse,crit}}$ (3.9 (a) and $\widehat{p}_{\text{eff,crit}}$ (3.9(b) as a function of $\mathcal{R}_V$ for $\mathcal{R}_0 = 12$. At the scales represented there is no detectable difference between the curves.

Since the behaviour of $\widehat{p}_{\text{eff,crit}}$ and $\widehat{p}_{\text{pulse,crit}}$ is practically equivalent, the discussion of Figure 3.8 in section §3.4 applies to $\widehat{p}_{\text{pulse,crit}}$. Hence, we see that for pulse vaccination the critical pulse vaccination proportion is bounded below by

$$p_{\text{pulse,crit}}(\mathcal{R}_V, \mathcal{R}_0) \geq p_{\text{pulse,crit}}(0, \mathcal{R}_0)\left(1 - \frac{\mathcal{R}_V}{\mathcal{R}_0}\right), \tag{3.87}$$

where $p_{\text{pulse,crit}}(0, \mathcal{R}_0)$ is the critical pulse vaccination proportion for standard pulse vaccination (no contact vaccination). Reiterating the statements of section §3.1.2, there is little difference between the bounding curve for continuous vaccination and the one for annual vaccination pulses, but the difference increases as the pulsing period T is increased.

Values of $p_{\text{pulse,crit}}(0, \mathcal{R}_0)$ are shown in Figure 3.7(b) for pulsing periods of 1, 2 and 6 years. Notice that for $T = 6$ and $\mathcal{R}_0 \approx 17$ in the absence of contact vaccination nearly 100% of the susceptible population must be vaccinated in

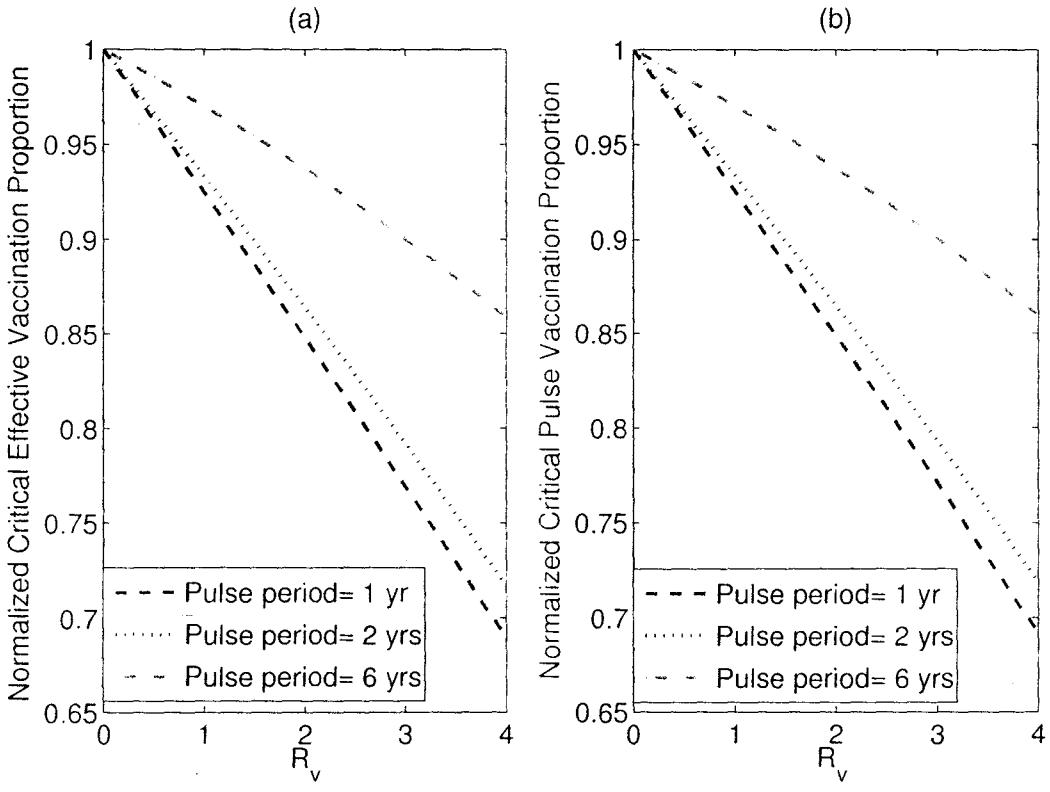

Figure 3.9: Normalized critical effective vaccination proportion $\widehat{p}_{\text{eff,crit}}$ (3.86b) (a) and Normalized critical pulse vaccination proportion $\widehat{p}_{\text{pulse,crit}}$ (3.85) (b)as a function of vaccine virus basic reproduction number ($\mathcal{R}_V$) for a wild virus of $\mathcal{R}_0 = 12$ and a range of pulsing periods. Notice $\widehat{p}_{\text{pulse,crit}} \approx \widehat{p}_{\text{eff,crit}}$. This approximate equality holds across the range of childhood diseases $0 < \mathcal{R}_0 \leq 30$ and is a direct result of the fact that $S(T^-)$ though strongly dependent on $\mathcal{R}_0$ depends very weakly on $\mathcal{R}_V$ (3.8) (3.86b).

every pulse, which is unrealistic. However, for biennial and shorter pulsing periods, $p_{\text{pulse,crit}}(0, \mathcal{R}_0)$ lies in a realistic range.

Dependence on Infectious Period

The previous numerical results assumed a vaccine virus mean infectious period of $\frac{1}{\gamma^V} = 16$ days, which corresponds approximately to the infectious period of wild poliovirus [2]. However, the results we have described are in fact valid much more generally, demonstrating only a very weak dependence on the length of infectious period (for $\mathcal{R}_V$ fixed). Figure 3.10 shows the normalized critical pulse vaccination proportion $\widehat{p}_{\text{pulse,crit}}$, and the normalized critical effective vaccination proportion $\widehat{p}_{\text{eff,crit}}$ as a function of $\mathcal{R}_V$ for annual pulse vaccination campaigns and vaccine virus infectious periods of $\frac{1}{\gamma^V} = 1$ day, 16 days and 1 year. The wild virus reproduction number is set at $\mathcal{R}_0 = 16$. The range of mean infectious periods up to a year includes all childhood infections, of which most have duration less than 1 month [2].

In Figure 3.10(a), $\widehat{p}_{\text{pulse,crit}}$ is indistinguishable for the three different mean infectious periods, again lying slightly above the line $1 - \frac{\mathcal{R}_V}{\mathcal{R}_0}$. In Figure 3.10(b), for the vaccine virus infectious periods of 1 day and 16 days, the $p_{\text{eff,crit}}$ values are indistinguishable from each other, as well as from the corresponding normalized curves $\widehat{p}_{\text{pulse,crit}}$ in Figure 3.10(a). For the much larger vaccine virus infectious period of 1 year, there is a slight decrease (< 0.04) in $\widehat{p}_{\text{eff,crit}}$, in fact differing negligibly with $p_{\text{eff,crit}}$ for the continuous vaccination model.

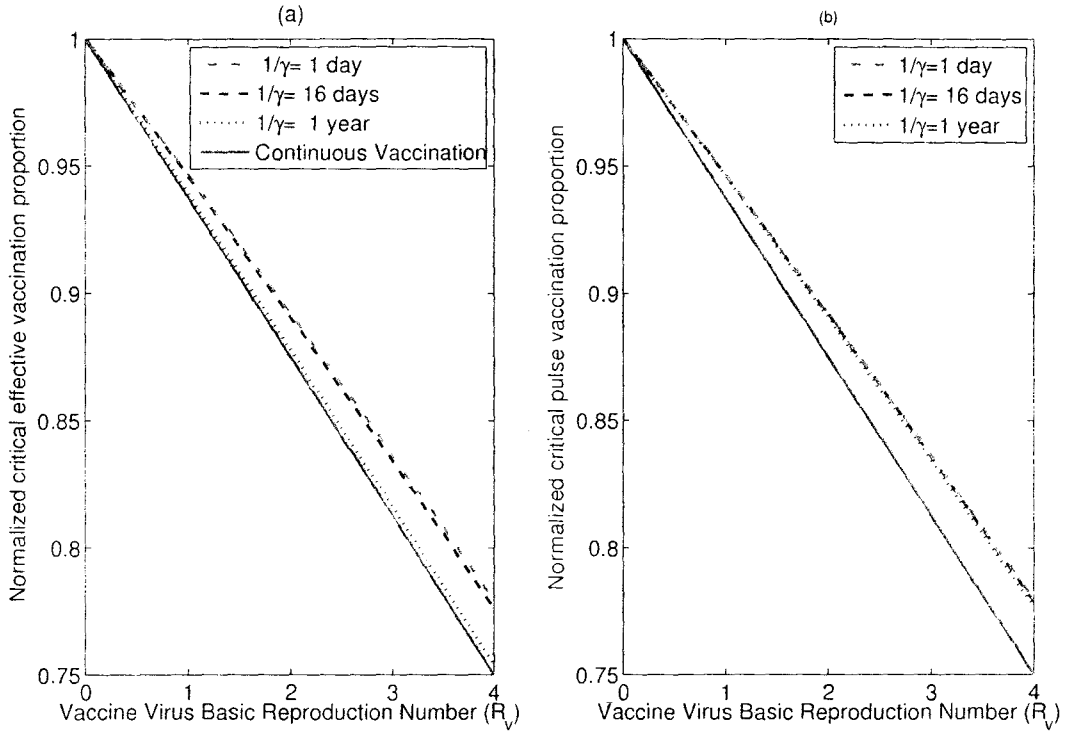

Figure 3.10: (a) Normalized critical effective vaccination proportion $\widehat{p}_{\text{eff,crit}}$ (3.86) for an annual pulse vaccination campaign ($\mathcal{R}_0 = 16$) as a function of vaccine virus reproduction number $\mathcal{R}_V$. Curves show a range of vaccine virus infectious periods $\frac{1}{\gamma_V}$ from 1 day to 1 year. The curves for vaccine virus infectious periods of 1 day and 16 days are indistinguishable, while for 1 year there is a slight decrease in $\widehat{p}_{\text{eff,crit}}$ differing negligibly with the continuous vaccination model (3.86a). (b) Normalized critical pulse vaccination proportion $\widehat{p}_{\text{pulse,crit}}$ for annual pulse vaccination campaigns as a function of vaccine virus reproduction numbers; parameter values as in (a). For vaccine virus mean infectious periods ranging from 1 day to 1 year there is negligible difference in $p_{\text{pulse,crit}}$. As well for mean vaccine virus infectious periods of 1 and 16 days the curves of $\widehat{p}_{\text{pulse,crit}}$ are negligibly different from the corresponding curves for $\widehat{p}_{\text{eff,crit}}$ in (a) as explained in section 3.4.2

Biologically, this decrease in $p_{\text{eff,crit}}$ for longer vaccine virus mean infectious periods is a result of the fact that a longer period gives a higher probability that an individual will still be vaccine infectious long after the pulse at which time susceptibles will have been replenished via births. This allows for the infectious individual to have a greater number of secondary transmissions. However, this effect is noticeable only for very long infectious periods (as long as the pulsing period itself). For childhood diseases, we conclude that stability has no significant dependence on the vaccine virus infectious period. Since the stability threshold (3.80) derived analytically is independent of the wild virus mean infectious period, we conclude that—like for continuous vaccination—for pulse vaccination the stability threshold depends in practice only on the reproduction numbers $\mathcal{R}_0$ and $\mathcal{R}_V$.

3.5 Discussion

We investigated the phenomenon of contact vaccination in the use of live-attenuated virus vaccines. Specifically, we focused on the ability of contact vaccination to reduce the critical vaccination proportion to control/eradicate the wild virus strain in comparison to vaccination with an inactivated or dead vaccine. Most of our results are applicable to any live-attenuated virus vaccine system, but our primary focus was childhood infectious diseases. The use of the Oral Polio Vaccine (OPV) was of particular interest as in this case the practical benefit of contact vaccination has long been recognized.

We investigated models of both continuous and pulse vaccination under the assumption that the vaccine virus is stable with respect to back-mutation or reversion [32]. In the case of continuous vaccination in a homogeneously mixed population, a very general control criterion was established that depends only on the reproduction numbers of the wild pathogenic ($\mathcal{R}_0$) and vaccine viruses ($\mathcal{R}_V$). If the proportion (p) of the population that is vaccinated before entering the susceptible pool satisfies

$$p \geq p_{\text{crit}} \left(1 - \frac{\mathcal{R}_V}{\mathcal{R}_0}\right), \tag{3.88}$$

then the wild virus will be eradicated independent of the initial makeup of the population in terms of susceptible and infectious individuals. In expression (3.88), $p_{\text{crit}} = (1 - \frac{1}{\mathcal{R}_0})$ represents the critical vaccination proportion in the absence of any contact vaccination ($\mathcal{R}_V = 0$). This general criterion is valid regardless of the number of infectious stages and the distributions of durations in the various stages, for both the vaccine and pathogenic wild virus (§3.2.3). Thus, even if a vaccine virus and pathogenic wild virus have markedly different distributions of latent and/or infectious periods the threshold is unchanged, depending only on the virus reproduction numbers. Even for $\mathcal{R}_V < 1$, under which the vaccine virus would naturally fade from the population upon cessation of vaccination, Eq. (3.88) shows that there can be epidemiologically significant reduction of the critical proportion (Figure 3.4). Below this threshold level of vaccination it was shown that the virus

remains endemic in the population with prevalence given by the analytical expression (3.21) (i.e., that there is a globally asymptotically stable endemic equilibrium).

With respect to pulse vaccination, we restricted attention to exponentially distributed infectious periods for the vaccine and wild pathogenic virus. Many of our results are analogous to those obtained previously for continuous vaccination in simple contact vaccination models. We calculated the threshold vaccination level for eradication; we expressed this in terms of the number of vaccinations as a proportion of births during a pulse interval. We refer to this quantity as p_{eff}. This definition facilitates comparison with continuous vaccination strategies as in the continuous case p_{eff} reduces to the standard model parameter p (the proportion of vaccinated newborns). Furthermore, this quantity is of interest since in the absence of contact vaccination ($\mathcal{R}_V = 0$) both pulse and continuous vaccination campaigns predict the same critical or threshold value of p_{eff} for pathogen eradication, independent of the pulsing period [8, 29].

Taking contact vaccination into account, there are noticeable differences in the critical values of p_{eff} between the pulse and continuous vaccination strategies. Our numerical results showed that for pulse vaccination with a vaccine virus of a given $\mathcal{R}_V > 0$, the continuous vaccination strategy gives a lower bound on the critical effective vaccination proportion. In other words, continuous vaccination is optimal in the sense of maximizing the effect of contact vaccination. Furthermore, the threshold value of p_{eff} is seen to in-

crease with increased pulsing period T and increased wild pathogenic virus reproduction number $\mathcal{R}_0$. Biologically, this increase in p_{eff} results from the fact that vaccination pulses simultaneously result in a sudden increase in the pool of vaccine virus infectious individuals and a sudden decrease of equal magnitude in the susceptible population. This decrease results in fewer secondary vaccine virus transmissions for each individual, lowering the overall effect of contact vaccination.

For pulsing periods of several years, the benefits of contact vaccination are significantly reduced; however, for annual pulsing the critical effective vaccination proportion remains very close to the value for continuous strategy, even at relatively high $\mathcal{R}_0$ values. This is particularly important in the context of OPV, as some form of annual pulse vaccination campaign is currently in use in 55 countries around the world. [1] We conclude that there is no significant decrease in the benefits of contact vaccination for annual pulse OPV campaigns, noting that there may also be other epidemiological [32] as well as practical reasons for pursuing pulse campaigns [28, 30].

The pulse vaccination results were shown analytically to be independent of the length of wild virus infectious period, and numerically were demonstrated to have only weak dependence on the vaccine virus infectious period (and negligible dependence for infectious periods less than a month, which are characteristic of childhood diseases). We add that although the threshold vaccination levels were computed in terms of local stability of the *disease free solution*, numerical simulations with randomized initial conditions indicate

these local results are in fact most likely true globally, i.e., regardless of initial conditions.

In previous work, based on a highly idealized model, a simple threshold criterion was derived for eradication of wild virus using live-attenuated virus vaccines [12]. We have shown that this same threshold (3.88), which depends only on the basic reproduction numbers of the wild and vaccine viruses, applies to much more general and more realistic models, and does not depend on initial conditions.

Compared to use of an inactivated (non-live) vaccine, even for low vaccine virus reproduction numbers ($\mathcal{R}_V < 1$), there is a significant reduction of threshold vaccination levels. However, to assess the importance of contact vaccination quantitatively for a given pathogen, an estimate of $\mathcal{R}_V$ is required. Beyond anecdotal evidence and limited case studies [27], there has been no emphasis on the estimation of vaccine-virus reproduction numbers. Such estimation is extremely difficult as, short of performing detailed serological studies, there is no way to distinguish immunity acquired from the wild or vaccine virus.

The models that we have considered here assume that infection and vaccination (whether primary or contact) result in complete and lifelong immunity. This is an excellent approximation for most childhood diseases [17], but for other diseases more work is needed to address the role of partial and decaying immunity. Firstly, the level of immunity provided by contact vaccination must be compared to primary vaccination. Secondly, in cases where primary

immunization results in only partial or decaying immunity, the role of contact vaccination in boosting immunity levels needs to be addressed. In addition to contact vaccination of completely susceptible individuals, boosting immunity levels in previously vaccinated individuals may be another significant benefit of live-attenuated virus vaccines.

3.6 Appendix

A standard result is that for any set of positive real numbers

$$g_i > 0, \qquad i = 1, \ldots, m, \tag{3.89}$$

the arithmetic mean is greater than or equal to the geometric mean, i.e.,

$$\frac{1}{m}\sum_{i=1}^{m} g_i \geq \Big(\prod_{i=1}^{m} g_i\Big)^{1/m}. \tag{3.90}$$

If $\prod_{i=1}^{m} g_i = 1$, then it follows immediately that

$$m - \sum_{i=1}^{m} g_i \leq 0\,, \tag{3.91}$$

with equality if and only if $g_i = 1$ for all i.

3.7 Appendix

It can be shown by a sequence of elementary arguments that for the *disease free equilibrium*

$$S^* \leq \frac{1}{\mathcal{R}_0} \iff p \geq \left(1 - \frac{1}{\mathcal{R}_0}\right)\left(1 - \frac{\mathcal{R}_V}{\mathcal{R}_0}\right) \tag{3.92}$$

From (3.17a) we have

$$S^* = \frac{1}{2} + \frac{1}{2\mathcal{R}_V} - \sqrt{\frac{1}{4}(1 - \frac{1}{\mathcal{R}_0})^2 + \frac{p}{\mathcal{R}_V}} \leq \frac{1}{\mathcal{R}_0} \tag{3.93a}$$

$$\iff \frac{1}{2} + \frac{1}{2\mathcal{R}_V} - \frac{1}{\mathcal{R}_0} \leq \sqrt{\frac{1}{4}(1 - \frac{1}{\mathcal{R}_0})^2 + \frac{p}{\mathcal{R}_V}} \tag{3.93b}$$

We note that since $\mathcal{R}_V < \mathcal{R}_0$ and $\mathcal{R}_0 > 1$ we have $\frac{1}{2} + \frac{1}{2\mathcal{R}_V} - \frac{1}{\mathcal{R}_0} > 0$. Therefore, we have

$$(\frac{1}{2} + \frac{1}{2\mathcal{R}_V} - \frac{1}{\mathcal{R}_0})^2 \leq \frac{1}{4}(1 - \frac{1}{\mathcal{R}_V})^2 + \frac{p}{\mathcal{R}_V} \tag{3.94a}$$

$$\iff p \geq 1 - \frac{\mathcal{R}_V}{\mathcal{R}_0} + \frac{\mathcal{R}_V}{\mathcal{R}_0^2} - \frac{1}{\mathcal{R}_0} \tag{3.94b}$$

$$\iff p \geq \left(1 - \frac{1}{\mathcal{R}_0}\right) - \mathcal{R}_V(\frac{1}{\mathcal{R}_0} - \frac{1}{\mathcal{R}_0^2}) \tag{3.94c}$$

$$\iff p \geq \left(1 - \frac{1}{\mathcal{R}_0}\right)\left(1 - \frac{\mathcal{R}_V}{\mathcal{R}_0}\right) \tag{3.94d}$$

3.8 Appendix

We utilize the following results proved in [4]. Consider a system

$$\begin{aligned} \frac{dx}{dt} &= f(t,x), & t &\neq \tau_k \\ \Delta x &= L_k(x) & t &= \tau_k \end{aligned} \tag{3.95}$$

where $\Delta x = x(\tau_k^+) - x(\tau_k^-)$, and $t \in \mathbb{R}, k \in \mathbb{Z}, x \in \Omega \subset \mathbb{R}^n$. The following conditions are also imposed,

1. $f(t+T,x) = f(t,x), \quad L_{k+q}(x) = L_k(x), \quad \tau_{k+q} = \tau_k + T, \; \exists q \in \mathbb{N}$

2. *the function* $f : \mathbb{R} \times \Omega \to \mathbb{R}^n$ *is continuous.*

3. *The functions* $L_k(x)$ *are continuous for* $x \in \Omega$

Furthermore a set $\mathcal{D} \subset \Omega$ is defined to be *canonical* if it satisfies the following three properties:

4. *the domain* $\mathcal{D}$ *is a bounded convex set*

5. *the closure of* $\mathcal{D}$ *can be expressed by a finite number of inequalities*

$$\Phi_i(x) \leq 0 \tag{3.96}$$

where $\Phi_i : \mathbb{R}^n \to \mathbb{R}$ *are smooth functions.*

6. *if both* $x \in \partial\mathcal{D}$ *and* $\Phi_i(x) = 0$ *then the Jacobian matrix* $\frac{\partial \Phi_i}{\partial x}(x) \neq 0$

The primary result we apply may be stated as follows [4] :

Theorem 1. *Suppose the conditions 1- are satisfied, the set $\mathcal{D}$ is canonical, $\Phi_i(x + L_k(x)) \leq 0, \forall i, \forall x \in \mathcal{D}$ and lastly the directional derivative of Φ along the flow at the boundary must satisfy*

$$\frac{\partial \Phi_i}{\partial x}(x) f(t, x) \leq 0 \quad (t \in \mathcal{R}, x \in \partial\mathcal{D}, i \in \alpha(x)) \tag{3.97}$$

where $\alpha(x) = \{i : \Phi_i(x) = 0\}$

Then Eq. (3.95) has a T-periodic solution $y(t)$ which is contained in $\mathcal{D}$ for all $t \in \mathbb{R}$.

It should be noted that conditions (97) combined with the condition $\Phi_i(x + L_k(x)) \leq 0, \forall i, \forall x \in \mathcal{D}$ are equivalent to the property that the set $\mathcal{D}$ is positively invariant with respect to the system (3.95).

Table 3.1: Table of Notation

Symbol	Definition	Place Defined
p	(continuous) vaccination proportion	§3.2
β^{I}	wild virus transmission rate	§3.2.1
β^{V}	vaccine virus transmission rate	§3.2.1
γ^{I}	wild virus recovery rate	§3.2.1
γ^{V}	vaccine virus recovery rate	§3.2.1
ε^{I}	wild virus specific death rate	§3.2.1
ε^{V}	vaccine virus specific death rate	§3.2.1
B	total birth rate	§3.2.1
$\mathcal{R}_0$	wild virus basic reproduction number	§3.2 and 3.2.
$\mathcal{R}_{\mathrm{V}}$	vaccine virus basic reproduction number	§3.2 and 3.2.
p_{crit}	critical (continuous) vaccination proportion $\mathcal{R}_{\mathrm{V}} = 0$	§3.2
S	susceptible class	§3.2
E_{V}	vaccine virus latent class	§3.2
E_{I}	wild virus latent class	§3.2
V	vaccine virus latent or infectious class	§3.2.1
I	wild virus latent or infectious class	§3.2
R	immune class	§3.2.1
N	total population size	§3.2.1
L_{DFE}	Lyapunov function for the *disease free equilibrium*	§3.2.3
L_{EE}	Lyapunov function for the *endemic equilibrium*	§3.2.3
ν	*per capita* birth rate	§3.3
μ	*per capita* natural death rate	§3.2
p_{pulse}	pulse vaccination proportion	§3.3
T	period of pulse vaccination	§3.3
$\Psi(t)$	fundamental matrix solution	§3.3.2
p_{eff}	effective vaccination proportion	§3.4.1
$p_{\mathrm{eff,crit}}$	critical effective vaccination proportion	§3.4.1
$\widehat{p}_{\mathrm{eff,crit}}$	normalized critical effective vaccination proportion	§3.4.1
$S(T^-)$	proportion of susceptibles immediately before vaccination pulse	§3.4.1
$p_{\mathrm{pulse,crit}}$	critical pulse vaccination proportion	§3.4.2
$\widehat{p}_{\mathrm{pulse,crit}}$	normalized critical pulse vaccination proportion	§3.4.2
$\mathcal{D}$	open set	Appendix 3.8

Bibliography

[1] (2008), Polio Eradication.org. Technical report, URL polioeradication.org/content/fixed/national.html.

[2] R. M. Anderson and R. M. May (1991), Infectious Diseases of Humans, Dynamics and Control, Oxford Science Publications.

[3] N. T. J. Bailey (1954), A statistical method for estimating the periods of incubation and infection of an infectious disease, Nature 174, 139-140.

[4] D. Bainov and P. Simeonov (1993). Impulsive Differential Equations: Periodic Solutions and Applications. Longman Scientific and Technical.

[5] C. T. Bauch and D. J. D. Earn (2003), Transients and attractors in epidemics, Proceedings of the Royal Society of London Series B. 270, 1573-1578.

[6] S. M. Blower, K. Koelle, D. E. Kirschner, and J. Mills (2001), Live attenuated HIV vaccines: predicting the trade-off between efficacy and

safety. Proceedings of the National Academy of Sciences 98(6), 3618–3623.

[7] O. Diekmann, J. A. P. Heesterbeek, and J. A. J. Metz (1990), On the definition and the computation of the basic reproduction ratio R0 in models for infectious-diseases in heterogeneous populations, Journal of Mathematical Biology 28(4), 18.

[8] A. d'Onofrio (2002), Stability properties of pulse vaccination strategy in SEIR epidemic model, Mathematical Biosciences 179, 57–72.

[9] A. d'Onofrio (2004), Mixed pulse vaccination strategy in epidemic model with realistically distributed infectious and latent times, Applied Mathematics and Computation 151, 181–187.

[10] A. d'Onofrio (2005), On pulse vaccination strategy in the SIR epidemic model with vertical transmission, Applied Mathematics Letters 18, 729–732.

[11] D. J. D. Earn, P. Rohani, B. M. Bolker, and B. Grenfell (2000), A simple model for complex dynamical transitions in epidemics, Science 287, 667–670.

[12] M. Eichner and H. K. P. (1995), Deterministic Models for the Eradication of Poliomyelitis: Vaccination with Inactivated (IPV) and Attenuated (OPV) Polio Virus Vaccine, Mathematical Biosciences 127, 149–166.

[13] H. I. Freedman and J. W. H. So (1985), Global Stability and Persistence of Simple Food Chains, Math. Biosci. 76, 69–86.

[14] K. J. Gough (1977), The estimation of latent and infectious periods, Biometrika 64, 559–565.

[15] H. Guo and M. Y. Li (2006), Global Dynamics of a Staged Progression Model for Infectious Diseases. Mathematical Biosciences and Engineering 3(3), 513–525.

[16] D. He and D. J. D. Earn (2007). Epidemiological effects of seasonal oscillations in birth rates. Theoretical Population Biology 72, 274- 291.

[17] H. W. Hethcote (2000), The Mathematics of Infectious Diseases. SIAM Review 42(4), 599–653.

[18] H. F. Hull, N. A. Ward, B. D. Hull. J. B. Milstien, and C. de Quadros (1994), Paralytic Poliomyelitis: seasoned strategies disappearing disease. Lancet 343, 1331-1337.

[19] A. Korobeinikov (2004). Lyapunov functions and global properties for SEIR and SEIS epidemic models, Mathematical Medicine and Biology 21, 75–83.

[20] A. Korobeinikov and P. K. Maini (2004), A Lyapunov Function and Global Properties for SIR and SEIR Epidemiological Models with Nonlinear Incidence, Math. Biosci. Eng. 1(1), 57–60.

[21] A. Korobeinikov and G. Wake (2002), Lyapunov Functions and Global Stability for SIR, SIRS and SIS Epidemiological Models, Applied Math Letters 15, 955–960.

[22] Y. A. Kuznetsov (1998), CONTENT- integrated environment for analysis of dynamical systems. Tutorial .

[23] J. P. La Salle and S. Lefschetz (1961), Stability by Liapunov's direct method with applications, Academic Press, New York.

[24] J. Lasalle (1976), The Stability of Dynamical Systems, Regional Conference Series in Applied Mathematics, SIAM.

[25] A. L. Lloyd (2001), Realistic Distributions of Infectious Periods in Epidemic Models: Changing Patterns of Persistence and Dynamics, Theoretical Population Biology 60, 59–71.

[26] J. Ma and D. J. D. Earn (2006), Generality of the final size formula for an epidemic of newly invading infectious disease, Bulletin of Mathematical Biology 68, 679–702.

[27] J. M. Neff, J. M. Lane, V. A. Fulginiti, and D. Henderson (2002), Contact-Vaccinia-Transmission of Vaccinia from Smallpox vaccination, JAMA 288(15).

[28] A. Sabin (1991), Mealses, killer of millions in developing countries: strategies of elimination and continuing control, European Journal of Epidemiology 7, 1–22.

[29] B. Shulgin, L. Stone, and Z. Agur (1998), Pulse vaccination strategy in the SIR epidemic model, Bulletin of Mathematical Biology 60, 1123–1148.

[30] L. Stone, B. Shulgin, and Z. Agur (2000), Theoretical examination of the pulse vaccination policy in the SIR epidemic model, Mathematical and Computer Modelling 31, 207-215.

[31] P. van den Driessche and J. Watmough (2002), Reproduction Numbers and Sub-Threshold Endemic Equilibria for Compartmental Models of Disease Transmission, Mathemiatcial Biosciences 180, 29–48.

[32] B. G. Wagner and D. J. D. Earn (2008), Circulating vaccine derived polioviruses and their impact on global polio eradication, Bulletin of Mathematical Biology 70, 253–280.

[33] G. C. Woodrow and M. M. Levine (1990), New Genearation Virus Vaccines, Marcel Dekker, Inc.

Chapter 4

The Effects of Demographic Stochasticity in Pulse Vaccination Campaigns

4.1 Introduction

It has long been realized that demographic stochasticity can have important consequences for epidemiological systems. In the case of measles, a childhood disease characterized by a relatively high transmission rate, field epidemiologists have observed apparently random extinctions or fade-outs, particularly for small isolated populations [11]. Such observations motivated some of the first mathematical discussions of the effects of stochasticity on pathogen persistence and recurrent epidemics by Bartlett [7, 8, 10, 9, 11] in the late 1950s.

Bartlett [8] introduced the important concept of the *critical community size* (CCS), essentially the minimum population size for which a pathogen will persist in a community without reintroduction.

Bartlett employed a compartmental stochastic model allowing for immigration of susceptible and infectious individuals but not deaths (either natural or disease specific) [6, 7]. Developing a recursive approximation for the stationary distribution of the model. Bartlett derived a quantity similar to the mean time to extinction which he termed the " mean recurrence time to zero infectives " [10, 11]. The difference in terminology results from the fact that use of stationary distributions necessitates the inclusion of some immigration of infectious individuals in the model. To confirm the validity of his model. Bartlett compared his theoretical results as well as those generated by Monte Carlo simulation methods to measles case notification data from England and the U.S.A [8, 9]. This work represents a milestone in understanding the importance of stochasticity in epidemiological dynamics.

Bartlett's early work has been extended significantly, most notably with the introduction of the idea of quasi-stationary distributions for finite state continuous time Markov chains [18, 45]. In the context of compartmental epidemiological models, much effort has been focused on analytical approximations of the quasi-stationary distribution [44, 45], which may be thought of as the stochastic analogue of a deterministic endemic equilibrium in a differential equation model. There has been particular interest in the computation of the mean and distributions for the time to stochastic extinction

of pathogens, as a function of population size [5, 44, 45, 52]. The dependence of the mean time to extinction on the population size is used to give a value for the CCS. Some recent work has explored the significance of the distribution of latent and infectious periods on disease persistence at the population level (by analytical methods [5] and by direct simulation [41]).

The effects of demographic stochasticity on the outcomes of *continuous vaccination* campaigns have been investigated previously [35], and analytical approximations of the CCS have been derived [5] (in the large population limit) as a function of the proportion of the population that is vaccinated. The key approximation that is made is that the distribution of initial states is the quasistationary distribution; from this it follows that the time to extinction is exponentially distributed [5, 15], and hence that the mean time to extinction specifies the full distribution of times to extinction (from which the CCS can be inferred). This work shows—in the large population limit—that the CCS is inversely proportional to the square of the mean infectious period.

The implications of stochasticity for *pulse vaccination* (whereby mass vaccination campaigns are undertaken at regular intervals) have yet to be significantly explored [36]. Deterministic compartmental ordinary differential equation models of pulse vaccination for childhood diseases have been explored extensively [1, 17, 22, 19, 20, 21, 46, 49, 50]. In particular, these works establish that there is a critical pulse interval such that if a fixed proportion of susceptibles is vaccinated in each pulse, then the pathogen will

certainly be eradicated if the pulse interval is shorter than the critical length [20, 21, 49, 50]. The existence of this critical pulse interval has also been proved for more general models, which include waning of maternal immunity and realistically (Gamma) distributed latent and infectious periods [20, 21].

In the deterministic setting, the threshold effective vaccination level (number of doses per unit time) required to ensure eradication has been proven to be identical in the simplest (SIR) framework [49, 50] and—based on numerical analysis—is conjectured to be identical more generally [21]. For vaccination below this threshold level, complicated dynamics are possible, including deterministic chaos for sufficiently long pulse intervals [19]. In addition, the pulse vaccination model can exhibit parametric resonance (resonant behaviour which appears when a control parameter exceeds a threshold value [30]), which can have the counter-intuitive effect of increasing disease prevalence when decreasing the pulse interval [17].

The stochastic epidemic theory cited above makes clear that demographic stochasticity can lead to dynamics that are substantially different from the behaviour of deterministic models. We are therefore motivated to investigate whether the conclusions drawn from deterministic pulse vaccination models remain valid in the presence of a realistic amount of demographic stochasticity. With specific emphasis on measles vaccination, we employ a mix of computational and partially analytical techniques. Our analysis has considerable practical importance, because some form of pulse vaccination is currently carried out for measles and poliomyelitis in many developing

countries (typically in the form of annual national immunization days) [48].

4.1.1 Methods of Analysis

Our analysis is based upon the standard Susceptible-Exposed-Infectious-Recovered (SEIR) compartmental framework [3, 33]. In its deterministic form, the model can be represented by the following set of impulsive differential Eqs. [20].

$$\frac{dS}{dt} = \nu N - \frac{\beta}{N} SI - \mu S - p_{\text{pulse}} \sum_{n=0}^{\infty} S(nT^-)\delta(t - nT) \tag{4.1a}$$

$$\frac{dE}{dt} = \frac{\beta}{N} SI - (\mu + \sigma)E \tag{4.1b}$$

$$\frac{dI}{dt} = \sigma E - (\mu + \gamma)I \tag{4.1c}$$

$$\frac{dR}{dt} = \gamma I + p_{\text{pulse}} \sum_{n=0}^{\infty} S(nT^-)\delta(t - nT) - \mu R \tag{4.1d}$$

$$S(nT^-) = \lim_{\varepsilon \to 0^+} S(nT - \varepsilon) \tag{4.1e}$$

Here, N is the total population size. Individuals are born into the susceptible class at *per capita* rate ν; regardless of disease status, individuals die at *per capita* rate μ, where $\frac{1}{\mu}$ is the average life-span (we ignore any disease-induced mortality). The fixed rates σ and γ imply that the latent and infectious periods are exponentially distributed with means $\frac{1}{\sigma}$ and $\frac{1}{\gamma}$, respectively. Vaccination occurs in pulses separated by time T; at each pulse, a proportion p_{pulse} of the susceptible population is vaccinated (and we assume that vaccination

confers lifelong immunity). Standard incidence ($\beta SI/N$) is assumed, so the transmission rate is β/N. The model ( ) is phrased in terms of absolute number of individuals, but it can straightforwardly be phrased in terms of proportions of the population by scaling the state variables (S, E, I, R) by the population N [32, 53].

The basic reproduction number—the average number of secondary infections resulting from a single infectious individual in a fully susceptible population, *in the absence of vaccination*—is easily calculated [51] and found to be

$$\mathcal{R}_0 = \frac{\beta\sigma}{(\gamma+\nu)(\sigma+\nu)}. \tag{4.2}$$

Solutions of the deterministic model ( ) correspond to the ensemble mean of the true stochastic system in the limit of large population size ($N \to \infty$) [39, 40]. The differential equations in the deterministic model implicitly specify a stochastic model in which waiting times for each system event are exponentially distributed with rates dependent on the current state (S, E, I, R) of the system. The population is made up of discrete individuals and each stochastic event results in the transfer of a finite number of individuals from one class to another. The transitions and rates associated with each event type are given in Table 4.1.1. With the exception of vaccination, all events involve a single individual. The number of individuals who are vaccinated in a given pulse depends on the number of susceptibles in the population at the event time. Note that, unlike the other events, the timing of vaccinations is

Event	Rate	Transition
Birth	νN	$S \rightarrow (S+1)$, $N \rightarrow N+1$
Infection	$(\beta/N)IS$	$S \rightarrow S-1$, $E \rightarrow E+1$
Infectious	σE	$E \rightarrow E-1$, $I \rightarrow I+1$
Recovery	γI	$I \rightarrow (I-1)$
Natural death	μX	$X \rightarrow (X-1)$, $N \rightarrow N-1$
Vaccination	$\sum_{n=0}^{\infty} \delta(t-nT) p_{\text{pulse}} S(nT^-)$	$S \rightarrow S - \lfloor p_{\text{pulse}} S \rfloor$

Table 4.1: Event rates for the stochastic SEIR model with pulse vaccination. X refers to any of the state variables (S, E, I or R). The notation $\lfloor x \rfloor$ denotes the largest integer less than or equal to x. Note that the pulse vaccination term $\sum_{n=1}^{\infty} \delta(t-nT) p_{\text{pulse}} S(nT^-)$ is deterministic with respect to time, with $\lfloor p_{\text{pulse}} S(nT^-) \rfloor$ individuals vaccinated at $t = nT$, $n = 0, 1, 2 \ldots$

deterministic, i.e., susceptible individuals are always vaccinated precisely at time $t = nT$ (for $n = 0, 1, 2, \ldots$).

The Gillespie Algorithm

We employ the standard Gillespie algorithm [27] to simulate the stochastic process specified by Table 4.1. This algorithm is an iterative (or chain) Monte Carlo method used to compute true realizations of (discrete state space) continuous time Markov processes (for which future system states depend only on the current state). Realizations are "true" in practice to the extent that our random number generators are truly random and generate data of the correct distribution. Each iteration of the algorithm has two steps, the first step selecting the time to the next event, and the second step selecting the event type.

The algorithm may be fully explained as follows. At a fixed time t_0 consider a Markov system defined by n possible events (transitions). We assume the state of the system at time t_0 is known. We denote the rate associated to each event as $\{a_i\}_{i=1}^n$. Therefore the probability of an event of type i occurring in time Δt is $a_i \Delta t + \mathcal{O}(\Delta t^2)$. We define two random variables: T_e, the time to the next event (of any type), and I_e, the index of the next event (i.e., the type of event that occurs next). The algorithm is based on the computation of the distributions for these two random variables.

Following [27] we compute the distribution for T_e. Using conditional probabilities for successive time intervals we may write

$$P(T_e > t + \Delta t) = P(T_e > t) \left(1 - \sum_{i=1}^{n} a_i \Delta t + \mathcal{O}(\Delta t^2) \right). \tag{4.3}$$

In Eq. (4.3) the first term represents the probability that there are no events in the time interval $[t_0, t_0 + t]$ while the second term represents the probability that there are no events in the time interval $[t_0 + t, t_0 + t + \Delta t]$. Rearranging Eq. (4.3) we see that

$$\frac{P(T_e > t + \Delta t) - P(T_e > t)}{\Delta t} = P(T_e > t) \left(-\sum_{i=1}^{n} a_i + \mathcal{O}(\Delta t) \right) \tag{4.4}$$

Taking limits as $\Delta t \to 0$ in (4.4) yields the linear differential equation

$$\frac{dP(T_e > t)}{dt} = P(T_e > t) \left(-\sum_{i=1}^{n} a_i \right). \tag{4.5}$$

Solving Eq. (4.4) (noting $P(T_e > 0) = 1$ and $P(T_e \leq t) = 1 - P(T_e > t)$) yields the distribution of T_e

$$P(T_e \leq t) = 1 - e^{-\sum_{i=1}^{n} a_i t}. \tag{4.6}$$

Eq. (4.6) establishes that T_e is exponentially distributed with parameter $\sum_{i=1}^{n} a_i$. Using the distribution of T_e the probability that the next event occurs in the time interval $[t_0 + t_1, t_0 + t_1 + \Delta t]$ and the event is of type j (i.e., $I_e = j$) may be calculated using conditional probabilities as

$$\begin{aligned} P(I_e = j, T_e \in [t, t + \Delta t]) &= P(T_e > t)\left(a_j \Delta t + \mathcal{O}(\Delta t^2)\right) \\ &= e^{-\sum_{i=1}^{n} a_i t}\left(a_j \Delta t + \mathcal{O}(\Delta t^2)\right) \end{aligned} \tag{4.7}$$

As in the computations for T_e dividing by Δt and taking the limit in (4.7) as $\Delta t \to 0$ yields the probability *density* associated to the distribution $P(T_e < t, I_e = j)$

$$p(t, j) = a_j e^{-\sum_{i=1}^{n} a_i t}. \tag{4.8}$$

The distribution of the random variable I_e may now be calculated by conditioning the expression for $P(T_e \leq t, I_e = j)$ on the time to the next event T_e. Assuming the next event occurs in some arbitrary (measurable) set

$\mathcal{A} \subset (0, \infty)$, the expression for this conditional probability is

$$\begin{aligned} P(I_e = j | T_e \in \mathcal{A}) &= \frac{P(I_e = j, T_e \in \mathcal{A})}{P(T_e \in \mathcal{A})} \\ &= \frac{a_j \int_{\mathcal{A}} e^{-\sum_{i=1}^n a_i t} dt}{\sum_{i=1}^n a_i \int_{\mathcal{A}} e^{-\sum_{i=1}^n a_i t} dt} \\ &= \frac{a_j}{\sum_{i=1}^n a_i}. \end{aligned} \tag{4.9}$$

Notice there is no dependence on the time of the event. Since the set $\mathcal{A}$ is arbitrary, Eq. (4.9) implies that the index of the next event I_e and the time to the next event T_e are independent random variables. Thus, the distribution of I_e is simply

$$P(I_e = j) = \frac{a_j}{\sum_{i=1}^n a_i}. \tag{4.10}$$

Using these results, the Gillespie algorithm can be performed through two independent steps:

1. The time to the next event T_e is chosen by selecting a variate from the exponential distribution with rate $\sum_{i=1}^n a_i$.

2. The index of the next event I_e is selected by choosing a variate from the discrete distribution (4.10).

In practise, the two steps are most often achieved using a uniform random number generator on the unit interval and straightforward transformations. We refer the reader to [27] for a complete discussion of implementation issues.

Event	Rate	Transition
Infection	βIS	$S \to S-1,\ I \to I+1$
Recovery	γI	$I \to I-1$

Table 4.2: Events rates and transitions for the SIR epidemic model without vital dynamics.

Moment Closure Models

To complement our numerical analysis based on particular realizations of the underlying Markov process specified in Table 4.1.1, we also consider differential equations for the time-evolution of the ensemble variances of the process. We derive these equations based on a moment-closure approximation [12, 15, 36, 37, 42].

To explain the derivation of the moment evolution equations, we consider an oversimplified two-event-type model. For the more complicated model that we have actually investigated, the equations are derived in an identical manner, but the algebra is much messier.

Consider a discrete-state, continuous-time Markov process with only two event types: infection and recovery (the SIR model without vital dynamics [33]). The system is defined in Table 4.2. For this Markov process, given a

time t, the probability that the system is in state (S, I) at time $t + \Delta t$ is

$$\begin{aligned} P(S, I, t + \Delta t) = &\beta(S + 1)(I - 1)P(S + 1, I - 1, t)\Delta t \\ &+ \gamma P(S, I + 1, t)\Delta t \\ &+ P(S, I, t)(1 - \beta SI\Delta t - \gamma\Delta t) + \mathcal{O}(\Delta t^2) \end{aligned} \tag{4.11}$$

The terms of Eq. (4.11) represent (in order) the probability of arriving at state (S, I) by a single infection, single recovery, or lack of any event in the time Δt. The probability of arriving at the state (S, I) through multiple transitions is incorporated into the $\mathcal{O}(\Delta t^2)$ term. Regrouping terms in Eq. (4.11) and shrinking Δt to zero, we arrive at the differential equation

$$\begin{aligned} \frac{dP(S, I, t)}{dt} = &\beta(S + 1)(I - 1)P(S + 1, I - 1, t) \\ &+ \gamma(I - 1)P(S, I - 1, t) \\ &- (\beta IS + \gamma)P(S, I, t) \end{aligned} \tag{4.12}$$

From Eq. (4.12) it is straightforward to obtain differential equations for the moments (of any order) of S and I by summing over all the system states,

$$\frac{d\langle S^q I^p\rangle}{dt} = \sum_{(S,I)} S^q I^p \frac{dP(S, I, t)}{dt}, \tag{4.13}$$

where $\langle\cdot\rangle$ denotes ensemble average and the sum is over the set $\{(S, I) : S \geq 0, I \geq 0, 0 \leq S + I \leq N\}$.

In principle, substituting Eq. (4.12) into the LHS of Eq. (4.13) specifies

the differential equations for the system moments (since the LHS of (4.13) can be expressed as a linear combination of powers of the two state variables). In practice, it is more convenient to look at ODEs for the moment (or cumulant) generating functions, the expansion coefficients of which are the moments (cumulants) of the system. The moment and cumulant generating functions are defined, respectively, as

$$\mathcal{M}(\theta_{\mathrm{I}}, \theta_{\mathrm{S}}) = \left\langle e^{\theta_{\mathrm{I}} I + \theta_{\mathrm{S}} S} \right\rangle \tag{4.14a}$$

$$\mathcal{K}(\theta_{\mathrm{I}}, \theta_{\mathrm{S}}) = \log\left(\mathcal{M}\right) . \tag{4.14b}$$

As in Eq. (4.13), the average in (4.14) is taken across all possible states (S, I). Differential equations for the moment (cumulant) generating function are constructed completely analogously to Eq. (4.13). The explicit moment equations up to second order for the SIR epidemic model (with vital dynamics) are given in [42].

We now return our attention to the $SEIR$ pulse vaccination model. Using the methods just discussed we compute the moment equations. Following [42], to simplify analysis we ignore fluctuations in the total population N, treating this term as deterministic. Also recall from the discussion of Gillespie algorithm simulations that pulse vaccination is modelled as a deterministic process. We use $\langle X \rangle$, $\mathrm{var}(X)$ and $\mathrm{cov}(X, Y)$ to denote the mean, variance

and covariance. Similarly the third order central moment is

$$\mathrm{M}_3(X,Y,Z) = \langle (X - \langle X \rangle)(Y - \langle Y \rangle)(Z - \langle Z \rangle) \rangle \ . \tag{4.15}$$

For the sake of generality, we give the equations for a mixed vaccination campaign in which there is both a pulse and continuous vaccination component with a proportion p of the population vaccinated at birth and a proportion p_{pulse} of susceptibles vaccinated in each pulse. The moment equations, up to second order, are then give by the following expression:

$$\begin{aligned}
\frac{d\langle S \rangle}{dt} &= (1-p)\nu N - \mu \langle S \rangle - \frac{\beta}{N}\mathrm{cov}(S,I) - \frac{\beta}{N}\langle S \rangle \langle I \rangle \\
&\quad - p_{\text{pulse}} \sum_{n=0}^{\infty} \delta(t - nT) \left\langle S(nT^-) \right\rangle && \text{(4.16a)} \\
\frac{d\langle E \rangle}{dt} &= \frac{\beta}{N}\mathrm{cov}(S,I) + \frac{\beta}{N}\langle S \rangle \langle I \rangle - (\mu + \sigma_1)\langle E \rangle && \text{(4.16b)} \\
\frac{d\langle I \rangle}{dt} &= \sigma_1 \langle E \rangle - (\mu + \gamma_1)\langle I \rangle && \text{(4.16c)} \\
\frac{d\mathrm{var}(S)}{dt} &= (1-p)\nu N + \mu \langle S \rangle - 2\mu \mathrm{var}(S) + \frac{\beta}{N}\mathrm{cov}(S,I) \\
&\quad + \frac{\beta}{N}\langle S \rangle \langle I \rangle - 2\frac{\beta}{N}\left(\langle S \rangle \mathrm{cov}(S,I) + \mathrm{var}(S)E(I) + \mathrm{M}_3(S,I,I)\right) \\
&\quad - p_{\text{pulse}}(2 - p_{\text{pulse}}) \sum_{n=0}^{\infty} \delta(t - nT)\mathrm{var}(S(nT^-)) && \text{(4.16d)}
\end{aligned}$$

$$\frac{d\text{var}(E)}{dt} = (\mu + \sigma_I)\left(\langle E\rangle - 2\text{var}(E)\right) + \frac{\beta}{N}\text{cov}(S,I) + \frac{\beta}{N}\langle S\rangle\langle I\rangle + 2\frac{\beta}{N}\left(\langle S\rangle\,\text{cov}(E,I) + \text{cov}(S,E)\langle I\rangle\right) + 2\frac{\beta}{N}\text{M}_3(S,E,I) \tag{4.16e}$$

$$\frac{d\text{var}(I)}{dt} = (\mu + \gamma_I)(\langle I\rangle - 2\text{var}(I)) + \sigma_I\left(\langle E\rangle + 2\text{cov}(E,I)\right) \tag{4.16f}$$

$$\frac{d\text{cov}(S,E)}{dt} = -(2\nu + \sigma_I)\text{cov}(S,E) - \frac{\beta}{N}\left(\text{cov}(S,I) + \langle S\rangle\langle I\rangle\right) - \frac{\beta}{N}\langle S\rangle\,\text{cov}(S,I) + \frac{\beta}{N}(\text{var}(S)\langle I\rangle - \langle S\rangle\,\text{cov}(E,I)) - \frac{\beta}{N}\text{cov}(S,E)\langle I\rangle - \frac{\beta}{N}\left(\text{M}_3(S,S,I) + \text{M}_3(S,E,I)\right) - p_{\text{pulse}}\sum_{n=0}^{\infty}\delta(t-nT)\text{cov}(S(nT^-),E(nT^-)) \tag{4.16g}$$

$$\frac{d\text{cov}(S,I)}{dt} = -(2\mu + \gamma_I)\text{cov}(S,I) + \sigma_I\text{cov}(S,E) - \frac{\beta}{N}\left(\langle S\rangle\,\text{var}(I) + \text{M}_3(S,I,I)\right) - \beta_I\langle I\rangle\,\text{cov}(S,I) - p_{\text{pulse}}\sum_{n=0}^{\infty}\delta(t-nT)\text{cov}(S(nT^-),I(nT^-)) \tag{4.16h}$$

$$\frac{d\text{cov}(E,I)}{dt} = -(2\mu + \sigma_I + \gamma_I)\text{cov}(E,I) - \sigma_I\left(\langle E\rangle - \text{var}(E)\right) + \frac{\beta}{N}\left(\langle S\rangle\,\text{var}(I) + \text{cov}(S,I)\langle I\rangle + \text{M}_3(S,I,I)\right) \tag{4.16i}$$

$$\frac{dN}{dt} = (\nu - \mu)N \tag{4.16j}$$

Notice that the system of equations (4.16) is not closed, as the rates of change of second order moments depend on third order moments. In general, the rates of change of the kth moments will depend on the $(k+1)$th (and if non-mass-action mixing were assumed then there would be dependence on

higher order moments as well). In order to close the equations at some order, assumptions are typically imposed on the form of the distribution of states. We assume that the states of the system have a multivariate normal (MVN) distribution (i.e., at each time point, the distribution of states across all possible realizations is MVN). With this assumption, the system closes with moments no higher than second order, since third order central moments vanish for the MVN distribution . The MVN moment closure model is thus obtained by setting $M_3(X, Y, Z) = 0$ in (1.16). MVN moment-closure approximations for the SEIR model without vaccination are considered in [42].

Moment closure approximations allow us to investigate the dependence of results on population size without resorting to direct simulation. However, as these methods assume the form of the ensemble distribution, they cannot be used—at least not directly—to estimate the time to extinction. Furthermore, as we are assuming normal distributions for non-negative state variables, we expect that the approximation will become worse as the standard deviation becomes comparable in size to the mean. Numerically, breakdown is manifested by divergence of integrations of Eq. (1.16). Such divergence has been noted for the standard MVN SIR and SEIR models in [42]. This breakdown is not specific to the MVN approximation; it has also been observed when analyzing a multivariate lognormal moment closure approximation [25]. Bimodal distributions have been considered for simple two compartment SIS models [37]. In contrast to the MVN model, such methods involve imposi-

tion of a non-trivial functional relationship between higher and lower order moments (as dictated by the distribution).

In spite of the limitations imposed by specifying the ensemble distributions as MVN, our model does provide useful indirect information about the probability of extinction. We make indirect inferences by examining the coefficient of variation (CV) of state variables; the CV of X is

$$\mathrm{CV}(X) = \frac{\sigma(X)}{\langle X \rangle}, \tag{4.17}$$

where $\sigma(\cdot)$ denotes standard deviation and $\langle \cdot \rangle$ denotes mean. If $\mathrm{CV}(X)$ is of order unity then X is frequently near zero. Consequently, as $\mathrm{CV}(E)$ and $\mathrm{CV}(I)$ approach unity, there will be a high probability of extinction or fade-out. Unfortunately, as previously discussed, when the coefficient of variation approaches 1, the MVN approximation is more prone to error. Nevertheless, we will show in the following sections that the MVN model makes useful predictions regarding stochastic extinctions for the pulse vaccination model. Some previous work has demonstrated MVN models often provide good approximations of the mean and variance, even for true distributions that are known to be far from normal [34].

4.2 Results

In the following sections we focus specifically on vaccination for measles. Unless otherwise noted, we assume standard epidemiological parameters for measles ($\mathcal{R}_0 = 17.5$, mean latent period $\frac{1}{\sigma} = 8$ days, mean infectious period $\frac{1}{\gamma} = 5$ days). In addition, we assume a birth rate $\nu = 0.02\text{yr}^{-1}$, a constant transmission rate β (no temporal variation in β), and identical rates of birth and death ($\nu = \mu$).

We begin by describing the results of many Gillespie simulations covering a range of population sizes and proportions vaccinated. These results are compared with the predictions of the MVN pulse SEIR model. We highlight the differences in measles extinction probabilities predicted by continuous and pulse vaccination programs. We show that demographic stochasticity leads to eradication thresholds that are much lower than those predicted by the deterministic model (1.1), for populations of (at least) the size of large cities and small countries.

4.2.1 Stochasticity and Pulse Vaccination

Gillespie simulations

Figure 4.1 shows the results of Gillespie simulations of the pulse SEIR vaccination model for measles, with pulse intervals (from top to bottom) of $T = 1, 2, 3, 6$ years and an (initial) population size of 10 million. As a result of demographic stochasticity, the actual population size fluctuates about the

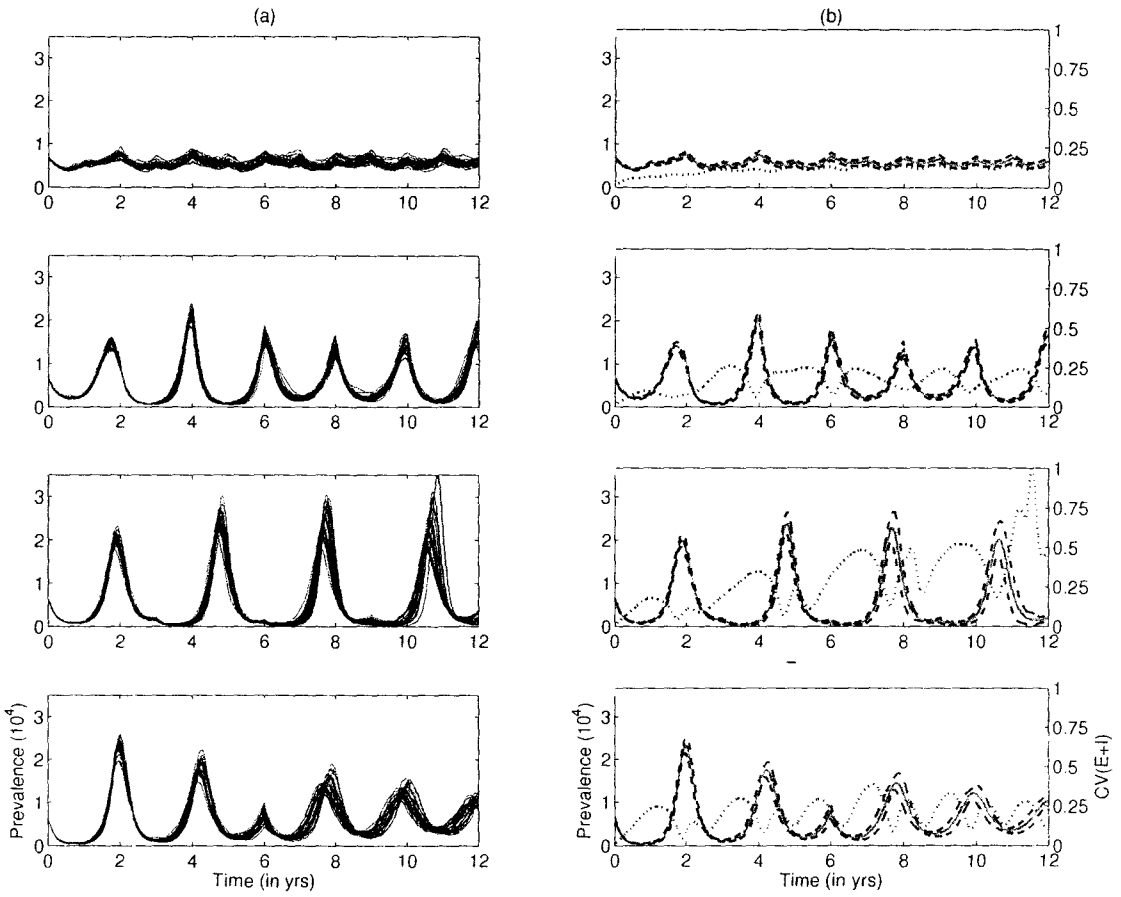

Figure 4.1: Prevalence time series for Gillespie simulations of the pulse $SEIR$ model (4.1) in a population of 10 million. Initial conditions for are taken to be the globally asymptotically stable equilibrium of (4.1) for a previously unvaccinated population. From top to bottom each row represents pulsing periods of 1, 2, 3 and 6 years, with pulse vaccination proportions of $p_{\text{pulse}} = 0.05, 0.105, 0.17$ and 0.30, respectively. For $T = 1, 2, 3$ years, these values correspond to $p_{\text{eff}} \approx 0.16$ (4.18). Panels in column (a) show thirty sample realizations, while panels in column (b) give the mean of 1000 realizations. Dashed curves in (b) denote differences of one standard deviation, while the dotted curve gives the coefficient of variation for the prevalence $\text{CV}(E + I)$ (4.17). Longer pulsing periods give rise to higher epidemic peaks and deeper epidemic troughs. For $T = 3$ years, the standard deviation in the epidemic trough is comparable in size to the mean, indicating a potential for stochastic extinction.

initial values. The left panel gives a 12 year time series of measles prevalence $(E + I)$ for 30 stochastic realizations. The right hand side shows the ensemble mean of 1000 realizations, with dashed lines indicating differences of one standard deviation. Note that the proportion of susceptibles vaccinated in each pulse (p_{pulse}) is different in each of the four pairs of panels in Figure 4.1, in order to keep constant the number of doses administered over the 12 year time period (facilitating a more useful comparison among the different pulse intervals); we make this concept more precise is section § 4.2.2.

The same set of initial conditions is used for each realization, namely the discrete state closest to the globally asymptotically stable endemic equilibrium [31, 38] of the deterministic model (4.1) in the absence of vaccination. The deterministic endemic equilibrium may be thought of as the mean of the quasi-stationary distribution of the corresponding stochastic model [2, 4]. From a biological perspective, these simulations amount to initiating a pulse vaccination program in a population where measles is endemic and there has previously been a negligible level of vaccination.

It is evident from Figure 4.1 that for periods of 2, 3 and 6 years, pulse vaccination leads to substantially larger epidemic peaks, as well as deeper epidemic troughs. Though larger epidemic peaks are an undesirable consequence, lower epidemic troughs may increase the probability of stochastic eradications. The effect of lower troughs is particularly evident for $T = 3$ years. The standard deviation is of comparable size to the mean in the epidemic troughs (as indicated by CV$(E+I)$), implying that stochastic fadeouts

may be possible for slight increases in vaccination proportion p_{pulse} .

We further investigate the possibility of stochastic extinction in Figure 4.2, which gives the probability of stochastic measles extinction within 12 years of the introduction of a pulse vaccination campaign as a function of the pulse vaccination proportion p_{pulse}. Curves are shown for population sizes of 1, 5 and 10 million individuals, essentially representing small to large metropolitan populations.

It is immediately apparent from Figure 4.2 that eradication is achieved at feasible levels [54] of pulse vaccination, below 35 percent for each of the pulse intervals and population sizes considered. Systematic effects of demographic stochasticity are also clear in this figure: For fixed pulse intervals, the vaccination level at which complete measles eradication occurs increases with population size, and there is a substantial narrowing of the range of p_{pulse} over which the probability of extinction rises from 0 to 1. For populations of 10 million, we see threshold-type behaviour, with almost zero probability of extinction below the threshold and nearly certain extinction beyond it. This feature is especially apparent for the 1, 2 and 3 year pulse intervals.

Deterministically, one would expect the pulse vaccination proportion required for eradication to increase with pulse interval, but Figure 4.2 shows that stochastically this is not necessarily the case. There is a small increase in the required p_{pulse} as the pulse interval is increased from 1 to 2 years, but at 3 years the required proportion *decreases* noticeably. We will discuss this counter-intuitive result at length in §4.[illegible]. As alluded to in the discussion

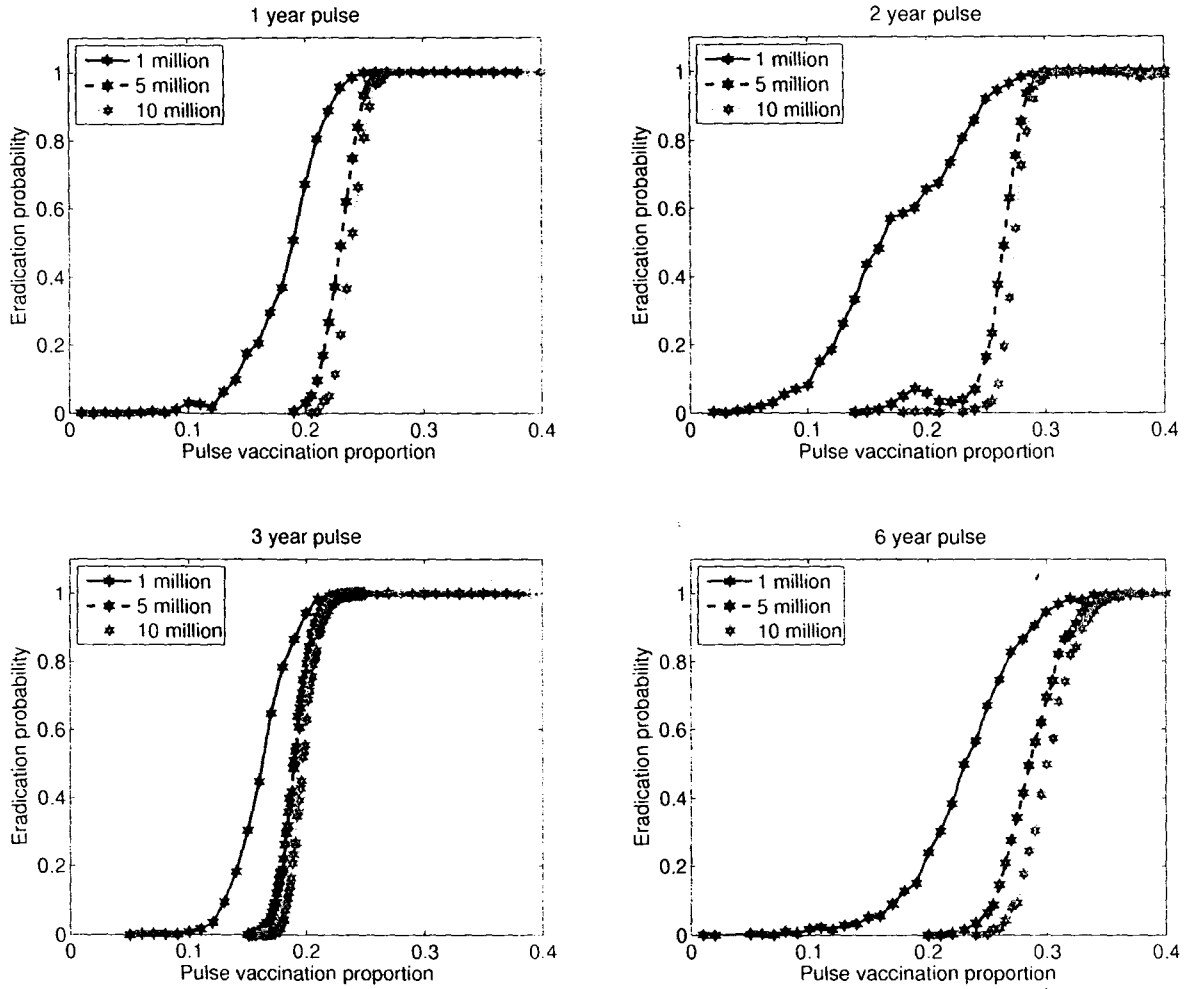

Figure 4.2: Probability of eradication within 12 years of initiation of vaccination for pulse vaccination with intervals of $T = 1, 2, 3, 6$ years and populations of $N = 1, 2, 10$ million as a function of pulse vaccination proportion p_{pulse}, computed through Gillespie simulations based on Table 4.1.1. Required vaccination levels for stochastic eradication are seen to increase with population size N, and there is a thresholding effect whereby the range of p_{pulse} over which the probability of eradication changes from 0 to 1 becomes extremely narrow. Eradication is achieved for a 3 year pulse interval at a lower vaccination proportion than for annual or biennial pulses, suggesting the dynamics are non-trivially dependent on the length of pulse interval.

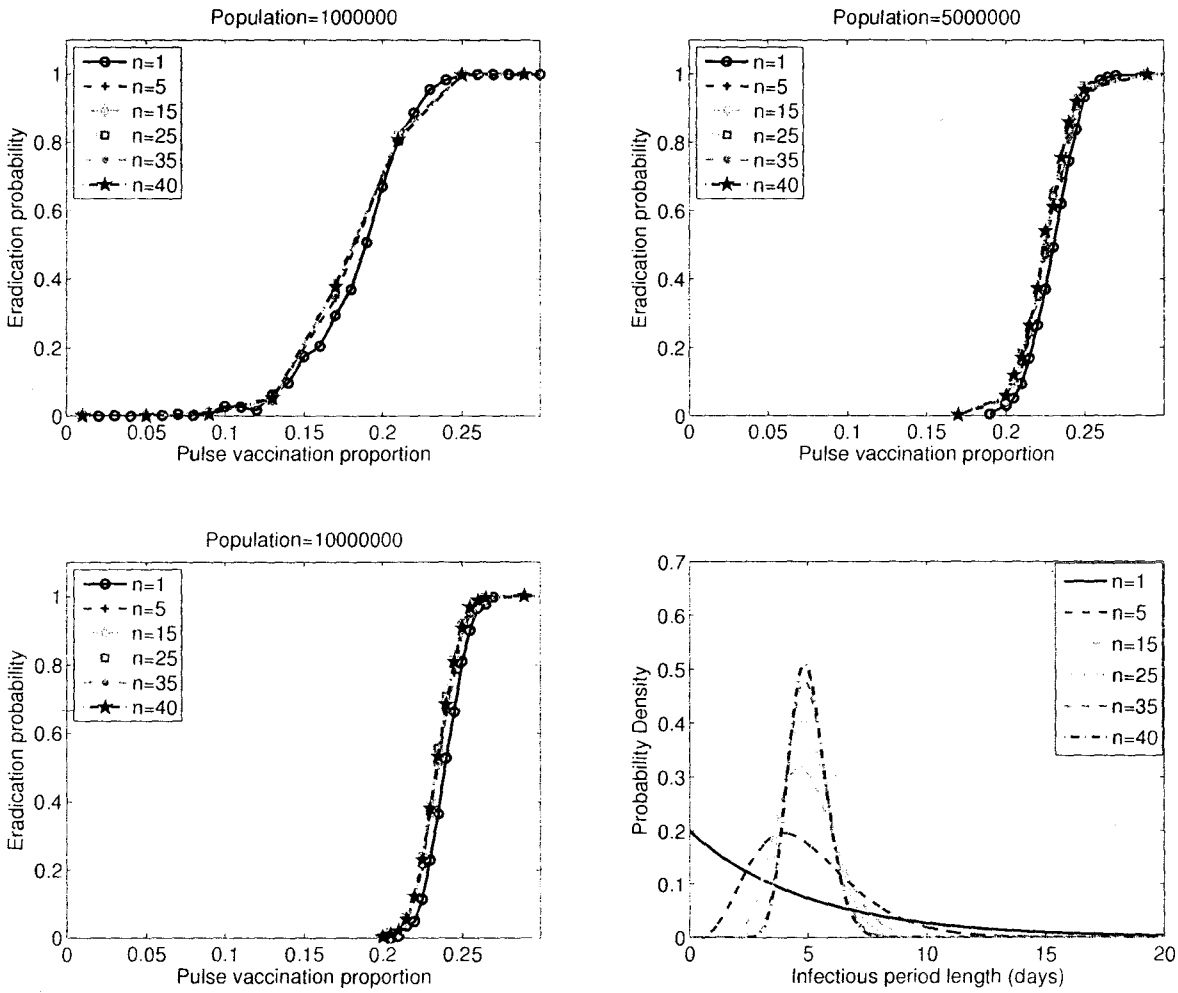

Figure 4.3: Probability of measles eradication within 12 years of initiation of annual pulse vaccination for Erlang (Gamma) distributed latent and infectious periods Gamma(n, $\frac{1}{n\sigma}$), Gamma(n, $\frac{1}{n\gamma}$) as a function of pulse vaccination proportion p_{pulse}. The bottom right panel shows the *probability density* for selected Erlang distributions with shape parameter n and a mean infectious period of 5 days. Eradication is seen to depend very weakly on changes in distribution.

of the prevalence time series, we will argue that (stochastically) eradication potential is strongly and non-trivially dependent of the length of pulse interval, not simply the pulse vaccination proportion or even the overall number of vaccinations in a given time period.

Additionally, we note that behaviour is negligibly affected by the distribution of the latent and infectious periods. We performed Gillespie simulations using more realistic Erlang distributed latent and infectious periods [28] with the identical mean. The eradication probability for annual pulse campaigns with Erlang distributed latent and infectious periods (both with the same shape parameter n) is given in Figure . Note that $n = 1$ corresponds to the exponential distribution of the SEIR model. Results are practically identical, even for $n = 40$ which represents very tightly focused distribution.

MVN Model

Many of the results of the pulse SEIR Gillespie simulations in the previous sections can be predicted—some albeit indirectly—using the MVN moment-closure approximation (4.16).

Figure 4.4 shows the 12 year prevalence time series for the MVN model (4.16) for the identical pulse vaccination proportions (and initial conditions) depicted for the Gillespie algorithm simulations of Figure 4.1. The solid curve denotes the mean, while dashed lines indicate differences of one standard deviation. The MVN model captures the epidemic peaks and troughs of the Gillespie simulations while giving comparable standard deviation values.

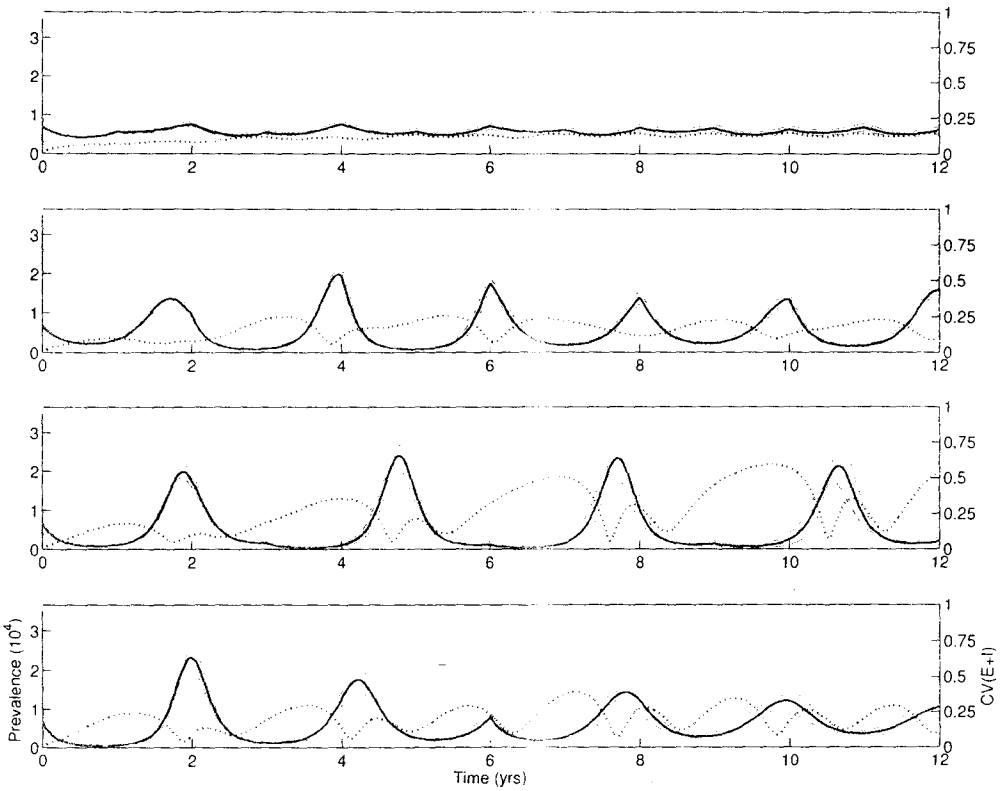

Figure 4.4: Prevalence (E+I) time series for the pulse SEIR model as calculated by the MVN moment closure model (1.16). From top to bottom panels represent pulsing intervals $T = 1, 2, 3, 6$ years and pulse vaccination proportions $p_{\text{pulse}} = 0.05, 0.105, 0.17$ and 0.20. Note these are the identical parameters as in the Gillespie simulations of Figure 1.1. Solid curves indicate the mean, while dashed curves indicate differences of one standard deviation. Dotted curves give the coefficient of variation $\text{CV}(E + I)$ (1.17) (right axis). The MVN model captures the epidemic peaks and troughs of the Gillespie simulations while giving comparable standard deviation (coefficient of variation) values.

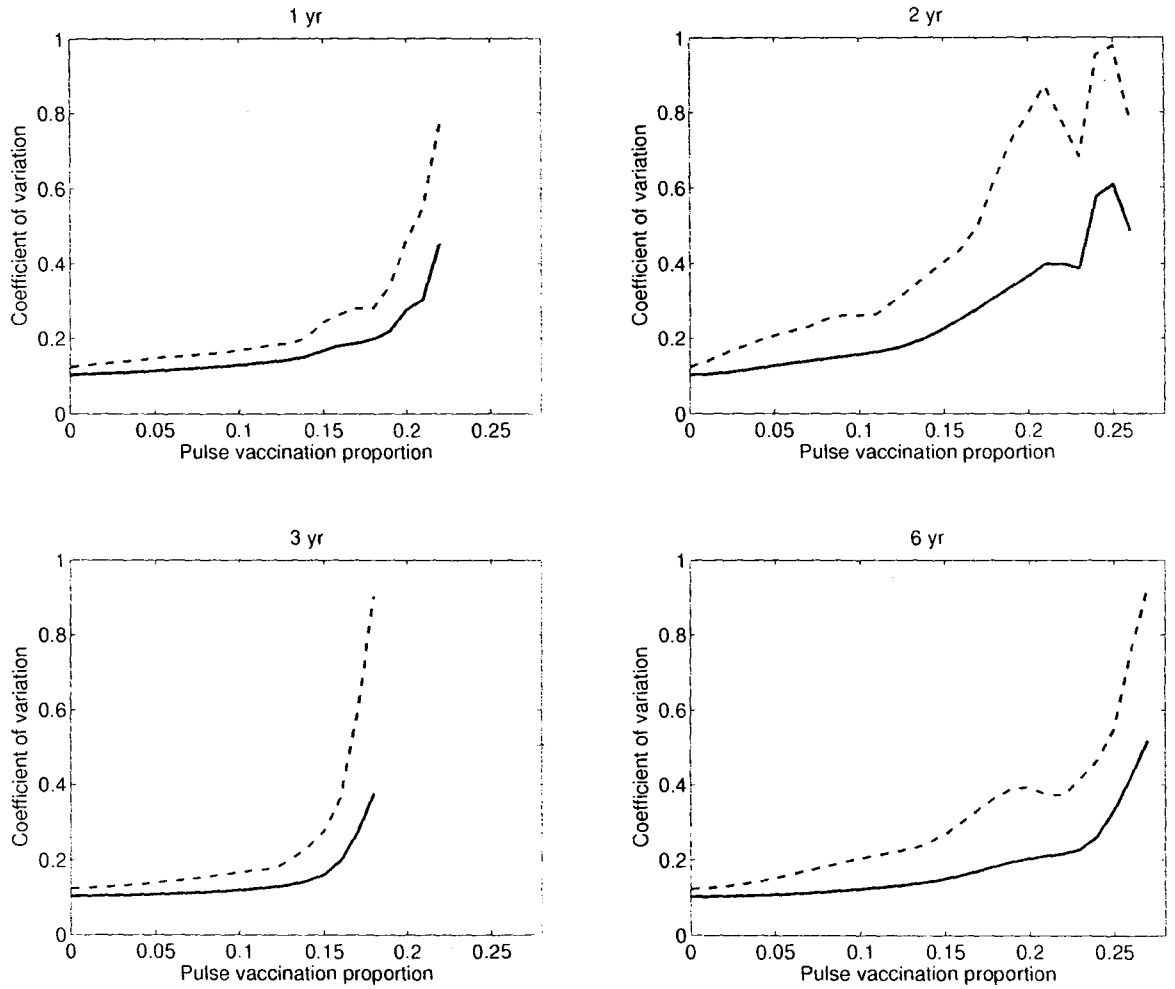

Figure 4.5: Coefficient of variation of disease prevalence, CV$(E + I)$, as a function of pulse vaccination proportion predicted by the MVN pulse SEIR model (4.16) in a population of 10 million. Initial conditions correspond to the Gillespie simulations of Figure . The dashed line indicates the maximum over a 12 year period from the initial pulse, while the solid line indicates the mean. The parameter range at which CV$(E + I)$ increases towards unity, indicating a high probability of stochastic eradication, exhibits good agreement with the parameter region in which stochastic extinctions occur in the corresponding Gillespie algorithm simulations in Figure 4.2.

It is more instructive to look at the coefficient of variation for the prevalence CV$(E+I)$. If this value tends towards one, fluctuations in prevalence are nearly as large as the mean, indicating a high probability of stochastic eradication. We compute the coefficient of variation as a function of the pulse vaccination proportion p_{pulse}, paying particular attention to the values of p_{pulse} for which eradication is observed in the Gillespie algorithm simulations (Figure 4.2). In fact, results show that the MVN model is able to successfully predict the parameter ranges for which extinctions are likely.

Figure 4.5 shows (as a function of pulse vaccination proportion p_{pulse}) the coefficient of variation CV$(E+I)$ ( ) of disease prevalence, for pulse intervals of $T = 1$, 2, 3 and 6 years and a population of $N = 10$ million individuals. The initial conditions are the same as in our Gillespie simulations (Figure 4.1, 4.2). From the point of view of our moment-closure approximation (4.16), these initial conditions correspond to setting the initial variances and covariances to zero, since every realization of the process begins in exactly the same state.

The solid curve in Figure 4.5 shows the mean CV$(E+I)$ over a 12 year period while the dashed curve corresponds to the maximum. The results accurately predict the parameter range in which stochastic extinctions are observed in the Gillespie simulations depicted in Figure 4.2. For each pulse interval T, as p_{pulse} is increased the CV increases, eventually approaching unity; at this point a high probability of extinction is expected (since fluctuations are as large as the mean) and the MVN hypothesis itself begins

to break down as the true distribution of states becomes far from normal. Comparing the results to Figure 4.2, we see that the parameter values where CV$(E + I)$ rapidly increases toward 1 correspond to the narrow range of p_{pulse} at which extinctions are observed in the Gillespie simulations. Note, in particular, that the somewhat counter-intuitive result that a lower p_{pulse} is required to achieve eradication for $T = 3$ years (compared with $T = 1$ or 2 years) is clearly evident in Figure 4.5. There is a steep increase in CV$(E+I)$ to a value above 0.9 before $p_{\text{pulse}} = 0.19$, at which point the MVN model becomes divergent as the hypothesis of a normal distribution of states breaks down.

4.2.2 Comparison of Pulse and Continuous Vaccination

Continuous vaccination targets individuals at the moment that they enter the susceptible population, whereas pulse vaccination targets all susceptible individuals, regardless of their age. Thus p is a proportion new recruits, whereas p_{pulse} is a proportion of all susceptibles. In order to make fair comparisons between continuous and pulse vaccination, we need to use the same measure to assess both.

One sensible metric is the number of doses of vaccine administered per unit time. Equivalently, we consider the *effective vaccination proportion*, p_{eff}, which we define to be the average number of vaccinations per pulse interval

T, as a proportion of the input of new susceptibles (births) over the same period, i.e.,

$$p_{\text{eff}} = \frac{V(T)}{\nu T N} \tag{4.18}$$

where $V(T)$ is the average number of vaccinations per pulse interval T. For continuous vaccination, we have $V(T) = p\nu TN$ for any time period T, so $p_{\text{eff}} = p$. Note that for any type of vaccination program, p_{eff} is directly proportional to the cost of the campaign (ignoring logistical issues and associated costs that differ among different strategies).

Twelve year prevalence time series for a continuous vaccination campaign with $p_{\text{eff}} = 0.16$ are given in Figure 4.6. Note that this is approximately the same value of p_{eff} depicted for the 1, 2, and 3 year pulse interval Gillespie algorithm simulations in Figure (4.1). In contrast to the pulse vaccination results the continuous vaccination model does not exhibit substantial epidemic peaks or troughs and fluctuations in prevalence remain far less than the mean ($< 20\%$).

It is instructive to compare the stochastic eradication results for continuous vaccination to the pulse results in terms of p_{eff}. Figure 4.7 gives the probability of eradication within 12 years of the initiation of either annual pulse or continuous vaccination campaigns (as a function of p_{eff}).

The continuous vaccination model exhibits the same thresholding effect noted previously for pulse vaccination. However, even for populations of 5 or 10 million, the continuous vaccination threshold approaches the deterministic

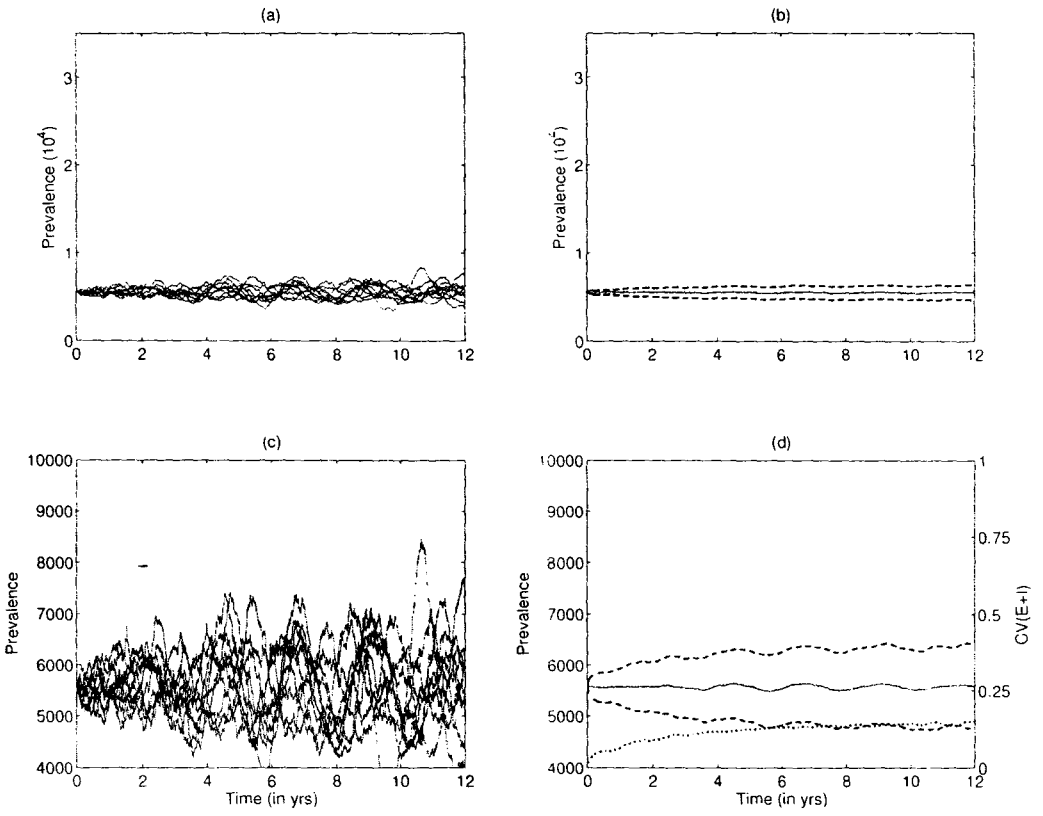

Figure 4.6: Prevalence time series for continuous vaccination Gillespie algorithm simulations, $p = p_{\text{eff}} = 0.16$, $N = 10,000,000$. Panel (a) shows 20 realizations while panel (b) gives the mean for 1000 realizations. The bottom panels (a) and (c) give the same prevalence as in (b) and (d) respectively, but with a different prevalence scale (vertical axis). The scale in (a),(b) corresponds to Figure (4.1). Dashed lines in panels (b),(d) indicate differences of one standard deviation, while the dotted curve in (d) gives the coefficient of variation $\text{CV}(E+I)$ (4.17). In comparison to the 3 year pulse vaccination campaign for the same value of p_{eff} (Figure 4.1), the continuous vaccination strategy does not result in large epidemic peaks and troughs.

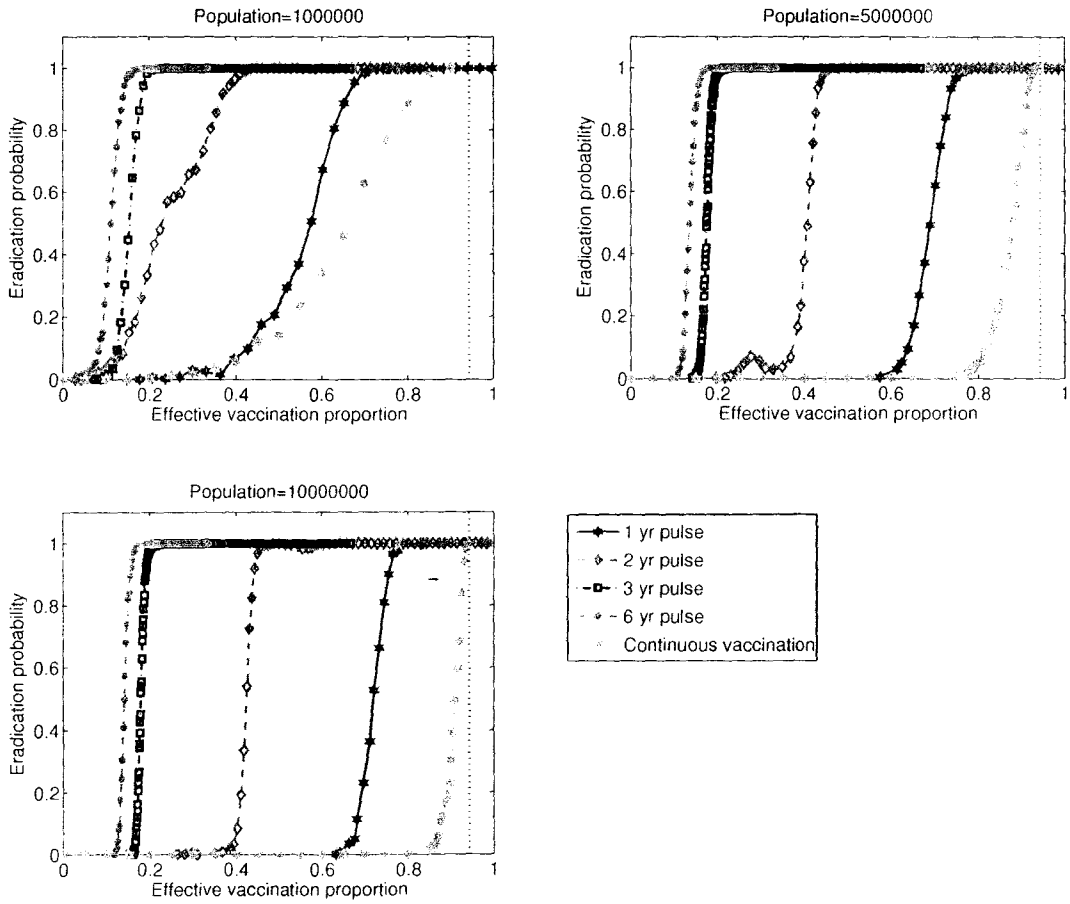

Figure 4.7: Probability of measles eradication within 12 years of initiation of vaccination for pulse campaigns of $T = 1, 2, 3, 6$ years and continuous campaigns with populations of $1, 5, 10$ million as a function effective vaccination p_{eff} (4.18). Results are computed through Gillespie simulations of (4.1) over 1000 realizations. Eradication occurs at a significantly lower value of p_{eff} for pulse vaccination campaigns. As population size increases, in the continuous vaccination campaigns the eradication threshold approaches the deterministic threshold $p_{\text{crit}} = 1 - \frac{1}{\mathcal{R}_0} \approx 0.94$ indicated by the dashed vertical line.

limit (denoted by the vertical line),

$$p_{\text{eff}} \rightarrow p_{\text{crit}} = 1 - \frac{1}{\mathcal{R}_0}. \tag{4.19}$$

Deterministically, p_{crit} is the critical vaccination proportion required for eradication, for both continuous and pulse vaccination [20, 50]. For $\mathcal{R}_0 = 17.5$, Eq. (4.19) yields an eradication threshold of $p_{\text{eff}} \simeq 0.94$.

For the 1 year pulse vaccination campaign, we see in Figure 4.7 that the results are still far from deterministic, with eradication almost certain for $p_{\text{eff}} < 0.8$, even for populations of 10 million. For longer pulse intervals, the difference between the eradication thresholds for continuous and pulse vaccination campaigns becomes extremely pronounced.

4.2.3 Deep Troughs and the Pulse Interval Length

For longer pulse intervals, we have observed a dramatic decrease in the effective vaccination proportion (p_{eff}) that is required for eradication. The creation of deep troughs following vaccination pulses is the key to understanding why the effective vaccination proportion (p_{eff}) required for eradication decreases as the pulse interval (T) is increased. In the deterministic limit, the disease fails to persist if and only if the total number of vaccinations reaches a critical proportion of births. With a finite population size, the depth of the inter-epidemic trough can be more important than the overall number of individuals vaccinated (in terms of increasing the probability of

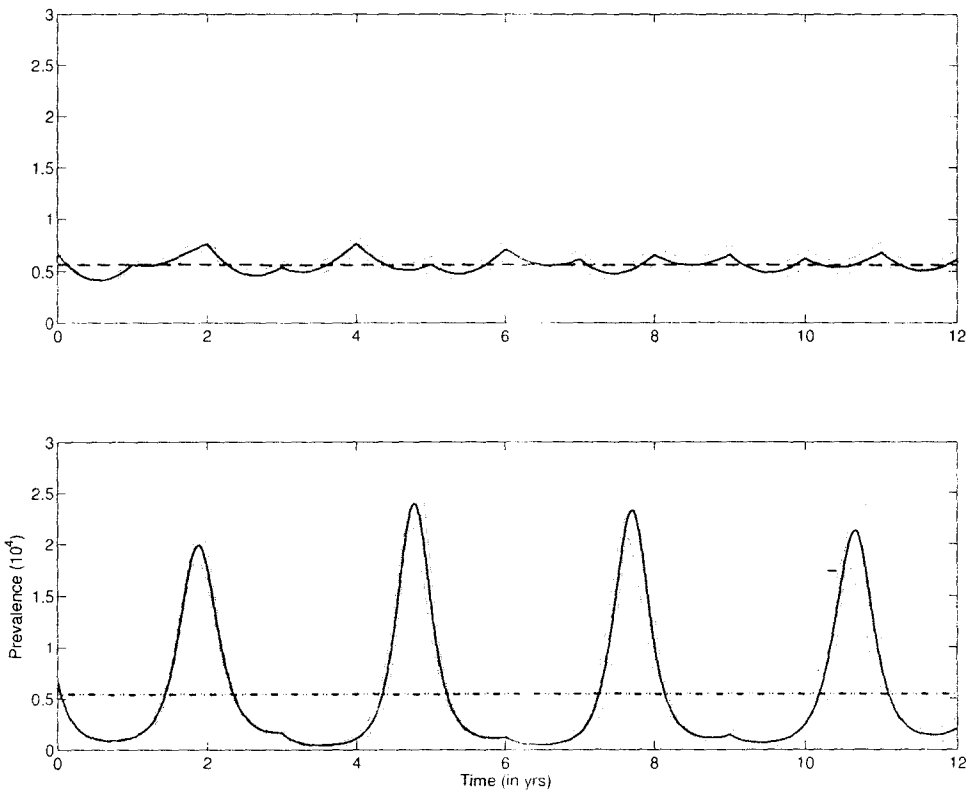

Figure 4.8: Prevalence $(E+I)$ as a function of time as predicted by the MVN pulse SEIR model (4.16) for (top panel) an annual pulse vaccination campaign with $p_{\text{eff}} = 0.17$ (4.18) ($p_{\text{pulse}} = 0.05$) and (bottom panel) a triennial pulse vaccination campaign with $p_{\text{eff}} = 0.16$ ($p_{\text{pulse}} = 0.17$) in a population of $N = 10$ million. Time is measured from the initiation of the pulse vaccination campaign, and the population is assumed to be previously unvaccinated. Dashed horizontal lines indicate the mean prevalence over the 12 year period. The 3 year pulse results in deeper troughs in prevalence (suggesting increased probability of stochastic extinction), as well as substantially larger peaks. However, the mean prevalence over the 12 year period for the two scenarios is equivalent.

extinction).

Figure 1.8 shows the prevalence of infectious individuals as a function of time over the 12 year period from the initiation of vaccination for annual (a) and triennial (b) pulses both with $p_{\text{eff}} \approx 0.16$ ($p_{\text{pulse}} = 0.05, 0.17$) in a population of $N = 10$ million (using the MVN moment closure approximation (1.16)). The solid line represents the mean prevalence while the dashed lines denote differences of one standard deviation. The horizontal line represents the time-average prevalence over the 12 year period. As previously discussed the triennial pulse exhibits significantly larger prevalence peaks and deeper troughs. However (for equivalent p_{eff}), the annual, triennial pulse, and continuous strategy (not shown) exhibit the same time-average prevalence over the 12 year period. Thus in terms of eradication, the triennial pulse strategy is superior in achieving eradication without adversely affecting mean prevalence despite its effect on increasing peak prevalence.

In the case of the annual pulse, we see that vaccination is applied as prevalence is increasing, preventing the epidemic from reaching its full peak height, but at the same time resulting in higher troughs. In the case of the triennial pulse the interval is long enough that the epidemic has reached its maximum, and is descending rapidly into a trough. In this way vaccination in the triennial pulse serves to deepen the epidemic troughs increasing the potential for stochastic extinction.

The tendency for large amplitude oscillations in disease prevalence when the pulse vaccination level is below the deterministic eradication threshold

has been noted previously [17, 49], though the ramifications for stochastic extinction have not been explored before. Higher peaks in prevalence are clearly undesirable from a public health perspective, but the costs of these temporary spikes in prevalence must be balanced against reduction in mean prevalence (as compared to other strategies with equivalent p_{eff}) and the higher probability of extinction.

4.3 Discussion

Previous work [20, 49, 50] based on deterministic models has indicated that continuous vaccination and pulse vaccination programs always incur the same cost (in terms of the number of vaccine doses required to achieve eradication). In this work, we have shown that significant differences arise when the effects of demographic stochasticity are considered.

We focused on measles vaccination and considered both continuous vaccination and pulse vaccination (with pulse intervals of 1, 2, 3 and 6 years). We found that a given probability of eradication can be achieved using less vaccine if pulse vaccination is employed rather than continuous vaccination, and that less vaccine is generally required if a longer pulse interval is employed (assuming the same number of vaccinations per unit time). These conclusions are valid for very large populations (up to at least 10 million). Furthermore, the proportion of the susceptible population that must be vaccinated in each pulse is in a realistic range (less than 35% of susceptibles,

even for triennial pulses, whereas the ability to reach 70% of all children has been demonstrated in some cases [54]).

The length of the pulse interval is as important as the magnitude of the pulse or the total number of vaccinations. Judicious choice of pulse intervals can serve to deepen troughs in disease prevalence, increasing the probability of stochastic fadeout.

We compared the results of many exact realizations of stochastic epidemics [27] to a multivariate normal moment-closure approximation of the underlying process [42]. The two approaches yielded similar results, and we conclude that moment closure is an effective tool for analyzing the stochastic effects of pulse vaccination programs on pathogen eradication. Moment closure models cannot directly yield the distributions of states in the parameter range where pathogen extinction probability is high, but they accurately predict the parameter ranges in which stochastic extinctions are significant. Thus, these methods provide a useful way to examine effects of demographic stochasticity without resorting to intensive computational simulations.

Throughout this work, we have assumed that the populations we are dealing with are isolated, and that transmission rates do not vary with time. In reality, populations are linked by migration and travel, which can lead to "rescue effects" [16] whereby infection is transferred into a community where the pathogen has gone extinct. In addition, transmission rates for measles and other childhood infectious diseases typically vary seasonally [13, 25, 43]. The present work represents a first step in the analysis of more realistic

situations which would include spatially linked populations as well as seasonal forcing.

Pulse vaccination has previously been suggested as a strategy to avoid rescue effects, as it might synchronize prevalence troughs in different spatial locations [23, 24, 26, 29, 36]. How well this might work in practice has yet to be determined. Continuous vaccination programs have been shown both to increase and to decrease epidemic synchrony, depending on the disease in question [47]. If future work establishes that pulse vaccination does have the potential to synchronize prevalence troughs, then our present analysis suggests that eradication efforts will be further enhanced by the stochastic advantage of vaccinating in pulses.

Bibliography

[1] Z. Agur, L. Cojocaru, G. Mazor, R. M. Anderson, and Y. L. Danon (1993), Pulse mass measles vaccination across age cohorts, Proceedings of the National Academy of Science USA 90, 11698–11702.

[2] L. J. S. Allen and A. M. Burgin (2000), Comparison of deterministic and stochastic SIS and SIR models in discrete time, Mathematical Biosciences 163, 1–33.

[3] R. M. Anderson and R. M. May (1991), Infectious Diseases of Humans. Dynamics and Control, Oxford Science Publications.

[4] H. Andersson and T. Britton (2000). Stochastic Epidemic Models and Their Statistical Analysis, Lecture Notes in Statistics, Springer.

[5] H. Andersson and T. Britton (2000). Stochastic epidemics in dynamic populations: quasistationarity and extinction, Journal of Mathematical Biology 41, 559–580.

[6] N. T. J. Bailey (1975), The Mathematical theory of Infectious Diseases and its Applications. Hafner Press.

[7] M. S. Bartlett (1956), Deterministic and stochastic models for recurrent epidemics, Proc. Third Berkeley Symp. Math. Statistic. and Prob. 4, 81–109.

[8] M. S. Bartlett (1957), Mealses Periodicity and Community Size, Journal of the Royal Statistical Society A. 120(1), 48–70.

[9] M. S. Bartlett (1960), The critical community size for measles in the United States, J.R. Statist. Soc., Ser. A. 123, 37–44.

[10] M. S. Bartlett (1960), Some Population Models in Ecology and Epidemiology, Metheun.

[11] M. S. Bartlett (1960), Some stochastic models in ecology and epidemiology, Contributions to Probability and Statistics: Essays in Honor of Harold Hotelling, Stanford University Press, pp. 89–96.

[12] C. Bauch and R. D. R. (2000), A moment closure model for sexually transmitted disease transmission through a concurrent partnership network, Proceedings of the Royal Society of London B. 1456, 2019-2027.

[13] C. T. Bauch and D. J. D. Earn (2003), Transients and attractors in epidemics, Proceedings of the Royal Society of London Series B. 270, 1573–1578.

[14] F. L. Black (1966), Measles endemicity in insular populations; Critical community size and its evolutionary implications, Journal of Theoretical Biology 11(2), 207–211.

[15] B. Bolker and S. W. Pacala (1997). Using moment equations to understand stochastically driven spatial pattern formation in ecological systems, Journal of Theoretical Population Biology 52, 179–197.

[16] J. H. Brown and A. Kodric-Brown (1977), Turnover rates in insular biogeography: effect of immigration on extinction, Ecology 58, 445–449.

[17] M. Choisy, J. F. Guegan, and P. Rohani (2006), Dynamics of infectious diseases and pulse vaccination: Teasing apart the embedded resonance effects, Physica D 223, 26–35.

[18] J. N. Darroch and E. Seneta (1967). On quasi-stationary distributions in absorbing and continuous time finite Markov Chains, Journal of Applied Probability 4, 192–196.

[19] A. d'Onofrio (2002), Pulse vaccination strategy in the SIR epidemic model: Global asymptotic stable eradication in the presence of vaccine failures, Mathematical and Computer Modelling , 473–489.

[20] A. d'Onofrio (2002), Stability properties of pulse vaccination strategy in SEIR epidemic model, Mathematical Biosciences 179, 57–72.

[21] A. d'Onofrio (2004), Mixed pulse vaccination strategy in epidemic model

with realistically distributed infectious and latent times, Applied Mathematics and Computation 151, 181–187.

[22] A. d'Onofrio (2005), On pulse vaccination strategy in the SIR epidemic model with vertical transmission, Applied Mathematics Letters 18, 729–732.

[23] D. J. D. Earn and S. A. Levin (2006), Global asymptotic coherence in discrete dynamical systems, Proceedings of the National Academy of Science USA 103(11), 3968–3971.

[24] D. J. D. Earn, S. A. Levin, and P. Rohani (2000), Coherence and conservation. Science 290(5495), 1360–1364.

[25] D. J. D. Earn, P. Rohani, B. M. Bolker, and B. Grenfell (2000), A simple model for complex dynamical transitions in epidemics, Science 287, 667–670.

[26] D. J. D. Earn, P. Rohani, and B. T. Grenfell (1998), Persistence, chaos and synchrony in ecology and epidemiology, Proceedings of the Royal Society of London Series B-Biological Sciences 265(1390), 7–10.

[27] D. T. Gillespie (1976), A General Method for Numerically Simulating the Stochastic Time Evolution of Coupled Chemical Reactions, Journal of Computational Physics 22, 403–434.

[28] K. J. Gough (1977), The estimation of latent and infectious periods, Biometrika 64, 559–565.

[29] B. Grenfell and J. Harwood (1997). (Meta)-population dynamics of infectious diseases, Trends in Ecology and Evolution 12, 395–399.

[30] Z. Grossman (1980). Oscillatory phenomena in a model of infetious diseases, Theoretical Population Biology 18, 204–243.

[31] H. Guo and M. Y. Li (2006), Global Dynamics of a Staged Progression Model for Infectious Diseases, Mathematical Biosciences and Engineering 3(3), 513–525.

[32] D. He and E. D. J. D. (2007), Epidemiological effects of seasonal oscillations in birth rates, Theoretical Population Biology 72, 274–291.

[33] H. W. Hethcote (2000), The Mathematics of Infectious Diseases, SIAM Review 42(4), 599–653.

[34] V. Isham (1995), Stochastic models of host-macroparasite interaction, Annals of Applied Probability 5, 720–740.

[35] W. Katzman and K. Dietz (1985), Evaulation of age-specific vaccination strategies, Journal of Theoretical Population Biology 23, 125–137.

[36] M. J. Keeling, O. N. Bjornstadt, and B. T. Grenfell (2004), Ecology, Evolution, and Genetics of Metapopulations, chapter Metapopulation Dynamics of Infectious Diseases, pp. 415–451.

[37] I. Kirshnarajah, A. Cook, G. Marion, and G. Gibson (2005), Novel mo-

ment closure approximations in stochastic epidemics, Bulletin of Mathematical Biology 67, 855–873.

[38] A. Korobeinikov and P. K. Maini (2004), A Lyapunov Function and Global Properties for SIR and SEIR Epidemiological Models with Nonlinear Incidence, Math. Biosci. Eng. 1(1), 57–60.

[39] T. Kurtz (1971), Limit Theorems fo Sequences of Jump Markov Processes Approximating Ordinary Differential Equations, Journal of Applied Probability 8(2), 344–356.

[40] T. G. Kurtz (1980), Relationships between stochastic and deterministic population models, Lecture Notes in Biomathematics 38, 449–467.

[41] A. L. Lloyd (2001), Realistic Distributions of Infectious Periods in Epidemic Models: Changing Patterns of Persistence and Dynamics, Theoretical Population Biology 60, 59–71.

[42] A. L. Lloyd (2004), Estimating variability in models for recurrent epidemics assessing the use of moment closure techniques, Theoretical Population Biology 65, 49–65.

[43] W. P. London and J. A. Yorke (1973), Recurrent outbreaks of measles, chickenpox, and mumps. I. Seasonal variation in contact rates, Am. J. Epidemiol. 98, 453–468.

[44] I. Nasell (1996), The Quasi-Stationary Distribution of the Closed Endemic SIS Model, Advances in Applied Probability 28(3), 895–932.

[45] I. Nasell (1999), On the time to extinction in recurrent epidemics, Journal of the Royal Statistical Society B. 61, 309–330.

[46] J. Nokes and J. Swinton (1997), Vaccination in pulses: a strategy for the global eradication of measles and polio?, Trends in Microbiology 5, 14-19.

[47] P. Rohani, D. J. D. Earn, and B. T. Grenfell (1999), Opposite Patterns of Synchrony in Sympatric Disease Metapopulations, Science 286, 968–971.

[48] A. Sabin (1991), Mealses, killer of millions in developing countries: strategies of elimination and continuing control, European Journal of Epidemiology 7, 1–22.

[49] B. Shulgin, L. Stone, and Z. Agur (1998), Pulse vaccination strategy in the SIR epidemic model, Bulletin of Mathematical Biology 60, 1123-1148.

[50] L. Stone, B. Shulgin, and Z. Agur (2000), Theoretical examination of the pulse vaccination policy in the SIR epidemic model, Mathematical and Computer Modelling 31, 207-215.

[51] P. van den Driessche and J. Watmough (2002), Reproduction numbers and sub-threshold endemic equilibria for compartmental models of disease transmission, Mathematical Biosciences 180(Sp. Iss.), 29–48.

[52] O. A. van Hewaarden and J. Grasman (1995), Stochastic epidemics: major outbreaks and the duration of the endemic period, Journal of Mathematical Biology 33, 581–601.

[53] B. G. Wagner and D. J. D. Earn (2008), Circulating vaccine derived polioviruses and their impact on global polio eradication, Bulletin of Mathematical Biology 70, 253–280.

[54] P. L. F. Zuber, K. S. G. Conombo, A. D. Traore, A. Millogo, J. D.and Ouattara, I. B. Ouedraogo, and A. Valian (2002), Mass Measles vaccination in urban Burkina Faso 1998, Bulletin of the World Health Organization 79(4), 296–300.

Chapter 5

Conclusions

In this work we dealt with a number of topics related to vaccination strategies for the eradication of childhood infectious disease. We proposed and analyzed "endgame" vaccination strategies for poliomyelitis to allow for the worldwide cessation of vaccination. We investigated the dynamical effects of contact vaccination in the use of live-attenuated virus vaccines, whereby vaccine recipients may pass on the vaccine virus to contacts resulting in secondary immunizations. Lastly we looked at the stochastic implications of pulse vaccinations, in which mass vaccinations are performed at regular intervals (as opposed to continuously). Specifically we focused on the ability of pulse vaccination to cause stochastic extinctions in measles vaccination campaigns. The mathematical models employed include standard SIR or $SEIR$ [19] type compartmental differential equations models and their analogous representation as discrete state continuous time Markov chains for finite pop-

ulations. We employed a mix of analytical and computational techniques. In our analysis of stochasticity we used direct simulation methods as well as moment closure approximation methods. In the analysis of compartmental differential equations models we employed such analytical techniques as the construction of Lyapunov functions [32] and the use of numerical bifurcation analysis routines [31].

Our analysis of so called "endgame" strategies for poliomyelitis vaccination focused on the use of the Oral Polio Vaccine, the primary polio vaccine used in the developing world [23]. Though providing an effective immune response, this live-attenuated virus is genetically unstable and may revert back to virulence and transmissibility resulting in circulating vaccine derived polioviruses [28]. Through the use of a compartmental ordinary differential equation model, we assessed the risks associated with reversion in continuous OPV vaccination programs. We established that although the impact of reversion is not significant when the wild virus is endemic, it is significant from the standpoint of the eventual cessation of vaccination (when the wild virus in nearly eradicated). We proposed and analyzed transition strategies to achieve complete eradication and allow for the cessation of vaccination. These strategies include the use of the Inactivated Polio Vaccine (IPV), the use of strictly pulse-vaccination OPV, as well as a one time pulse vaccination with IPV. Using stochastic simulation methods we found that a one time IPV pulse may be feasible, while a strictly pulse OPV campaign can be effective as long as a higher level of vaccination coverage is maintained.

We examined the benefits of contact vaccination in lowering critical vaccination thresholds for the eradication of wild viruses. For continuous vaccination programs, we established that thresholds are independent of the latent and infectious period distributions of both viruses, depending only on the reproduction numbers of both the wild and vaccine virus. Contact vaccination substantially lowers the (wild virus) critical vaccination proportion, even when the vaccine virus reproduction number is below 1, in which case the vaccine virus fades from the population upon cessation of vaccination. We also examined the effects of contact vaccination in pulse vaccination campaigns. Pulse vaccination leads to a decrease in the benefits of contact vaccination. However, we concluded that for annual pulse OPV vaccinations this decrease is not significant. This result is of practical importance since some form of annual pulse OPV campaign is conducted in 55 countries around the world [4], and the benefits of contact vaccination in OPV use have long been empirically observed by epidemiologists [23].

For pulse measles vaccination campaigns we found that, for populations on the order of large cities or small countries, taking demographic stochasticity into account may lead to significant differences with deterministic models. Particularly, we found that stochastic eradication is predicted for significantly lower levels of vaccination (in terms of total number of vaccinations) than for deterministic models or the equivalent stochastic model for continuous vaccination. The length of the pulse interval has a non-trivial effect on the eradication threshold. A pulse interval of sufficient length to allow inter pulse

epidemics to reach their maximum peak height can serve to deepen inter epidemic troughs, significantly increasing the probability of stochastic extinction. Though the deepening of troughs is accompanied by a corresponding increase in peak disease prevalence, the average prevalence over the entire pulse interval differs negligibly from the continuous vaccination scenario (for the equivalent number of vaccinations). In light of recent results which show pulse vaccination may be able to synchronize epidemic troughs in spatially coupled populations [15, 26], our work suggests that there may be significant stochastic advantages to employing pulse vaccination strategies worldwide.

A central theme of this thesis is that eradication of infectious disease is a worldwide problem that requires well coordinated global solutions. In making public policy decisions a multitude of factors must be considered ranging from the specific characteristics of the vaccine to the timing of vaccinations. As we have illustrated in this work, consideration of such factors may be the difference between successful worldwide eradication and persistence of the pathogen. Mathematical models, both stochastic and deterministic, can shed light on the relative importance of these factors and allow us to formulate and assess strategies to overcome potential barriers.

Bibliography

[1] Hakan Andersson and Tom Britton. *Stochastic Epidemic Models and Their Statistical Analysis.* Lecture Notes in Statistics. Springer. 2000.

[2] Hakan Andersson and Tom Britton. Stochastic epidemics in dynamic populations: quasistationarity and extinction. *Journal of Mathematical Biology*, 41:559–580, 2000.

[3] [Anon]. Diseases and conditions: Polio. Technical report, Centers for Disease Control and Prevention, 2005.

[4] [Anon]. Polio eradication.org. Technical report, January 2008.

[5] M. S. Bartlett. Measles periodicity and community size. *Journal of the Royal Statistical Society A.*, 120:48–70, 1957.

[6] M. S. Bartlett. The critical community size for measles in the us. *Journal of the Royal Statistical Society A.*, 123:37–44, 1960.

[7] B. M. Bolker and B. T. Grenfell. Chaos and biological complexity in measles. *Proc. R. Soc. Lond. B*, 251:75–81, 1993.

[8] S. Bunimovich-Mendrazitsky and L. Stone. Modeling polio as a disease of development. *Journal of Theoretical Biology*, 237:302–315, 2005.

[9] Centers for Disease Control and Prevention. Epidemioogy of measles-united states. *MMWR*, 48:749–753. 1999.

[10] Centers for Disease Control and Prevention. Global measles control and regional elimination. *MMWR*, 48:1124–1130, 1999.

[11] Centers for Disease Control and Prevention. Progress toward global poliomyelitis eradication. *MMWR*, 48:416–421, 1999.

[12] Centers for Disease Control and Prevention. Notice to readers: 25th anniversary of the last case of naturally acquired smallpox. *MMWR*, 51(42):952, 2002.

[13] A. d'Onofrio. Pulse vaccination strategy in the SIR epidemic model: Global asymptotic stable eradication in the presence of vaccine failures. *Mathematical and Computer Modelling*, pages 473–489, 2002.

[14] D. J. D. Earn, P. Rohani, B. M. Bolker, and B.T. Grenfell. A simple model for complex dynamical transitions in epidemics. *Science*, 287:667 - 670, 2000.

[15] D. J. D. Earn, P Rohani, and B. T. Grenfell. Persistence, chaos and synchrony in ecology and epidemiology. *Proceedings of the Royal Society of London Series B-Biological Sciences*, 265(1390):7–10, 1998.

[16] P. E. M Fine and J. A. Clarkson. Measles in england and wales - analysis of factors underlying seasonal patterns. *Int. J. Epidem.*, 11:5–15, 1982.

[17] Hongbin Guo and Michael Y. Li. Global dynamics of a staged progression model for infectious diseases. *Mathematical Biosciences and Engineering*, 3(3):513–525, 2006.

[18] D. He and D. J. D. Earn. Epidemiological effects of seasonal oscillations in birth rates. *Theoretical Population Biology*, 72:274–291, 2007.

[19] Herbert W. Hethcote. The mathematics of infectious diseases. *SIAM Review*, 42(4):599–653, 2000.

[20] David L. Heymann. Roland W. Sutter, and R. Bruce Aylward. A global call for new polio vaccines. *Nature*, 434:699–700, April 2005.

[21] H. F. Hull, N. A. Ward, B. D. Hull. J. B. Milstien, and C. de Quadros. Paralytic poliomyelitis: seasoned strategies disappearing disease. *Lancet*, 343:1331–1337, 1994.

[22] Harry F. Hull and Philip D. Minor. When can we stop using oral poliovirus vaccine? *Journal of Infectious Disease*. 192:2033–2035, 2005.

[23] T. J. John. A developing country perspective on vaccine-associated paralytic poliomyelitis. *Bulletin of the World Health Organization*, 82(1):53 - 57, 2004.

[24] M. J. Keeling. Metapopulation moments: coupling, stochasticity and persistence. *J. Anim. Ecol.*, 69:726–736, 2000.

[25] M. J. Keeling. Multiplicative moments and measures of persistence in ecology. *Journal of Theoretical Biology*, 205:269–281, 2000.

[26] M. J. Keeling, O. N. Bjornstadt, and B. T. Grenfell. *Ecology, Evolution, and Genetics of Metapopulations*, chapter Metapopulation Dynamics of Infectious Diseases, pages 415–451. 2004.

[27] W. O. Kermack and A. G. McKendrick. A contribution to the mathematical theory of epidemics. *Proceedings of the Royal Society of London Series A*, 115:700–721, 1927.

[28] Olen M. Kew, Peter F. Wright, Vadim I. Agol, Francis Delpeyroux, Shimizu Hiroyuki, Neal Nathanson, and Pallansch Mark A. Circulating vaccine-derived polioviruses: current state of knowledge. *Bulletin of the World Health Organization*, 82(1), 2004.

[29] Andrei Korobeinikov. Lyapunov functions and global properties for SEIR and SEIS epidemic models. *Mathematical Medicine and Biology*, 21:75–83, 2004.

[30] Andrei Korobeinikov and Philip K. Maini. Non-linear incidence and stability of infectious disease models. *Mathematical Medicine and Biology*, 22:113–128, 2005.

[31] Yuri A. Kuznetsov. *Elements of applied bifurcation theory*, volume 112 of *Applied Mathematical Sciences*. Springer-Verlag, New York, second edition, 1998.

[32] J. P. La Salle and S. Lefschetz. *Stability by Liapunov's direct method with applications*. Academic Press, New York, 1961.

[33] Alun L. Lloyd. Realistic distributions of infectious periods in epidemic models: Changing patterns of persistence and dynamics. *Theoretical Population Biology*, 60:59–71, 2001.

[34] Alun L. Lloyd. Estimating variability in models for recurrent epidemics assessing the use of moment closure techniques. *Theoretical Population Biology*, 65:49–65, 2004.

[35] W. P. London and J. A. Yorke. Recurrent outbreaks of measles, chickenpox, and mumps. i. seasonal variation in contact rates. *Am. J. Epidemiol.*, 98:453–468, 1973.

[36] Ingemar Nasell. On the time to extinction in recurrent epidemics. *Journal of the Royal Statistical Society B.*, 61:309–330, 1999.

[37] J. M. Neff, J. M. Lane, V. A. Fulginiti, and D. Henderson. Contact-vaccinia-transmission of vaccinia from smallpox vaccination. *JAMA*, 288(15), 2002.

[38] M. B. A. Oldstone. *Viruses, Plagues and History*. Oxford University Press, 1998.

[39] D. Schenzle. An age- structured model of pre- and post-vaccination measles transmission. *IMA J. Math. appl. med. Biol.*, 21:347–361, 1984.

[40] B. Shulgin, L. Stone, and Z. Agur. Pulse vaccination strategy in the SIR epidemic model. *Bulletin of Mathematical Biology*, 60:1123–1148, 1998.

[41] B. Singh, K. Suresh, Sanjiv Kumar, and P. Singh. Pulse polio immunization in Dehli- 1995-1996: A Survey. *Indian J. Pediatr.*, 64:57–64, 1996.

[42] L. Stone, B. Shulgin, and Z. Agur. Theoretical examination of the pulse vaccination policy in the SIR epidemic model. *Mathematical and Computer Modelling*, 31:207–215, 2000.

[43] P. L. F. Zuber, K. S. G. Conombo, A. D. Traore, A. Millogo, J. D.and Ouattara, I. B. Ouedraogo, and A. Valian. Mass measles vaccination in urban burkina faso 1998. *Bulletin of the World Health Organization*, 79(4):296–300, 2002.